SAND78-8188
Unlimited Release

MDAC/ROCKETDYNE Solar Receiver Design Review

Prepared by Sandia Laboratories, Albuquerque, New Mexico 87115 and Livermore, California 94550 for the United States Department of Energy under Contract AT(29-1)-789.

Printed November 1978

Sandia Laboratories
energy report

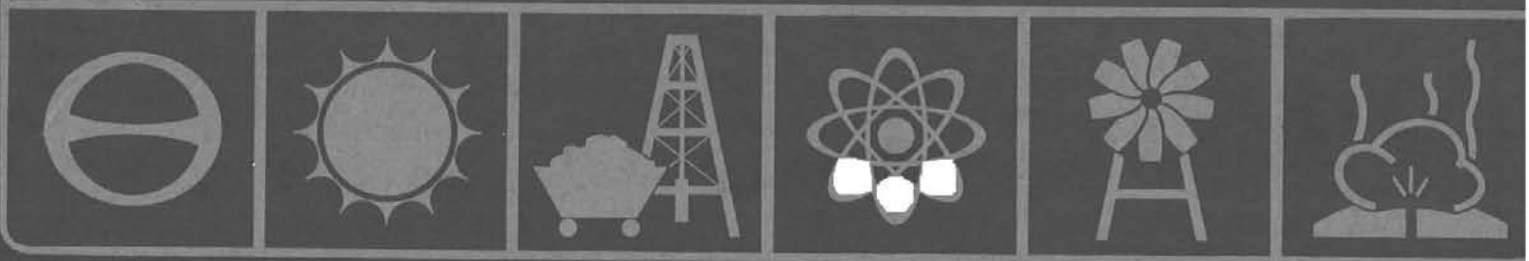

Issued by Sandia Laboratories, operated for the United States Department of Energy by Sandia Corporation.

NOTICE

Printed in the United States of America
Available from
National Technical Information Service
U. S. Department of Commerce
5285 Port Royal Road
Springfield, VA 22161
Price: Printed Copy $7.25 ; Microfiche $3.00

MDAC/ROCKETDYNE SOLAR RECEIVER

Design Review

FINAL REPORT

C-E Contract 17677

ASA 78-06

H. M. Payne
Project Leader
August 1978

Prepared for Sandia Laboratories
under Contract No. 18-2557

Combustion Engineering, Inc.
Power Systems Group
Windsor, Connecticut 06095

NOTICE

TABLE OF CONTENTS

LIST OF FIGURES

LIST OF TABLES

SECTION 1

INTRODUCTION AND SUMMARY

1.1 Introduction

This report presents the results of a review of the MDAC/Rocketdyne solar central receiver designs for both the 100 MWe commercial plant and the 10 MWe pilot plant. The major objective of this design review was to assess the adequacy of the design in meeting the requirements of the solar central receiver (boiler) over a commercial lifetime of 30 years.

The MDAC/Rocketdyne design consists of an external solar heated receiver, composed of a multiple of modular panels arranged in parallel and operating on the once-through steam generation principle. Each panel is composed of welded tangent tubes, connected between inlet and outlet headers. Subcooled water enters the bottom headers, flows upward, absorbs heat, produces saturated steam throughout the two phase region, and exits at the top as superheated steam. Tube size and material is the same for both the commercial and pilot plants. Panel sizes are different between the two plants. Commercial plant heat flux is approximately 2.8 times that of the pilot plant. Structural supports and attachments of both designs are similar. Control of final superheat temperature is maintained by varying the water flow to each of the panels, according to the thermal absorption of each panel. The pilot and commercial plant receiver designs are therefore similar in construction and mode of operation. They differ significantly, however, in thermal loading (heat flux).

1.2 Summary

1.2.1 MDAC and Rocketdyne design documents were examined initially, and potential problem areas were identified, in order to determine the analysis procedures required in the design review.

These initial observations and potential problem areas are listed in Reference 24. The tentative problem areas were identified as:

1. Lack of CHF test data at the high flux levels.
2. Tube wall thickness is greater than necessary.
3. A start-up rate of temperature rise may be too high.
4. ASME Code Case 1592 should be used for fatigue data.
5. Daily cyclic operation is only part of the potential fatigue stress problem to be addressed. CHF oscillations and cloud cover will contribute to fatigue damage, since Incoloy 800 does not show an endurance limit.
6. The weld joining tangent tubes may contribute stress concentration and is a potential source of cracking.

1.2.2 Thermal-Hydraulic Analysis

An existing C-E computer program was modified for the solar receiver configuration. This program performs an energy and mass balance on the receiver panels by a finite difference type integration of the heat flux curve. Outputs include tube metal temperatures, enthalpy, absorbed heat flux and pressure drop, as a function of panel length.

The design parameters of the solar receiver lie outside the ranges of existing C-E in-house standards for predicting CHF and the minimum film boiling coefficient. A literature search was conducted for suitable correlations of CHF and film boiling. It was determined that the MacBeth correlation was suitable for CHF prediction, and the Groeneveld correlation for film boiling. The Groeneveld correlation is conservative, compared to that used by Rocketdyne; i.e., it predicts higher metal temperatures.

Test data from Rocketdyne was analyzed for minimum film boiling coefficients. These were compared to values calculated by the two correlations above, and a wide variation was found. Generally speaking, the test data lies somewhere between the two correlations mentioned above. The Rocketdyne tests were limited in heat flux and mass flux. Further testing is needed, particularly at the higher mass and heat flux levels of the commercial plant.

Static stability analysis indicated that orificing of individual boiler tubes was not needed. Header sizing appears to be adequate as a check showed virtually no flow imbalance due to header and piping orientation.

Tube temperature calculations, using a two-dimensional steady-state heat conduction program, indicated that the maximum tube crown temperature for the pilot plant was 553°C (1027°F), in the superheater region. Maximum tube temperature for the commercial plant was 597°C (1106°F) at the minimum film coefficient and 626°C (1158°F) in the superheater region.

1.2.3 Stress Analysis

Stress analysis of the receiver panels indicated no problem with the pilot plant. Fatigue life in excess of 30 years should be achieved. The commercial plant design is subject to a reduced fatigue life due to the high panel temperature difference as a result of the CHF and film boiling problem. This causes the panel to tend to assume a "mattress" shape. Calculated panel stresses were well beyond yield (in compression) and an elastic analysis was conducted to simulate an inelastic analysis.

Results, while very conservative, indicate a serious fatigue problem as a result of the daily start-up and shut-down cycles of the receiver. Fatigue cracking would be expected on the outer surface of the tubes. High cycle fatigue due to CHF oscillations and cloud cover was not addressed in this review. Changing tubing size and material shows some improvement in fatigue stress but not enough to assure 30 years life. An inelastic analysis is recommended to further refine and clarify the fatigue life of the unit. The single most important factor in improving fatigue life would be to eliminate the CHF and film boiling in the high flux commercial plant. This might be accomplished by the use of rifled tubing in the evaporator region. An alternative would be a lower flux, but at some loss of efficiency.

A review of the CHF temperature oscillation problem indicated that further testing will be needed to establish the magnitude and frequency data needed to perform a fatigue analysis.

1.2.4 Water Chemistry Specifications

Water chemistry specifications and procedures were reviewed. In general, the specifications established for the receiver water quality control are satisfactory. Additional recommendations on pH control are included, along with C-E procedures for lay-up of once-through boilers.

1.2.5 Major Problems and Proposed Solutions

Major problem areas identified include the lack of accurate DNB and film boiling data for this design. Further testing at the heat flux and mass flux levels of the commercial design is

recommended. Analysis indicates that the pilot plant will not experience CHF, whereas the commercial plant will experience CHF and temperature oscillations, which may affect fatigue life. The pilot plant will give an optimistic view of the fatigue life expected in the commercial plant design, due to the CHF problem.

Preliminary review of a "turbulator" as a solution to the CHF problem in the commercial design was undertaken. Indications are that a rifled tubing evaporator section and a separate superheater section could be adapted to this external receiver without any adverse impact on receiver efficiency. Success of this method is predicated on results of testing of rifled tubing in this high flux environment.

SECTION 2

THERMAL-HYDRAULICS ANALYSIS AND WATER CHEMISTRY

2.1 Introduction

This section includes three major sub-sections. The first is a description of the thermal-hydrualics analysis of the pilot plant and commercial plant receiver designs. Secondly, an evaluation of the proposed 5-tube panel SRE retest is presented. Thirdly, the proposed plant water quality control is reviewed.

The method employed for the thermal analysis consisted of modifying an existing computer program to conform to the geometry of the MDAC/ Rocketdyne receiver configuration. This thermal analysis program is a finite difference calculation of the energy and mass balance on small increments axially along the length of a receiver panel tube. It is a one-dimensional calculation with a correction to account for the 2-D radial heat flow in the tube. Output consists of tube crown temperature profile, fluid enthalpy, and pressure losses. As existing standard correlations did not cover the ranges of parameters in this design, a literature review was made to select applicable correlations for the critical heat flux and the film boiling coefficients. Output of the thermal program served to generate input to the 2-D temperature and stress finite element programs, MARC-Heat, and MARC-Stress. The thermal analysis program was also employed to evaluate the proposed retest of the 5-tube panel. Each sub-section is discussed in detail below.

2.2 Thermal/Hydraulic Analysis of Pilot and Commercial Plants

2.2.1 Review of Correlations for Critical Heat Flux and Film Boiling

A review was made of available correlations for the calculation of the film boiling heat transfer coefficient. References are

listed at the end of the report. The review was conducted with the objective of selecting a correlation applicable to the range of design parameters of the MDAC receiver design:

Pressure	11.03 M Pa (1600 psia)
Tube Diameter (Inside)	6.858 mm (.27 in)
Inside Heat Flux	1.57 MW/M^2 (498,900 BTU/hr ft^2)
Mass Flux	2712 Kg/M^2-s (2×10^6 lbm/hr ft^2)
Flux Distribution	Heated 180^o Circumferentially (Approximate cosine shading)

Existing C-E standards for CHF and film boiling are not applicable to the above ranges. In addition to a correlation for film boiling, a correlation for predicting the critical quality (X_c) is also needed to establish the point of minimum film coefficient (X_{min}).

2.2.1.1 Correlation for X_c

Results of the review indicated that the Thompson-MacBeth correlation would be satisfactory for this analysis. It represents a large amount of world data in this pressure range. The MacBeth correlation is in two parts: one for low velocity, and another for high velocity. The transition from low to high velocity was determined as $G \geq 406.8$ Kg/M^2-S (0.3×10^6 lbm/hr ft^2) for the high velocity range. A description of this correlation is given in Appendix A.

The high mass flow correlation is shown graphically in Figure 2.1, for a range of CHF and mass flow rates

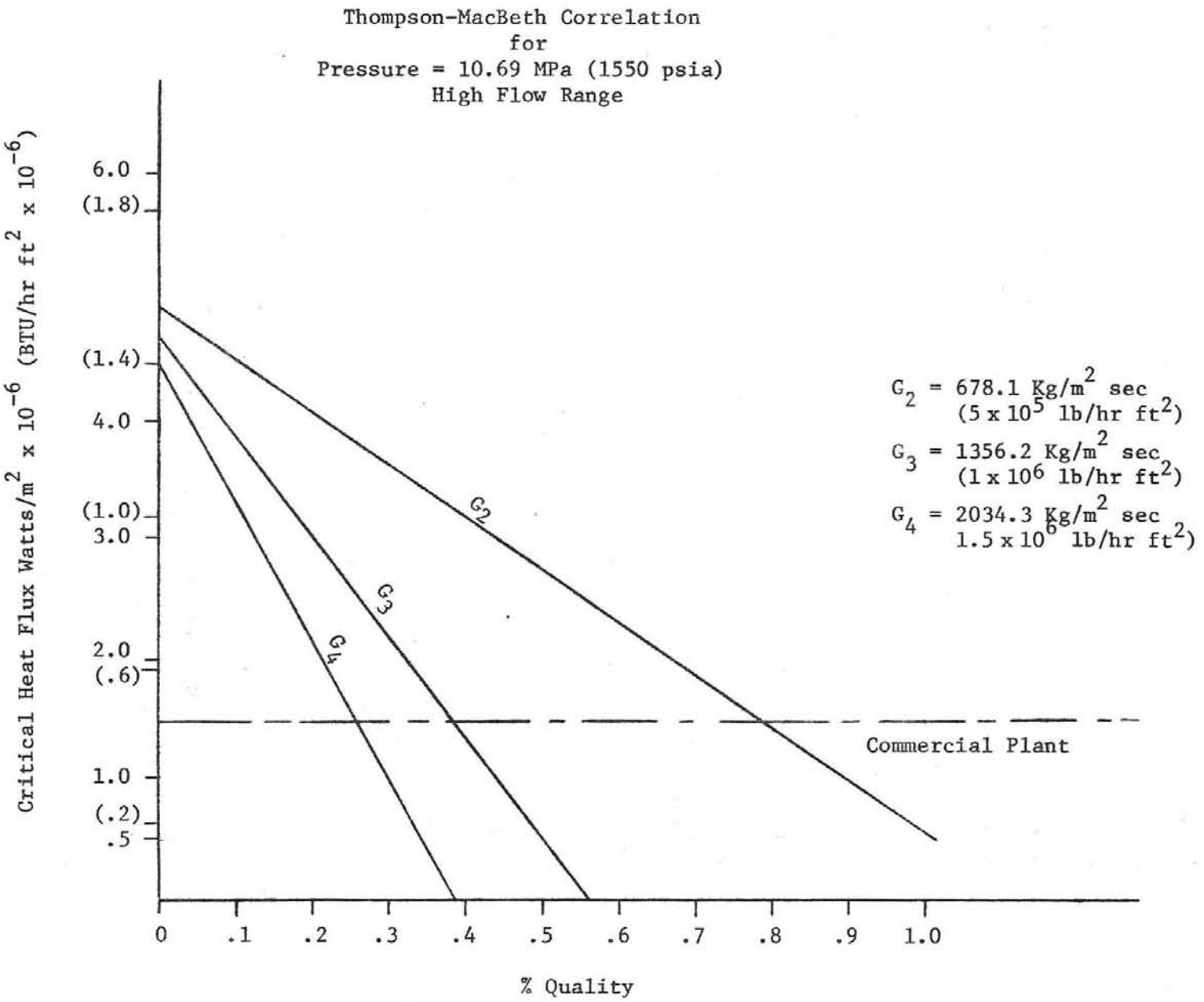
Thompson-MacBeth Correlation
for
Pressure = 10.69 MPa (1550 psia)
High Flow Range
Critical Heat Flux Watts/m² x 10⁻⁶ (BTU/hr ft² x 10⁻⁶)
6.0
(1.8)
(1.4)
4.0
(1.0)
3.0
2.0
(.6)
1.0
(.2)
.5
G2
G3
G4
Commercial Plant
0
.1
.2
.3
.4
.5
.6
.7
.8
.9
1.0
% Quality
G2 = 678.1 Kg/m² sec
(5 x 10⁵ lb/hr ft²)
G3 = 1356.2 Kg/m² sec
(1 x 10⁶ lb/hr ft²)
G4 = 2034.3 Kg/m² sec
1.5 x 10⁶ lb/hr ft²)

FIGURE 2.1

encountered in the solar receiver design. Figure 2.1 indicates the "inverse mass flow effect" in which an increase in mass flux results in a lower critical quality, q/A, being constant. This is the reverse of the trend at higher pressures.

The Thompson-MacBeth correlation is limited to a maximum pressure of 13.79 MPa, (2000 psia). The "change-over" to inverse mass flow effect is seen in other data at about the 13.79 MPa (2000 psia) pressure level. Constants in this correlation are listed for discrete pressure levels. For this analysis, these constants are interpolated lineraly between 10.68 MPa (1550 psia) and 13.79 MPa (2000 psia). Figure 2.2 shows a typical low mass flow correlation, used for pilot plant analysis.

2.2.1.2 Correlation for h_{min} and X_{hmin}

Having a method of predicting the critical quality above, it is now possible to predict the point of minimum film boiling, the minimum coefficient (h_{min}) and the coefficients existing from X_{hmin} to full saturated steam. Of the various film boiling correlations reviewed, practically all are variations on the Dittus-Boelter equation:

$$Nu = .023\ R_e^{.8}\ Pr^{1/3}$$

The correlation selected was a modified version of the Groeneveld correlation shown in Appendix B. It assumes equilibrium between the liquid and vapor phases.

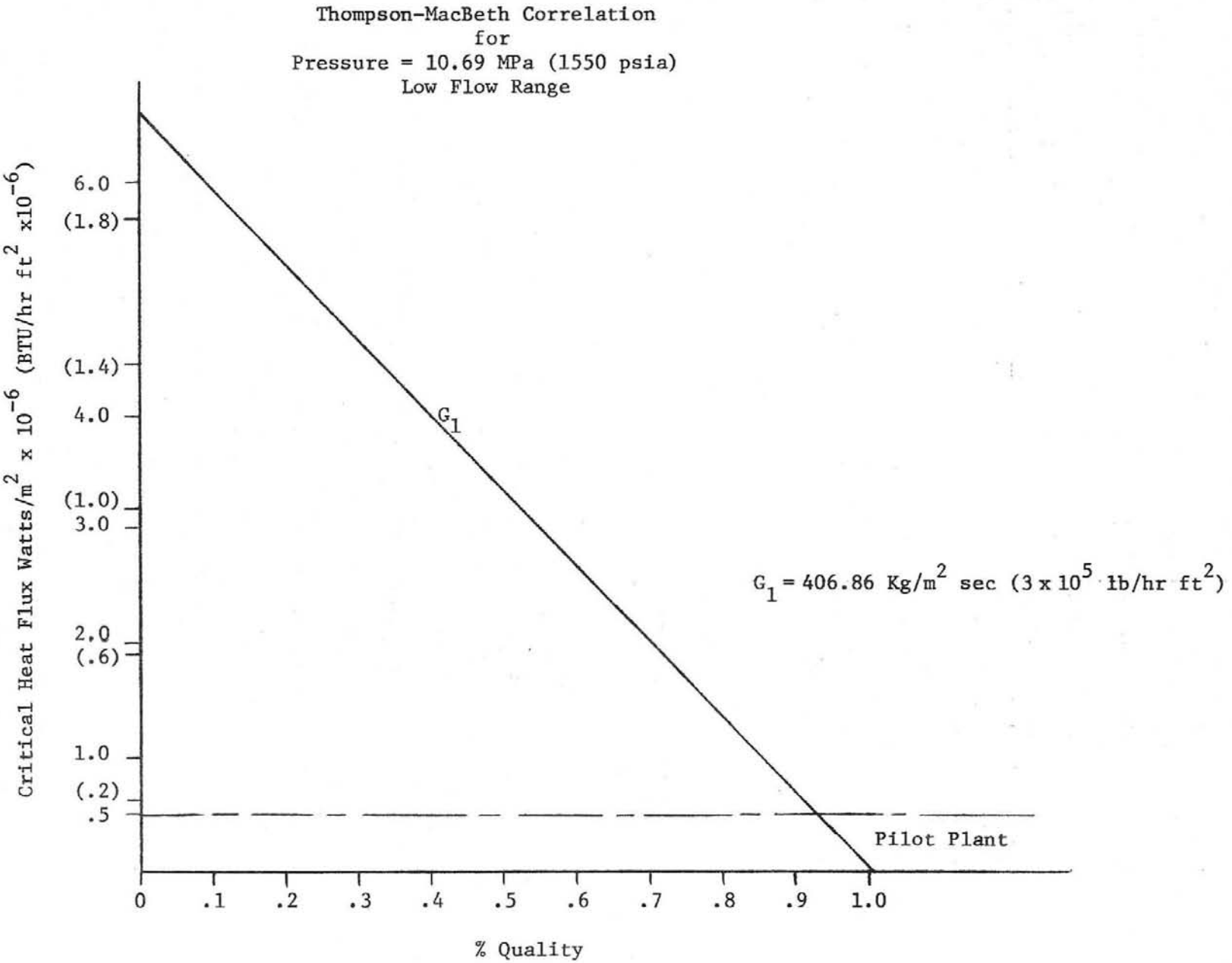
Thompson-MacBeth Correlation
for
Pressure = 10.69 MPa (1550 psia)
Low Flow Range
Critical Heat Flux Watts/m^2 x 10^{-6} (BTU/hr ft^2 x10^{-6})
6.0
(1.8)
(1.4)
4.0
(1.0)
3.0
2.0
(.6)
1.0
(.2)
.5
G_1
G_1 = 406.86 Kg/m^2 sec (3 x 10^5 lb/hr ft^2)
Pilot Plant
0
.1
.2
.3
.4
.5
.6
.7
.8
.9
1.0
% Quality

FIGURE 2.2

Values of h calculated for the commercial plant design conditions for the North panel are plotted on Figure 2.3. The value of h, at the calculated minimum film quality ($X_{h_{min}}$), is the minimum coefficient (h_{min}). Note that the Pr_w, evaluated at the wall temperature, requires an iterative procedure to determine the exact value. A $Pr_w = 1.0$ was assumed in Figure 2.3

This correlation is applicable for the following conditions:

Geometry	Tube
Flow Direction	Vertical and Horizontal
D, 5 to 25.4 mm	(0.2 to 1.0 in)
P, 6.89 to 21.5 MPa	(1000 to 3124 psia)
G, 284 to 4069 Kg/m^2-S	($.21 \times 10^6$ to 3×10^6 lbm/ft^2)
X, % wt.	10 to 90
Ø, .11 to 2 MW/m^2	(35×10^3 to 650×10^3 BTU/hr ft^2)
R_e Factor	6.6×10^4 to 1.3×10^6
Pr_w	.88 to 2.21
Y	.706 to .976

Accuracy of this correlation is $\pm$ 30% against experimental values, the majority of which were obtained with uniform 360^o circumferential heating. The effects of nonuniform 180^o heating on the solar boiler will be discussed in a later section.

2.2.2.2 Review of Experimental Heat Transfer Data as Reported by Rocketdyne/MDAC

Certain experiments were conducted by Rocketdyne during

Inside Film Coefficient vs. Quality
Using the Groeneveld Correlation
Commercial Plant
North Panel

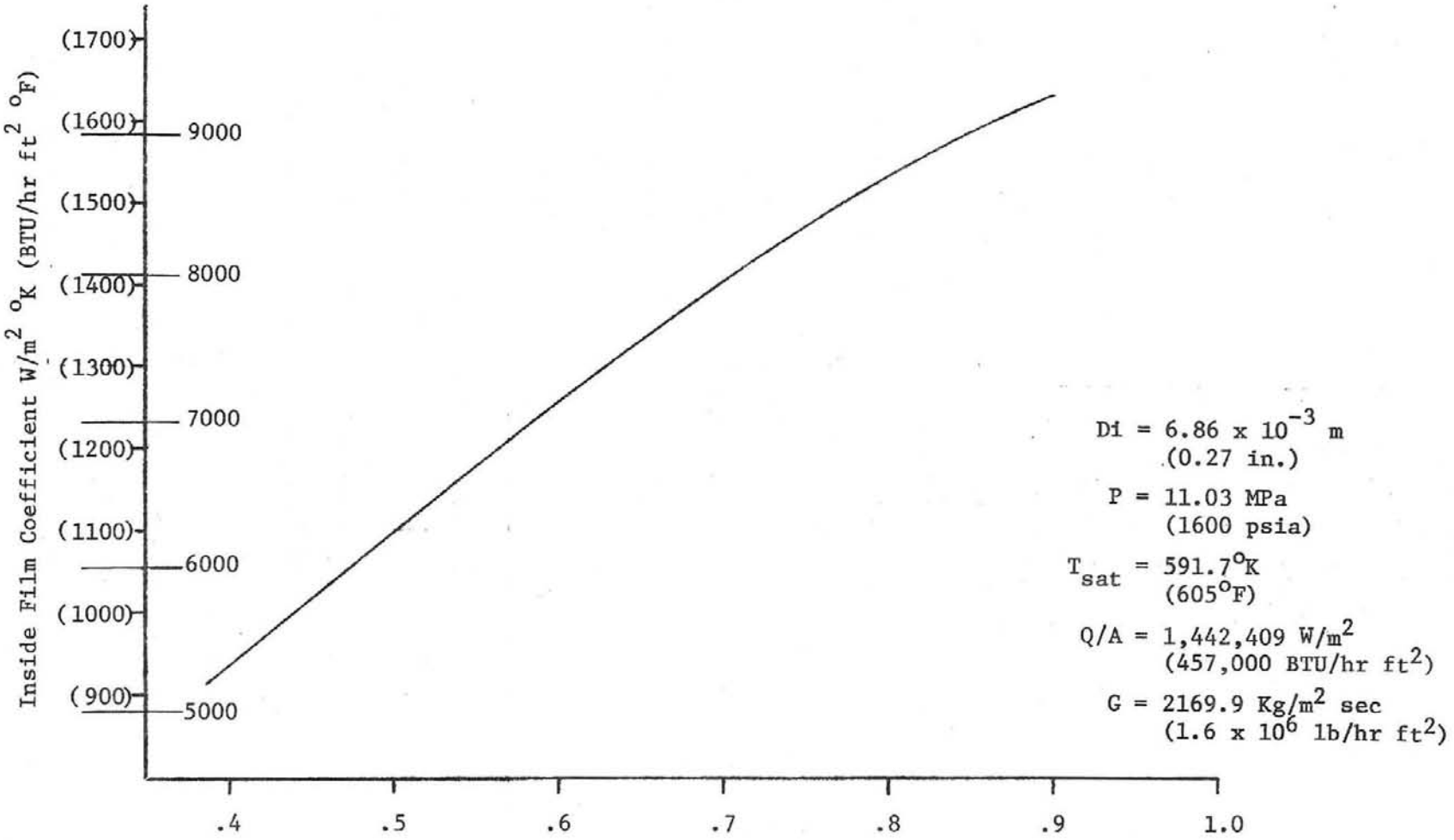

FIGURE 2.3

the solar receiver design development. These tests were reported in References 1 and 3.

Data as reported above, in tabular form and in the form of plots of tube temperatures, were analyzed with the objective of determining the minimum film boiling coefficient (h_{min}) and comparing these values with those calculated by the Groeneveld correlation, and with the correlation recommended by Rocketdyne. The tests analyzed are given in Table 2.1. These tests came from 3 sources: 1) electric resistance heated SS tubing, 2) 1- and 5-tube panels heated with radiant heaters (horizontal), and 3) SRE tests of 5-tube and 70-tube actual size panels mounted vertically and heated with radiant heaters.

Input data was taken from tables and graphs of measured tube and fluid temperatures as presented in Reference 1. Values of h_{min} were back-calculated using heat flux values determined to exist at the apparent location of the minimum heat transfer coefficient. Heat absorption to the fluid was calculated based on increase in fluid enthalpy. Heat flux locally was prorated according to the reported axial distribution of heater power for each test, in terms of power normalized against the average. Inside tube metal temperatures were calculated assuming radial flow based on measured outside crown temperatures, for the local calculated inside heat flux (radial flow). Film coefficient from the test data was then determined by:

TABLE 2.1

Rocketdyne Test Data

	Inputs						Measured		Predicted by Groeneveld				Predicted by Dittus-Boelter	
No.	O.D./I.D.	Tube L ft.	Tube K	P_{psia}	$q/A_i x 10^{-3}$	$Gx10^{-6}$	Tube O.D. Temp. °F	h_{min}	X_{DNB}	$X_{F.B.}$	Tube O.D. Temp.	h_{min}	Tube O.D. Temp.	h_{min}
Rocketdyne Base Tests, 360° Resistance Heated (Single Tube)														
	.25/.12	15.75	150	1750	244	1.55	1100	594	.27	.36	965	906	760	3809
	.25/.12	15.75	150	2000	244	1.55	1022	777	.28	.38	997	843	774	4103
	.25/.12	15.75	150	2400	244	1.55	824	2711	.80	.92	861	1920	787	5245
Horizontal Radiant Heated Tests, 180°, Single Tube Tests														
11	.375/.305	65	150	1900	149.8	.59	820	942	.55	.64	980	467	754	1580
12	.375/.305	65	150	1515	175.8	.56	----------				No Film Boiling		----------	
13	.375/.305	65	150	1590	210	.75	680	6774	.55	.64	1023	558	779	1586
14	.375/.305	65	150	----------			Two Phase Inlet - Most of Tube SH						----------	
20	.375/.305	65	150	1965	145.2	.59	850	789	.56	.66	968	475	774	1580
21	.375/.305	65	150	2250	239	.56	1000	683	.48	.59	1204	476	836	1792
22	.375/.305	65	150	1100	166.3	.62	825	618	.91	.99	960	451	757	1001
23	.375/.305	65	150	1775	143.3	.62	890	600	.58	.67	957	465	747	1465
SRE Tests, 5-Tube Panel Test No. 6-15, 70-Tube 12-Max.														
6	.5/.27	56	150	1500	15.36	.054	630	614	1.0	1.0	1095	31.5	691	181
15	.5/.27	56	150	1500	163.2	.254	1030	474	.88	.96	1437	218	934	663
12	.5/.27	56	150	1395	96.0	.04	1220	165	.93	1.0	3051	40	1181	181
13	.5/.27	56	150	1400	124.8	.043	1100	281	.91	.99	3674	41.5	1356	181
14	.5/.27	56	150	1485	134.4	.053	1070	336	.90	.98	3879	41.9	1415	181
16	.5/.27	56	150	1565	144.0	.043	1060	378	.89	.97	4105	42.2	1473	181
17	.5/.27	56	150	1550	124.8	.041	--	--	.91	.99	3674	41.5	1356	181
Max.	.5/.27	56	150	1550	182.4	.40	1080	480	.87	.95	1221	349	889	954
Extended SRE Tests														
1	.5/.27	56	150	1543	115.2	.062	1000	342	.92	1.0	2933	50.7	1199	214
2	.5/.27	56	150	1543	110.4	.062	975	352	.92	1.0	2844	50.5	1175	214
3	.5/.27	56	150	1543	115.2	.061	910	468	.92	1.0	2933	50.7	1199	214
4	.5/.27	56	150	1543	115.2	.058	965	383	.92	1.0	2933	50.7	1199	214
5	.5/.27	56	150	1543	124.8	.063	920	497	.91	.99	3099	51.3	1250	214
6	.5/.27	56	150	1543	144.0	.063	870	754	.89	.97	3455	52.2	1350	214

$$h = \frac{(q/A)i}{\Delta t_{film}}$$

These values are therefore the "measured" values of h_{min}.

Using the same test data inputs, an h_{min} was calculated using both the Groeneveld and Dittus-Boelter (MDAC recommended correlation). Note that the mass flux for the SRE tests falls below the lower limit for the Groeneveld correlation, thus invalidating this correlation for SRE tests.

A comparison of the calculated values and the measured values is presented in Figure 2.4 and Figure 2.5. Figure 2.4 presents the results of comparing the 360^{o} uniform heated data. The 180^{o}, one-side heated values are given in Figure 2.5.

For the 360^{o} heated data, Figure 2.4, the Groeneveld equation predicts the coefficient better than the Dittus-Boelter equation, but only one point lies within the $\pm$ 30% error band. Dittus-Boelter predicts coefficients much higher than measured.

For the 180^{o} heated data at the higher mass flux, the Dittus-Boelter predicts high coefficients, and the Groeneveld correlation predicts low values. The data mostly lie outside the $\pm$ 30% error band. In terms of metal temperatures, the Groeneveld correlation is conservative while the Dittus-Boelter is optimistic.

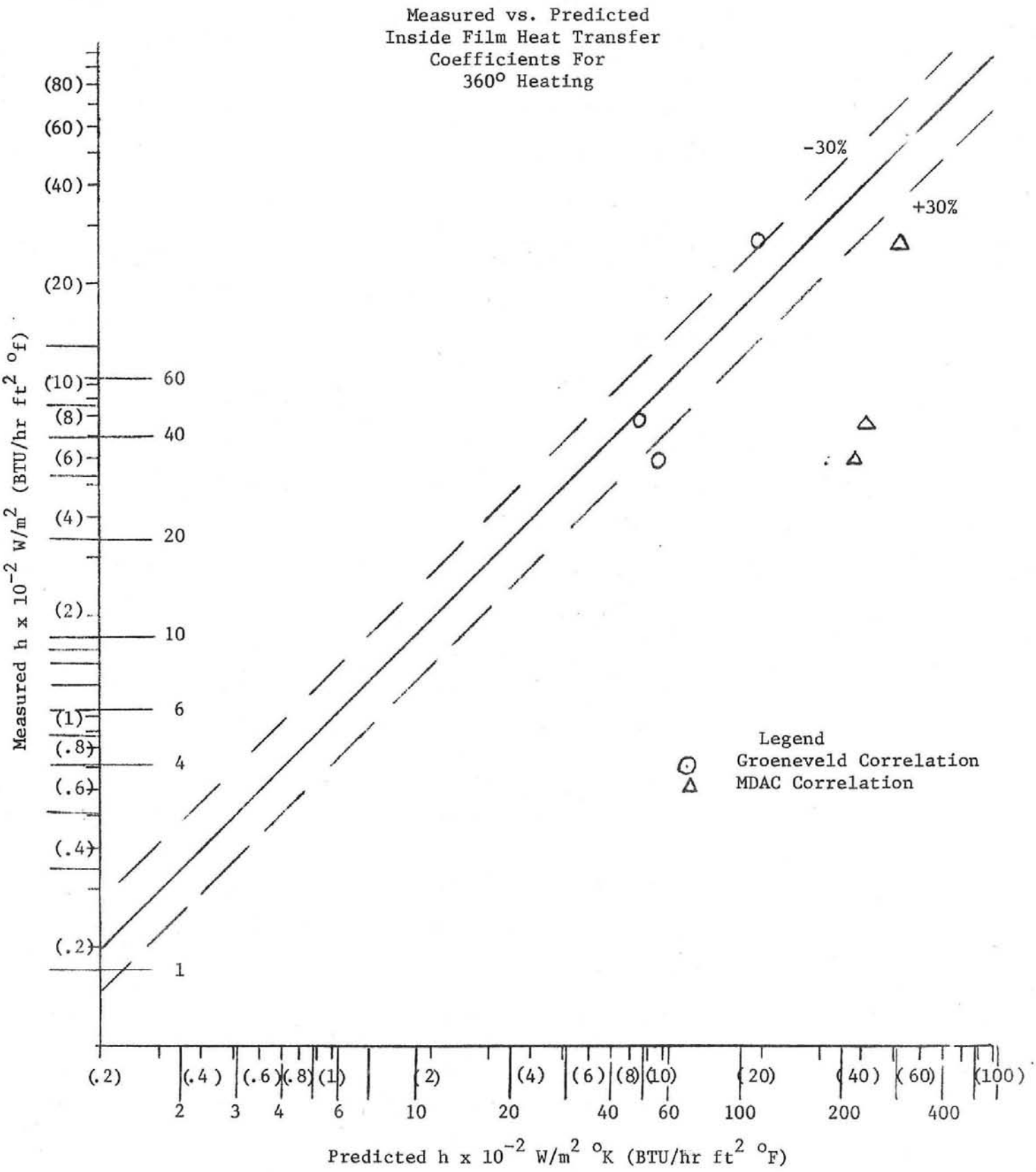
Measured vs. Predicted
Inside Film Heat Transfer
Coefficients For
360° Heating
-30%
+30%
Legend
Groeneveld Correlation
MDAC Correlation
Measured h x 10^-2 W/m^2 (BTU/hr ft^2 °f)
Predicted h x 10^-2 W/m^2 °K (BTU/hr ft^2 °F)
(80)
(60)
(40)
(20)
(10)
(8)
(6)
(4)
(2)
(1)
(.8)
(.6)
(.4)
(.2)
60
40
20
10
6
4
1
(.2)
(.4)
(.6)
(.8)
(1)
(2)
(4)
(6)
(8)
(10)
(20)
(40)
(60)
(100)
2
3
4
6
10
20
40
60
100
200
400

FIGURE 2.4

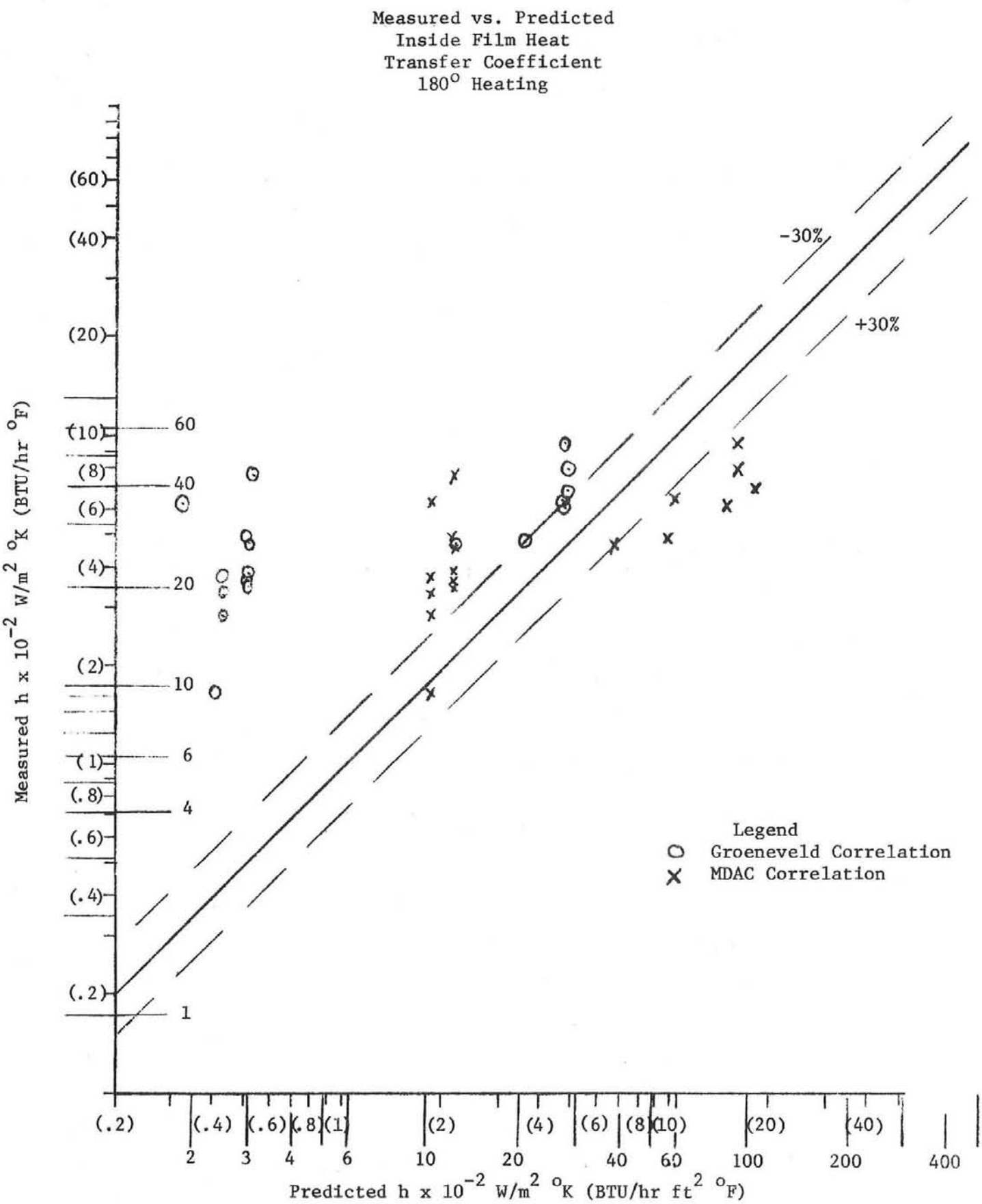
Measured vs. Predicted
Inside Film Heat
Transfer Coefficient
180° Heating
-30%
+30%
Legend
Groeneveld Correlation
MDAC Correlation
Measured h x 10^-2 W/m^2 °K (BTU/hr °F)
Predicted h x 10^-2 W/m^2 °K (BTU/hr ft^2 °F)
(60)
(40)
(20)
(10)
(8)
(6)
(4)
(2)
(1)
(.8)
(.6)
(.4)
(.2)
60
40
20
10
6
4
1
(.2)
(.4)
(.6)
(.8)
(1)
(2)
(4)
(6)
(8)
(10)
(20)
(40)
2
3
4
6
10
20
40
60
100
200
400

FIGURE 2.5

In the SRE tests, the mass flux was very low, 67.8 Kg/m^2 S ($.05 \times 10^6$ lbm/hr ft^2). The Groeneveld correlation is not valid below 271 Kg/m^2 s ($.2 \times 10^6$ lbm/hr ft^2). The Dittus-Boelter equation now predicts low coefficients for these low G rates. This analysis points out the wide variation existing between these two correlation methods. It is recommended that further testing be carried out, with higher mass flux and heat flux. If possible, the range of variables for both the pilot plant and the commercial plant should be tested with enough accuracy to determine the CHF, transition, and film boiling performance.

2.2.3 Thermal-Hydraulic Analysis Program

2.2.3.1 General Description

The computer program used to determine the thermal-hydraulic performance of an MDAC design solar panel employs a step-wise integrative calculational method. That is, the program performs an energy balance on a small element of the fluid, calculates heat absorption, the increase in enthalpy at the element outlet, the tube metal temperature and the fluid quality. This then becomes the input for the next element.

The program also calculates the inside film coefficients for each element, along with the pressure drop, using the homogeneous model, in the two-phase region. The homogeneous model for ΔP calculation was selected because of its simplicity. It can be shown, that in the case where small increments of flow are considered, the

homogeneous model agrees with the Martinelli-Nelson two-phase multiplier approach at the high mass flows. At lower flows, the agreement is within 20%.

The program is designed mainly for the axisymmetrical heat flux case, with a correction factor to account for the 2-D heat flow to the rear of the tube.

The program incorporates the flexibility to allow the user to calculate:

1. Preheat Panel Performance
2. Boiler Panel Performance
    a. With variable outlet conditions.
    b. With specified outlet conditions.
3. Multiples of the above.

Such flexibility allows calculations of design and off-design parameters. A description of the program is given in Appendix C.

2.2.3.2 Receiver Performance Results

Program output for the pilot plant and commercial plant maximum heat flux cases (N panels) are shown in Appendix C.

Tables 2.2 and 2.3 show the performance distribution data for the pilot and the commercial plant receivers, respectively. Figure 2.6 is a key plan, identifying the location of the panels by number. The receivers are symmetrical about the N-S axis. Boiler panel Nos. 1-9 were analyzed for each design. Panels 10, 11, and 12

TABLE 2.2

Predicted Performance (Rated Steam)
Pilot Plant

Full Power

Panel No.	Solar Flux MW/m^2 ($BTU/hr\ ft^2$)	Flow Kg/s (lb/hr)	Δ P KPa (psi)	Stability Index	Efficiency
1	.31 (98000)	1.06 (8419)	111 (16.06)	1.294	.89
3	.28 (87175)	.936 (7437)	94.7 (13.73)	1.198	.88
5	.25 (79250)	.843 (6697)	83.9 (12.18)	1.149	.88
7	.18 (57060)	.59 (4712)	59.6 (8.64)	1.016	.86
9	.13 (41210)	.41 (3265)	46.4 (6.73)	0.849	.82

Half Load

1	.15 (49000)	.5 (3970)	52.5 (7.61)	0.953	.84
3	.14 (43587)	.439 (3487)	48 (6.97)	0.885	.83
5	.13 (39625)	.39 (3114)	45.3 (6.57)	0.835	.81
7	.09 (28530)	.26 (2095)	38.9 (5.64)	0.711	.76
9	.07 (20605)	.17 (1372)	35.3 (5.13)	0.559	.69

Min. Control Load

1	.06 (19600)	.15 (1194)	33.6 (4.87)	0.532	.63
3	.055 (17435)	.147 (1170)	35.6 (5.16)	0.615	.70
5	.05 (15850)	.088 (697.7)	28.9 (4.20)	0.461	.46
7	.036 (11412)	*	*	*	*
9	.026 (8242)	*	*	*	*

*Not capable of producing rated steam.

TABLE 2.3

Predicted Performance (Rated Steam)
Commercial Plant

Full Power

Panel No.	Solar Flux MW/m^2 ($BTU/hr\ ft^2$)	Flow Kg/s (lb/hr)	ΔP MPa (psi)	Stability Index	Efficiency
1	.85 (269500)	15 (119100)	2.06 (299)	0.526	.91
3	.76 (239600)	13.4 (106300)	1.67 (242)	0.650	.91
5	.686 (217460)	12.1 (96330)	1.41 (204)	0.654	.91
7	.52 (164840)	9.1 (72600)	.89 (129)	0.477	.91
9	.37 (117600)	6.4 (51180)	.54 (78)	0.918	.90

Half Load

1	.425 (134750)	7.4 (58890)	.65 (94)	0.720	.90
3	.38 (119800)	6.6 (52300)	.55 (80)	0.711	.90
5	.34 (108730)	5.9 (47250)	.48 (70)	0.711	.89
7	.26 (82420)	4.4 (35170)	.34 (50)	0.736	.88
9	.185 (58800)	3.1 (24380)	.24 (35)	0.785	.85

Min. Control Load

1	.17 (53900)	2.8 (22200)	.22 (32)	1.155	.85
3	.15 (47920)	2.4 (19360)	.19 (27)	1.260	.83
5	.14 (43492)	2.2 (17300)	.17 (24)	1.038	.82
7	.104 (32968)	1.6 (12420)	.12 (17)	1.010	.78
9	.074 (23520)	1.0 (7942)	.09 (13)	0.692	.69

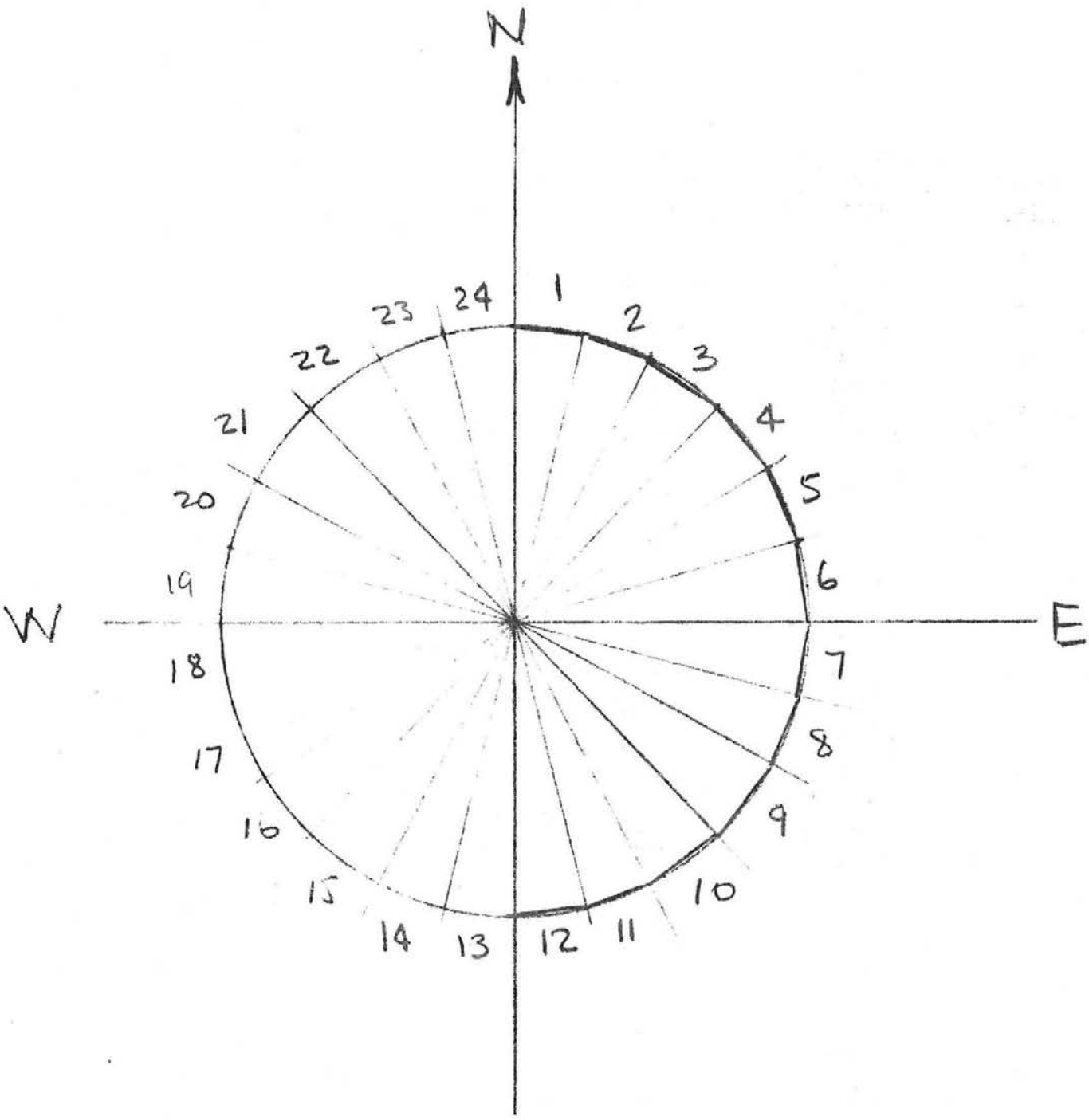

KEY PLAN

FIGURE 2.6

are preheat panels in the pilot palnt. Panels 11 and 12 are preheat penals in the commercial plant. The incident flux used was as given in Reference 1 for the panels shown in the pilot plant. Only the north panel flux was given directly for the commercial plant. The others were back-calculated from heat absorption data given in Reference 1. Three loads were selected to give a distribution of panel performance. In addition to the full load at maximum incident flux, half-load and a minimum load were picked. The minimum control load for producing rated steam 515.6°C (960°F) was set at 20% of full load. This proved to be too low for the pilot plant south-east panels to make rated steam (Table 2.2).

For these runs the bulk fluid inlet temperature was held constant at 260°C (500°F) for the pilot plant and 293°C (560°F) for the commercial plant. This was determined by running the preheater panels for full load in each case, and using the output as boiler input. In practice, the input temperature to the boiler panels would decrease with load. In this respect, the minimum control load may be too low for some of the panels indicated in Table 2.2. The heat absorption may not be enough to produce 515.6°C (960°F) final steam temperature with lower feedwater inlet temperatures. Since the thermal program does not iterate for a specified outlet pressure, input pressure is determined approximately, and the outlet

pressure is allowed to vary with flow rate. The program iterates flow to produce 515.6°C (960°F) final temperature ± 2.78°C (± 5°F).

The ΔP reported in Tables 2.2 and 2.3 is the sum of the friction, acceleration, and gravity components for the tubes only. These values do not include entrance and exit losses.

The panel efficiency is defined as the ratio of absorbed heat (W · ΔH) divided by the integrated incident heat flux profiles. This is a function of the back radiation and convection losses which are in turn dependent upon the tube metal temperature. This accounts for the greater losses, percentage-wise in the lightly-loaded panels. The loss model is the same for all cases. It can be seen that in cases of lightly loaded panels the superheater portion may actually experience a negative absorbed heat flux, resulting in a loss of fluid temperature in the top of the panels. In some cases, final temperature, 515.6°C (960°F), cannot be obtained, even with reduced flow. Such is the case with the pilot plant Panels 7 and 9 at minimum control load. As flow is reduced to increase enthalpy, the metal temperature increases, increasing the losses, which are then more than the incident heat flux.

Figures 2.7 and 2.8 show plots of the incident and absorbed flux profiles for the pilot and commercial plant's north panel. Figure 2.9 shows a minimum load for the pilot plant

Pilot Plant
North Panel
Absorbed and Incident Heat Flux

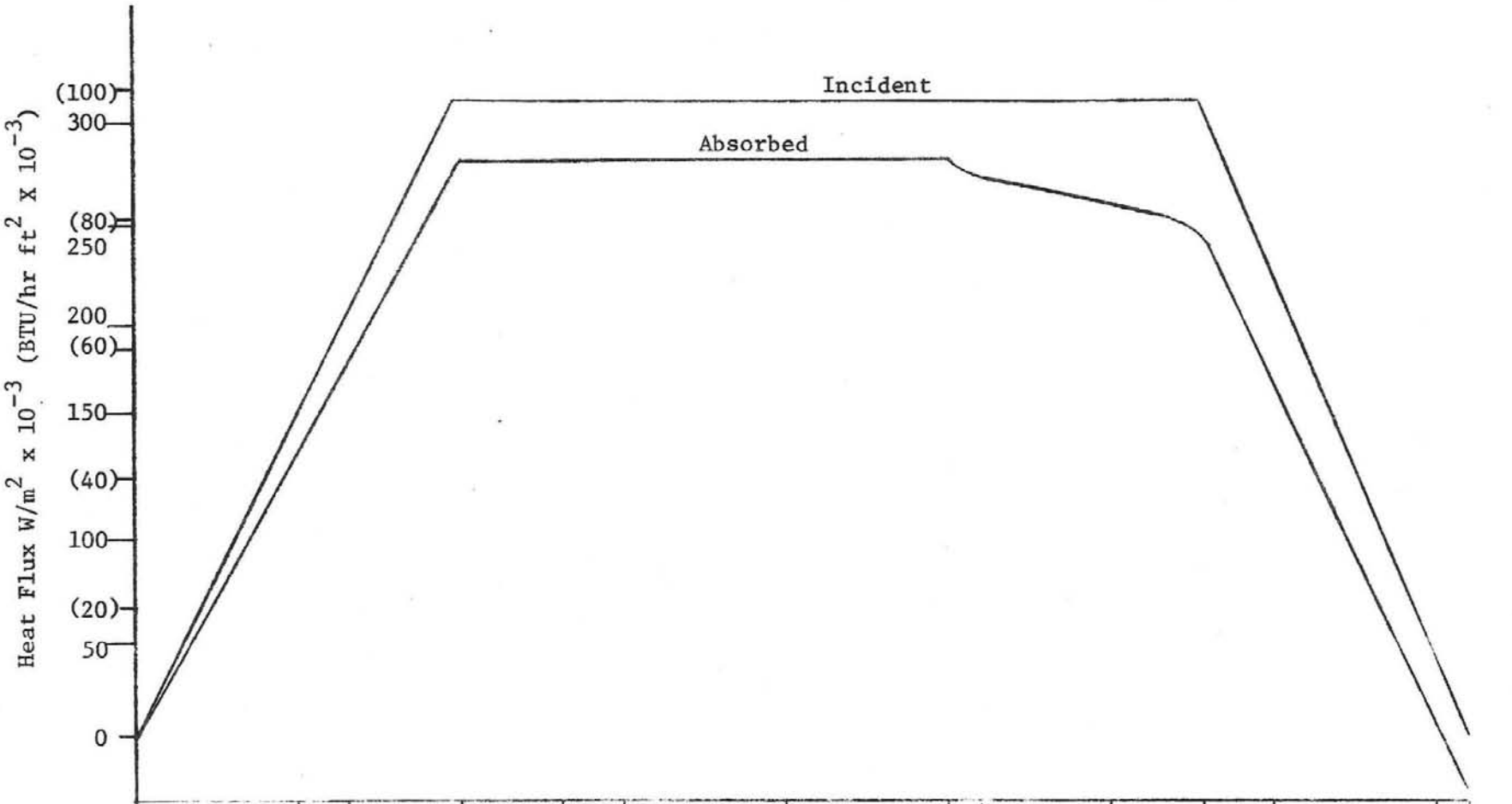

FIGURE 2.7

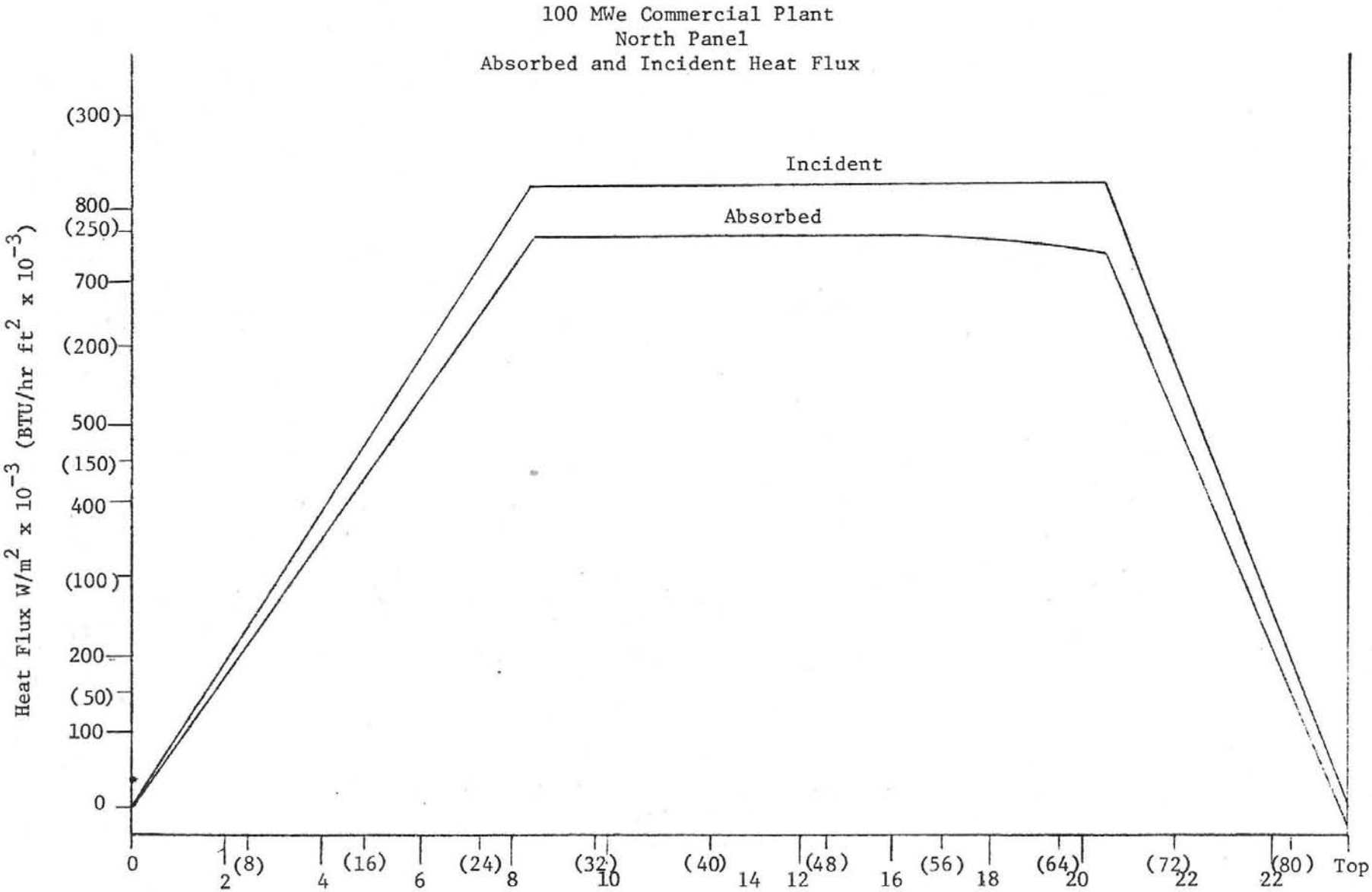
100 MWe Commercial Plant
North Panel
Absorbed and Incident Heat Flux
Incident
Absorbed
Heat Flux W/m^2 x 10^{-3} (BTU/hr ft^2 x 10^{-3})
(300)
800
(250)
700
(200)
500
(150)
400
(100)
200
(50)
100
0
0
2 (8)
4 (16)
6 (24)
8 (32)
10 (40)
14 12 (48)
16 (56)
18 (64)
20 (72)
22 22 (80) Top
Tube Length m (ft)

FIGURE 2.8

Pilot Plant Panel 7
Absorbed and Incident Heat Flux

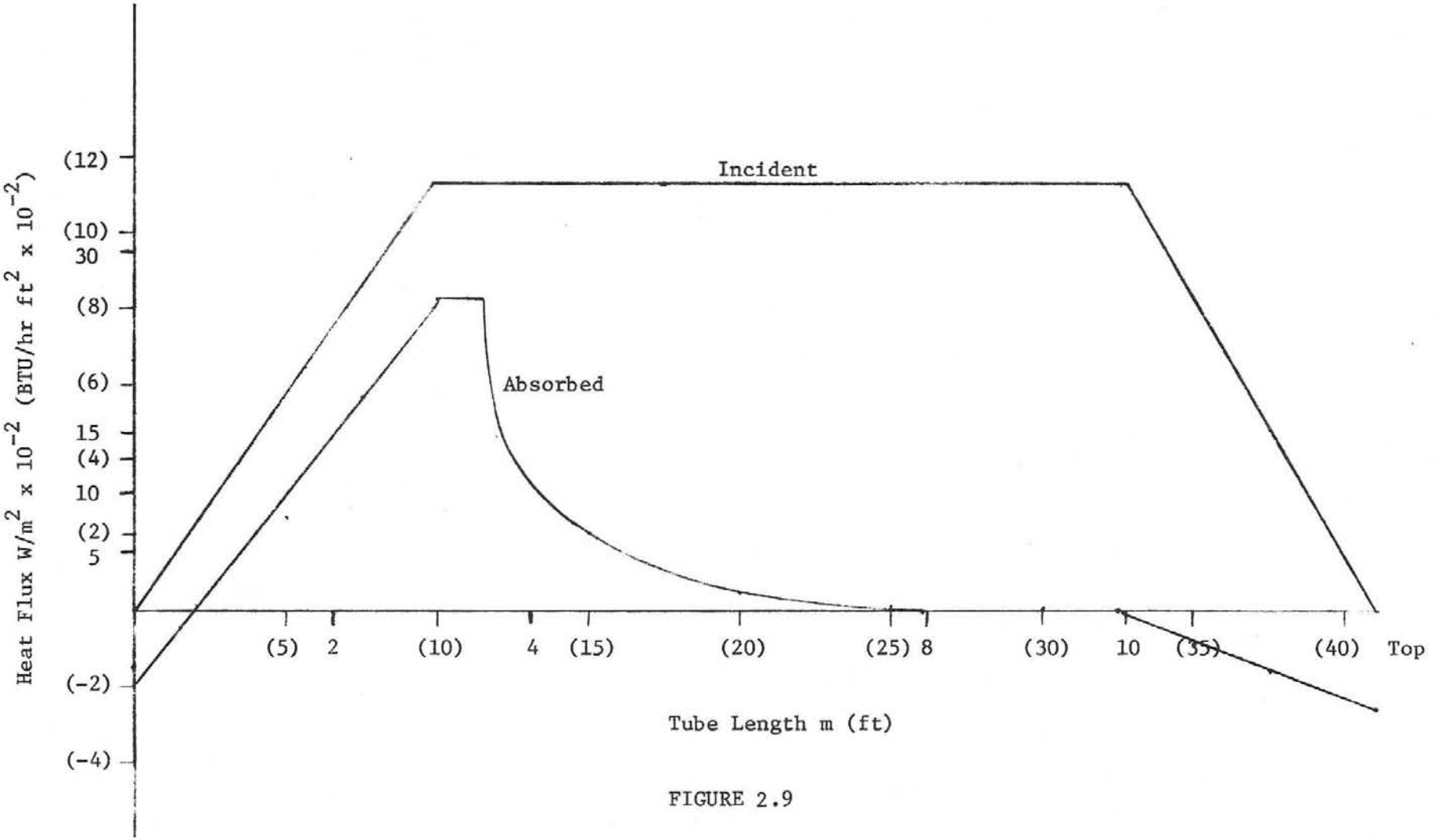

FIGURE 2.9

where the absorbed heat flux is largely negative in the superheater region.

2.2.3.3 Temperature Profiles

Figure 2.10 shows the temperature profile for the commercial plant N-panel. The tube temperatures are crown temperatures from the thermal analysis program. These are corrected for 2-D heat flow to the rear of the tube. As indicated, the CHF occurs at 17% quality. This puts the minimum film boiling coefficient at 27% quality. The portion of the curve in dashed line represents areas where there is uncertainty, or discrepancy in the correlations used. The peak temperature of 593.3°C (1100°F) at 9.14 m (30 feet) represents a point calculated from the Groeneveld correlation discussed previously. The distance from CHF to X_{hmin} is the transition boiling region, and is subject to oscillating temperature. The stable film boiling point is reached at 9.14 m (30 feet). Beyond the X_{hmin}, the Groeneveld correlation should predict metal temperature up to x = 1.0. However, there is a discontinuity when switching to the single phase correlation for the superheater. Until this is resolved by experiment, this region was smoothed to the single phase correlation at X = 1.0. The highest metal temperature occurs in the superheater, just before the heat flux curve starts to decrease.

Actual calculated temperatures are listed in Appendix C, on the program output sheets. The significant fact about

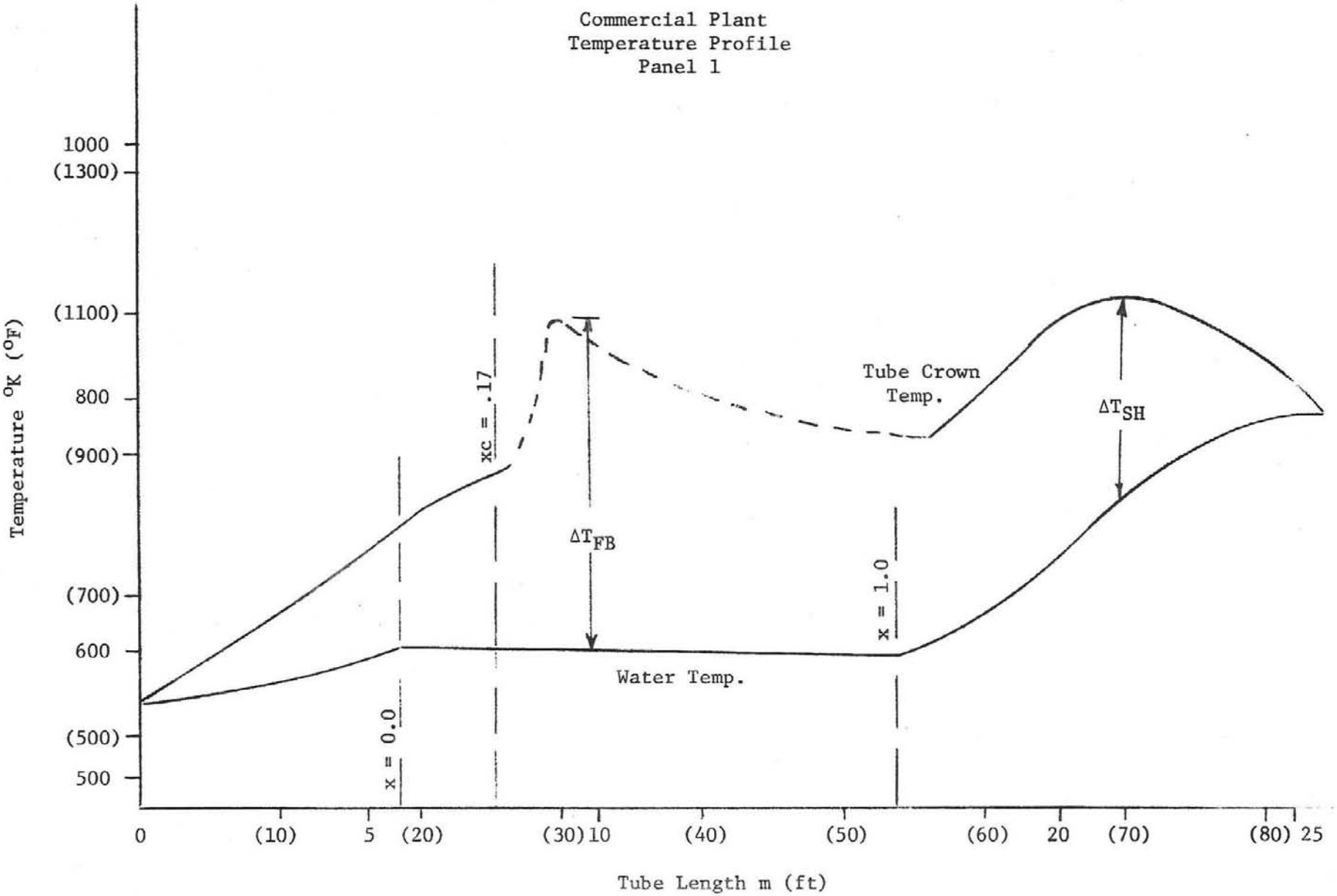
Commercial Plant
Temperature Profile
Panel 1
1000
(1300)
(1100)
800
(900)
(700)
600
(500)
500
Temperature °K (°F)
xc = .17
x = 0.0
x = 1.0
ΔT_FB
ΔT_SH
Tube Crown Temp.
Water Temp.
0
(10)
5
(20)
(30)
10
(40)
(50)
(60)
20
(70)
(80)
25
Tube Length m (ft)

FIGURE 2.10

these temperature profiles is the difference between the tube crown temperature and the bulk fluid temperature. In 2-D heat flow, the rear of the tube is at a temperature close to the bulk temperature. The front-to-back ΔT therefore represents a potential thermal stress condition if the panel is restrained in a certain way. The magnitude of this ΔT is the cause of the fatigue stress problem in the commercial plant. These temperature profiles are indications of the relative magnitude of this problem. The high ΔT is created by a combination of high heat flux, low film coefficient, tube thickness, and poor metal conductivity. There are two critical locations. One is at film boiling where a high ΔT exists. The other is where the superheater metal is at a higher average temperature, with less favorable metal properties.

Figure 2.11 shows the temperature profile for the No. 9 commercial plant panel for the full load condition. The lower flux results in a crown temperature of 471°C (880°F) while the CHF point has moved up the panel to approximately 10.67 m (35 feet).

Figures 2.12 and 2.13 show temperature profiles predicted for the pilot plant. The CHF occurs at vey high quality and there is no film boiling point outside the single phase superheat region. Maximum temperatures at the superheater location are 560°C (1040°F) and 526.7°C

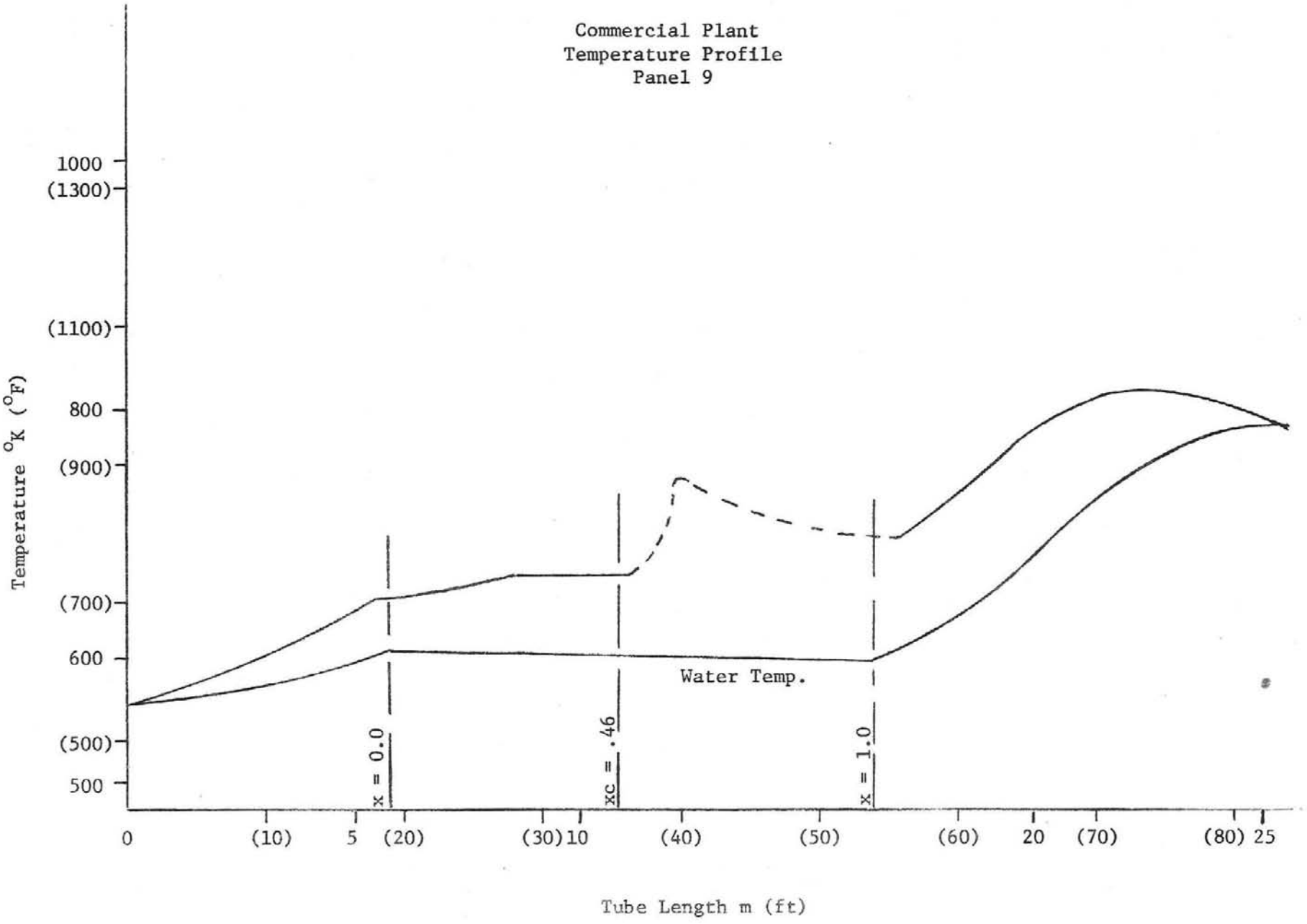
Commercial Plant
Temperature Profile
Panel 9
1000
(1300)
(1100)
800
(900)
(700)
600
(500)
500
Temperature °K (°F)
Water Temp.
x = 0.0
xc = .46
x = 1.0
0
(10)
5
(20)
(30)
10
(40)
(50)
(60)
20
(70)
(80)
25
Tube Length m (ft)

FIGURE 2.11

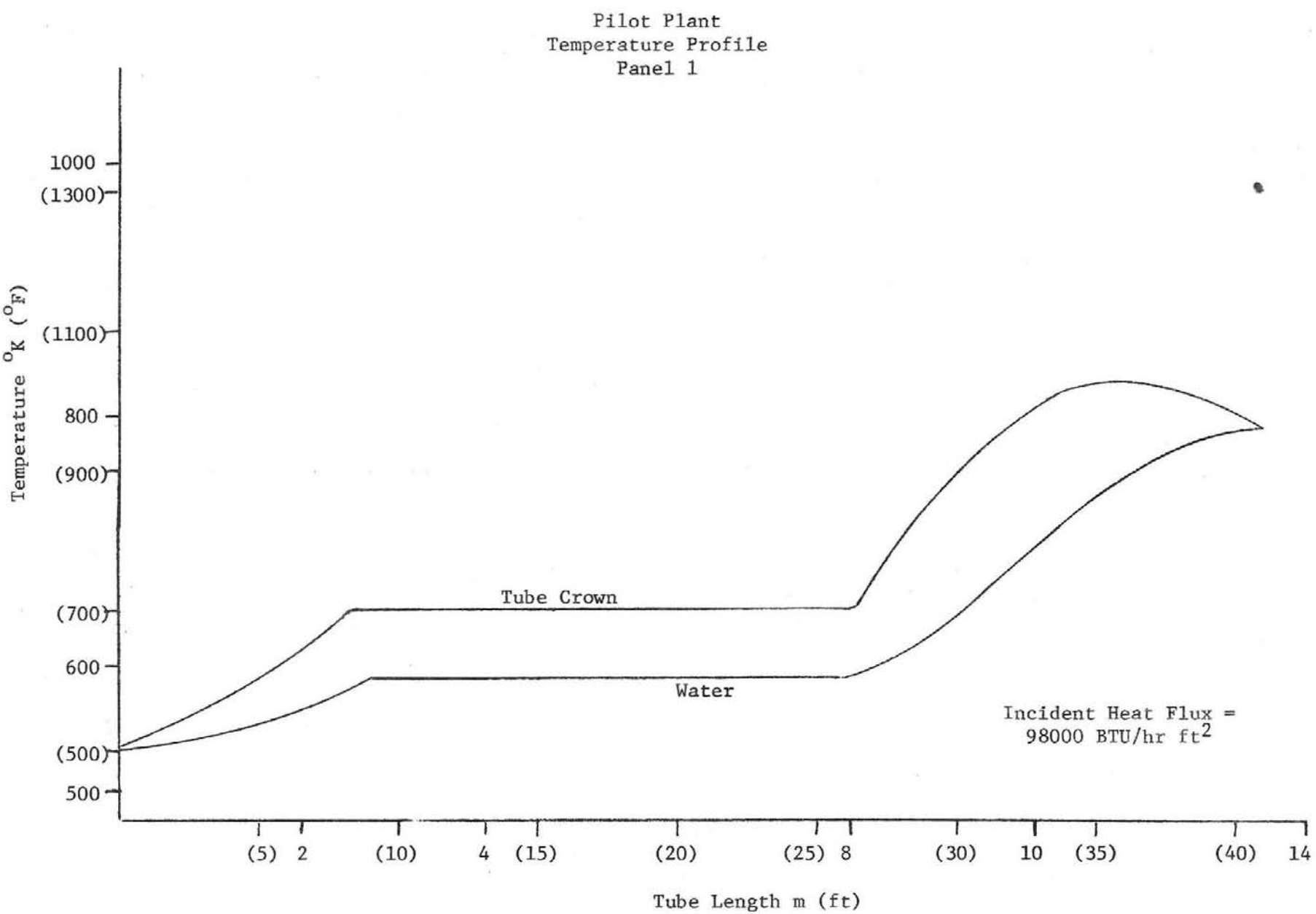
Pilot Plant
Temperature Profile
Panel 1
1000
(1300)
(1100)
800
(900)
(700)
600
(500)
500
Temperature °K (°F)
Tube Crown
Water
Incident Heat Flux =
98000 BTU/hr ft2
(5) 2
(10) 4
(15)
(20)
(25) 8
(30) 10
(35)
(40) 14
Tube Length m (ft)

FIGURE 2.12

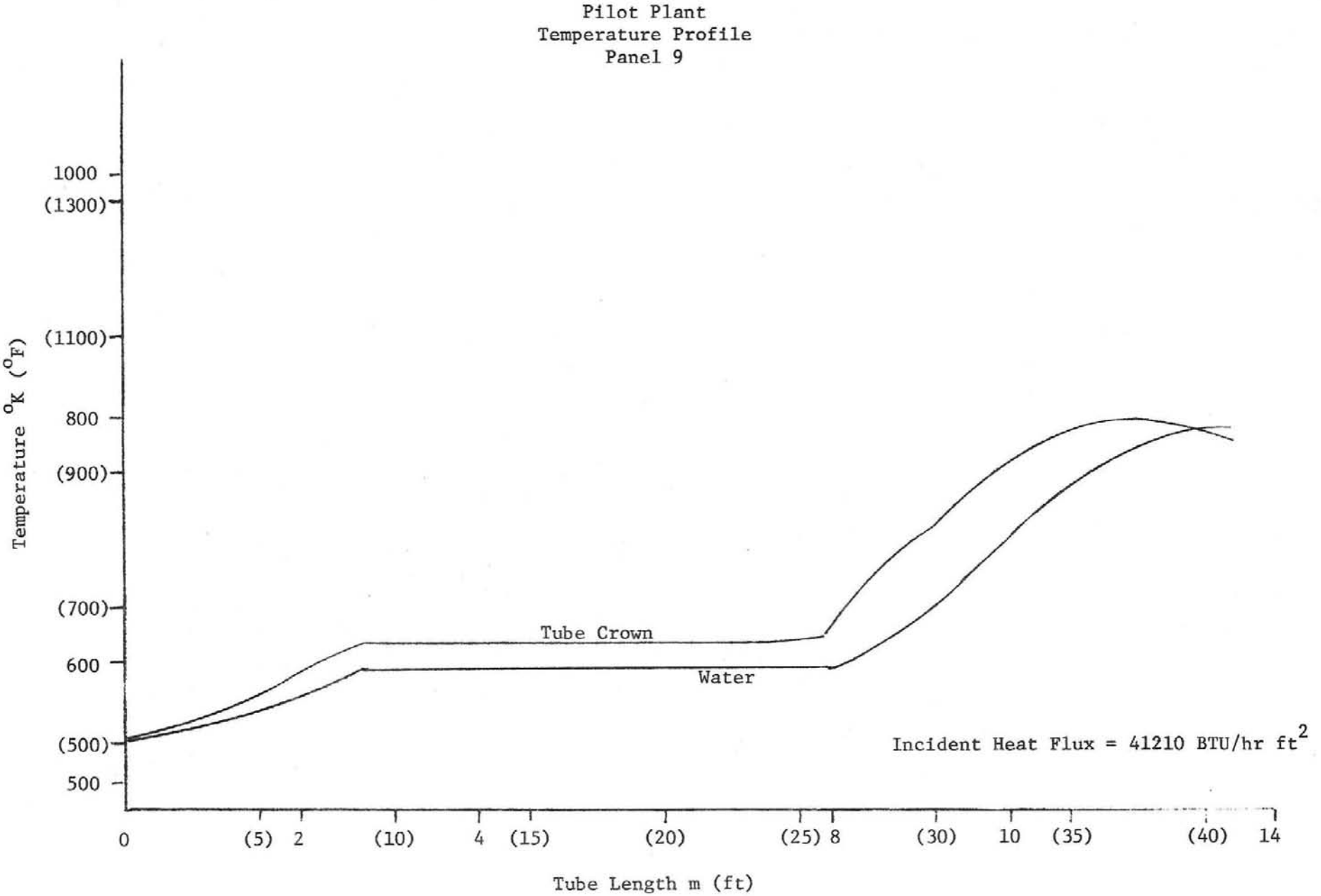
Pilot Plant
Temperature Profile
Panel 9
1000
(1300)
(1100)
800
(900)
(700)
600
(500)
500
Temperature °K (°F)
Tube Crown
Water
Incident Heat Flux = 41210 BTU/hr ft²
0
(5)
2
(10)
4
(15)
(20)
(25)
8
(30)
10
(35)
(40)
14
Tube Length m (ft)

FIGURE 2.13

(980°F), respectively. The ΔT is smaller in the pilot plant due to reduced heat flux. Consequently, the thermal stresses are smaller.

2.2.4 CHF Temperature Oscillations

The "boiling crisis" is invariably accompanied by temperature excursions at the point of the onset of CHF. Precise determination of the magnitude and frequency of these temperature excursions is virtually impossible without testing the particular design under consideration. A review of the literature reveals some general trends which may indicate relative orders of magnitude of the temperature oscillations. See Reference No. 21. For instance, if the crisis occurs at low quality, the temperature oscillations are likely to be more severe than at high quality. Thus it would be expected that the pilot plant would probably not experience temperature oscillations at dryout. On the other hand, the commercial design indicates a critical quality of 17%. Accompanied by high heat flux, the temperature excursions may be severe. The mass flux with commercial plant, however, is relatively high and the higher mass velocities will tend to reduce the magnitude of temperature oscillations (Reference 21).

Some typical temperature oscillations are shown in the above reference. For instance, Figure 6 of the above reference shows typical strip chart reproductions of tube metal temperatures measured mid-way through the tube wall of a high pressure boiler (P = 19 mPa (2755 psia)). At heat flux levels of .52 to .567 MW/m^2 (165,000 to 180,000 BTU/hr ft^2), the peak-to-peak temperatures reduce from 18.75°C to 10°C as the mass flux

increases from 1220 to 1763 Kg/m^2 s (.9 x 10^6 to 1.3 x 10^6 lbm/hr ft^2). This heat flux and mass flux are lower than those calculated for the commercial solar receiver. Frequency is difficult to determine from the charts. The traces are irregular, and a spectral density analysis would be needed. Figure 10 shows that the magnitude of temperature oscillations increases with heat flux.

The proposed 5-tube panel SRE retest has a major objective of measuring these temperature oscillations. This program is discussed further in the next sub-section.

A means of avoiding this problem would be the use of flow "turbulators", such as twisted tapes, or rifled tubes. These devices have been shown to be effective in certain designs in delaying the onset of CHF to higher qualities, thereby minimizing or eliminating the temperature excursions. A design study would be needed to assess these devices and a test program to confirm their performance for this application. Such a program will be recommended for use in the commercial plant design.

2.2.5 Static Stability Analysis

Figure 2.14 illustrates the concept of static stability. Problems arise when the system pressure curve has a zero or negative slope. Interactions with the pump flow/pressure curve could then cause flow excursions to occur. These, if severe, could cause eventual burnout.

To insure stability under these conditions, the slope of the ΔP flow curve must be positive. The greater the positive slope, the

Curve Illustrating Static
Instability

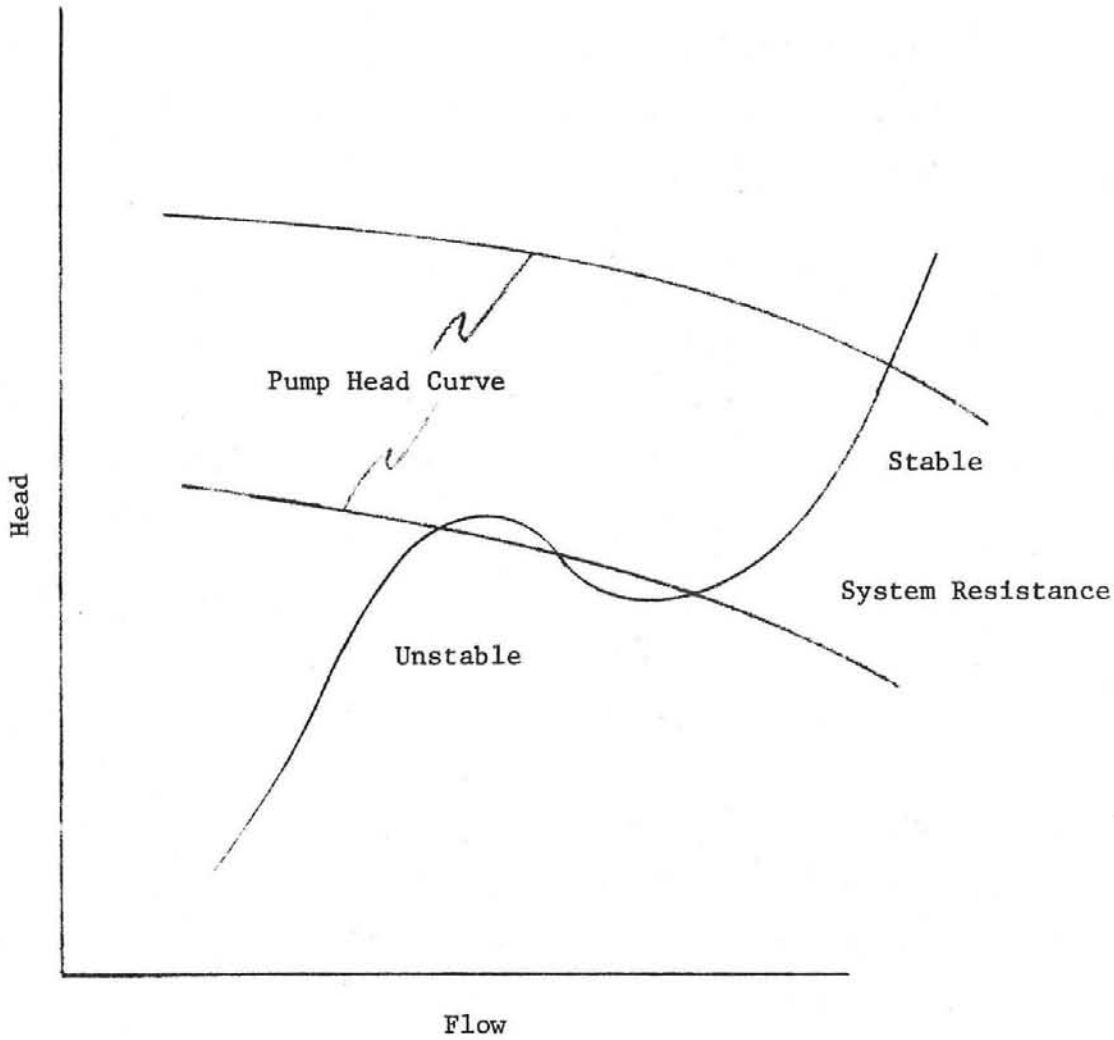

FIGURE 2.14

more stability is enhanced. Maximum slope is 2.0, the case if all single-phase substance is flowing.

The stability index is defined as follows:

$$SI = \frac{\log \frac{\Delta P_1}{\Delta P_0}}{\log \frac{G_1}{G_0}}$$

where: Subscript 0 refers to a particular point in question.

Subscript 1 denotes a flow increment change of +5% from the 0 point.

In the analysis, the ΔP term includes friction, momentum, and gravity terms.

This stability index (SI) was calculated for the load conditions in Tables 2.2 and 2.3. These are plotted on Figures 2.15 and 2.16. The absolute values of the SI are not significant. The fact that for all the steady state load points where rated 515.6°C (960°F) steam is generated, the SI values are positive, indicates static stability and no orificing of the tubes is needed.

Figures 2.17 and 2.18 show simulations of start-up conditions in a quasi-steady state. These curves were generated by holding the flow constant at 20% of the maximum steady state load point, then varying the heat flux from the 20% down to zero. This would simulate a normal start-up where a pre-determined flow is established, and the heat flux increased until rated steam conditions are produced at the panel outlet. This causes the ΔP to experience all points between full liquid phase to full steam quality phase at the panel outlet. Although the pilot plant results indicate the need for

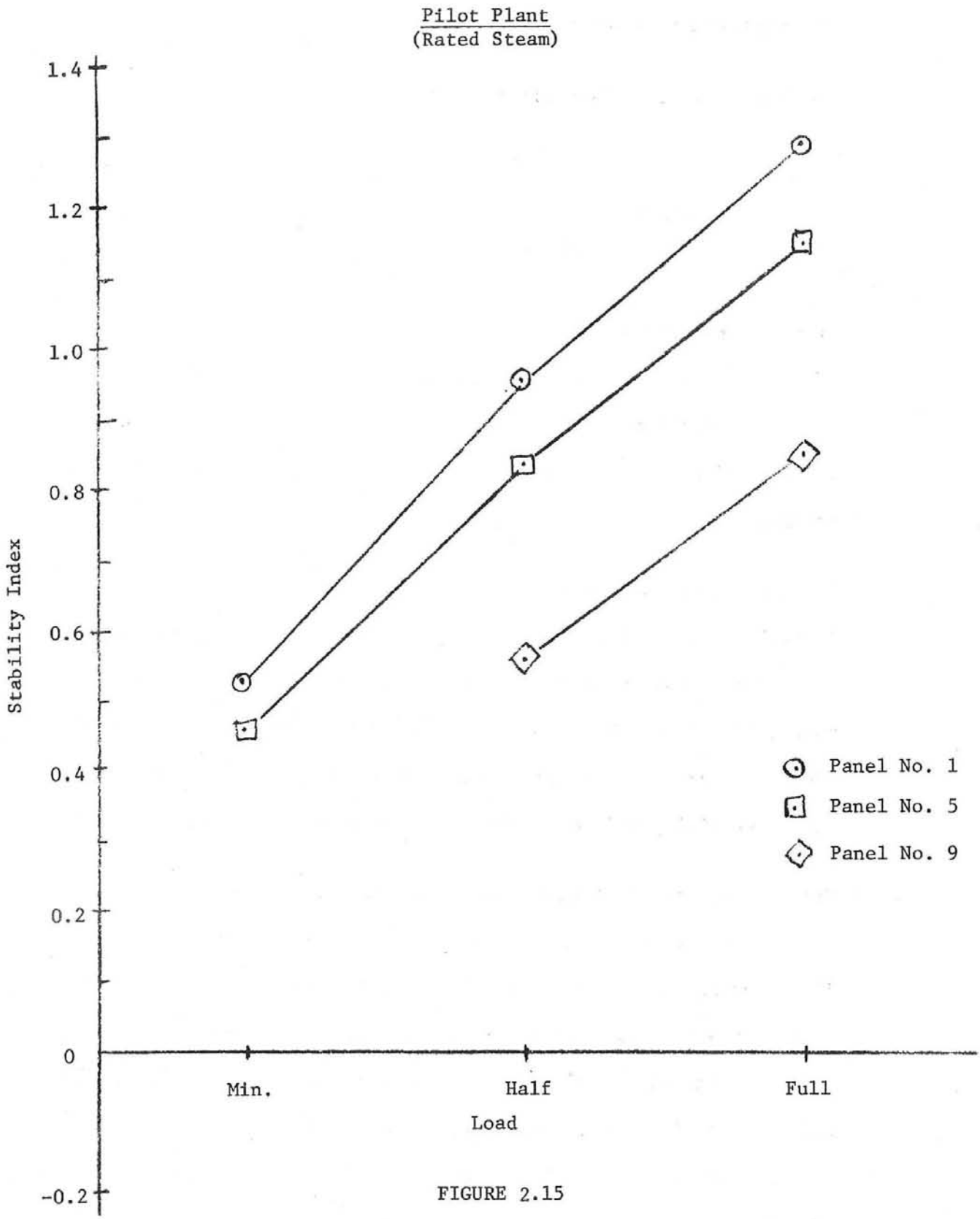
Pilot Plant
(Rated Steam)
1.4
1.2
1.0
0.8
0.6
0.4
0.2
0
-0.2
Stability Index
Min.
Half
Full
Load
Panel No. 1
Panel No. 5
Panel No. 9

FIGURE 2.15

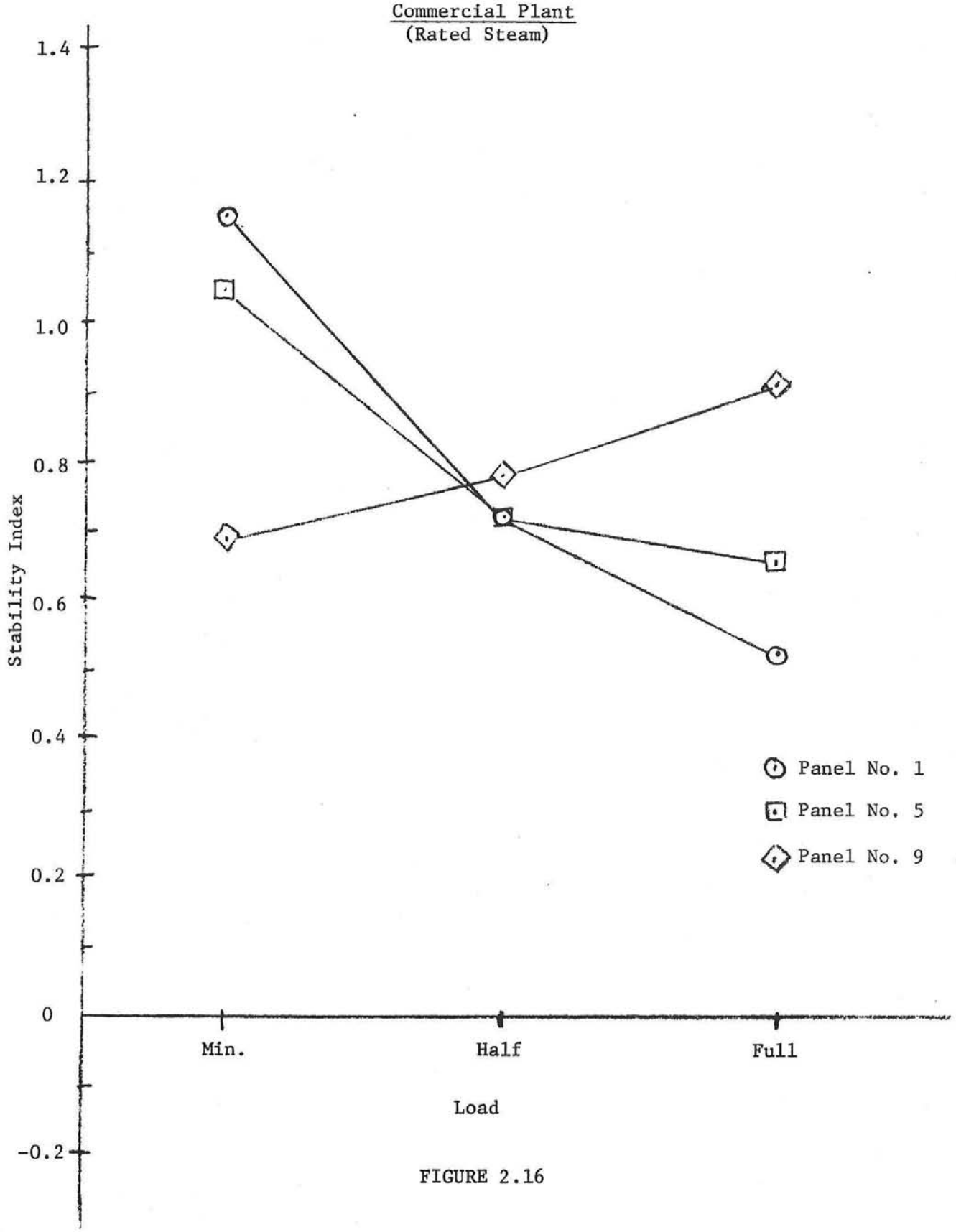
Commercial Plant
(Rated Steam)
1.4
1.2
1.0
0.8
0.6
0.4
0.2
0
-0.2
Stability Index
Min.
Half
Full
Load
Panel No. 1
Panel No. 5
Panel No. 9

FIGURE 2.16

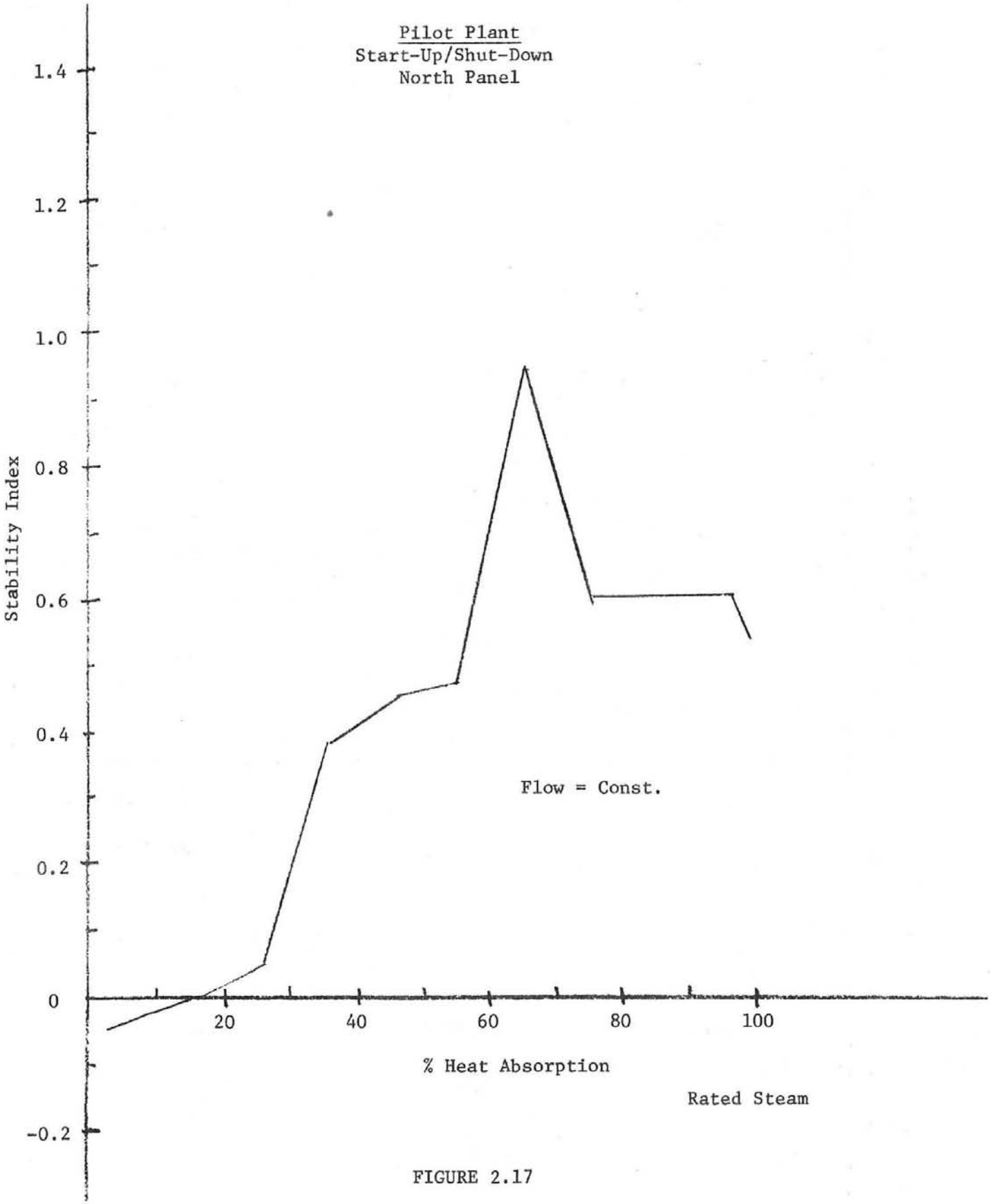
Pilot Plant
Start-Up/Shut-Down
North Panel
1.4
1.2
1.0
0.8
0.6
0.4
0.2
0
-0.2
Stability Index
Flow = Const.
20
40
60
80
100
% Heat Absorption
Rated Steam

FIGURE 2.17

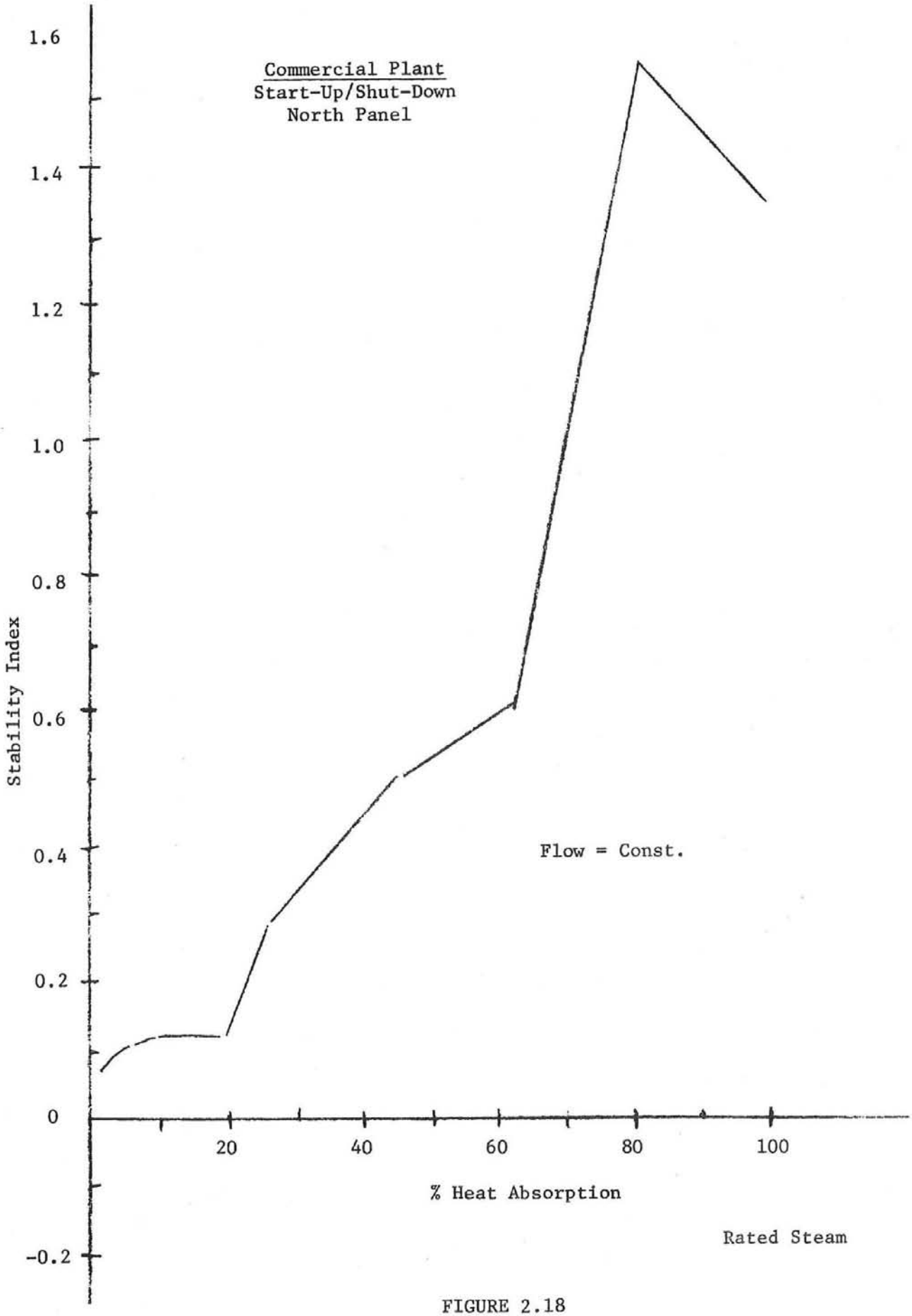
Commercial Plant
Start-Up/Shut-Down
North Panel
1.6
1.4
1.2
1.0
0.8
0.6
0.4
0.2
0
-0.2
Stability Index
Flow = Const.
20
40
60
80
100
% Heat Absorption
Rated Steam

FIGURE 2.18

orificing, only a small negative is indicated, and this is at very low heat flux level (20% of the minimum control load). If tests in the 5-tube and 70-tube panels confirm no serious instability, then orificing would not be necessary.

In Tables 2.2 and 2.3 each panel efficiency is tabulated for the load points investigated. This thermal efficiency is calculated by:

$$\eta = \frac{W \cdot \Delta H}{\int_0^A \dot{q}\, da}$$

where: $W \cdot \Delta H$ = heat absorbed

$\int_0^A \dot{q}\, da$ = total incident energy available

3.3 Evaluation of 5-Tube Panel Retest Program

An interim conclusion (Reference 24) was that further tests were needed to better define the CHF/film boiling region for this design. This subsection describes a thermal analysis of the MDAC/Rocketdyne 5-tube test panel with a recommended test matrix as input. The test matrix recommended is presented in Table 2.4.

The objective of the 5-tube panel retest is to obtain more accurate data in the CHF, transitional, and film boiling regions. In order to select the instrumentation, it is necessary to predict the locations on the panel where the CHF/film boiling region will occur under the test conditions specified in Table 2.4. Toward that end, the matrix points listed in Table 2.4 were inputted to the thermal analysis program. Program outputs gave the temperature profiles, locations, ΔP's, etc. for each test point.

TABLE 2.4

Test Matrix for 5-Tube Test Panel
DOE/MDAC Solar Receiver

Pressure In = 12.76, 11.72, 11 MPa (1850, 1700, 1600 psia)

Temperature In = 260, 293°C (500, 560°F)

Mass Flow Kg/m^2s ($lb/hr\ ft^2 \times 10^{-6}$)		Incident Heat Flux MW/m^2 ($BTU/hr\ ft^2 \times 10^{-3}$)				
		.6 (190.2)	.5 (160)	.41 (130)	.31 (98)	.15 (49)
2306	(1.7)	X	X	X	X+	X+
1763	(1.3)	X	X	X	X+	X+
1153	(.85)	X	X	X	X+	X+
879	(.648)	X				
732	(.54)		X			
678	(.50)	X*	X	X	X	X+
597	(.44)			X		
434	(.32)				X	
407	(.3)		X*	X*	X	X+
271	(.2)			X*	X*	X
207	(.153)					X
68	(.05)				X*	X*

+ No DNB indicated.

* 649°C (1200°F) final temperature reached before panel exit.

Maximum heat flux available for the test was .6 MW/m^2 or 70% of the commercial plant maximum. A range of 5 flux levels was selected. A range of 12 mass flux values was selected so as to provide at least 4 or 5 flows for each heat flux. The matrix is to be repeated for 12.75, 11.72, and 11.03 MPa (1850, 1700, and 1600 psia), and panel inlet temperature of 260 or 29.3°C (500 or 560°F). The upper (superheat) region is not of interest here, so the tests need not be carried out with the outlet temperatures as high as the results show. The thermal analysis program was stopped at 649°C (1200°F). Sometimes this occurred before the panel outlet. Sometimes superheat was not obtained, depending on the particular combination of test parameters. Runs are marked in Table 2.4 where no CHF was indicated. It is still necessary to run these points, to confirm the CHF locations. Tube sizes, material, and all other parameters were the same as for the pilot plant receiver analysis discussed previously.

Figure 2.19 shows the temperature profile for the highest heat flux, low flow case. Note that a 649°C (1200°F) final temperature was predicted. The flux profile at the upper end need not be used in the actual tests.

Figure 2.20 shows a similar profile for the same heat flux, but at maximum flow. Here the flow is so high that film boiling does not occur before the flux starts to drop. In this case, the flux profile should be shifted toward the top of the receiver, and the subcooling reduced. These two graphs serve to illustrate the large area of panel over which CHF may occur.

Results of the analysis are shown on the next three graphs. Figure 2.21 shows how the location of the CHF point is affected by heat flux as the parameter.

5-Tube Panel Test Predicted Performance

Max. Flux; Low Flow

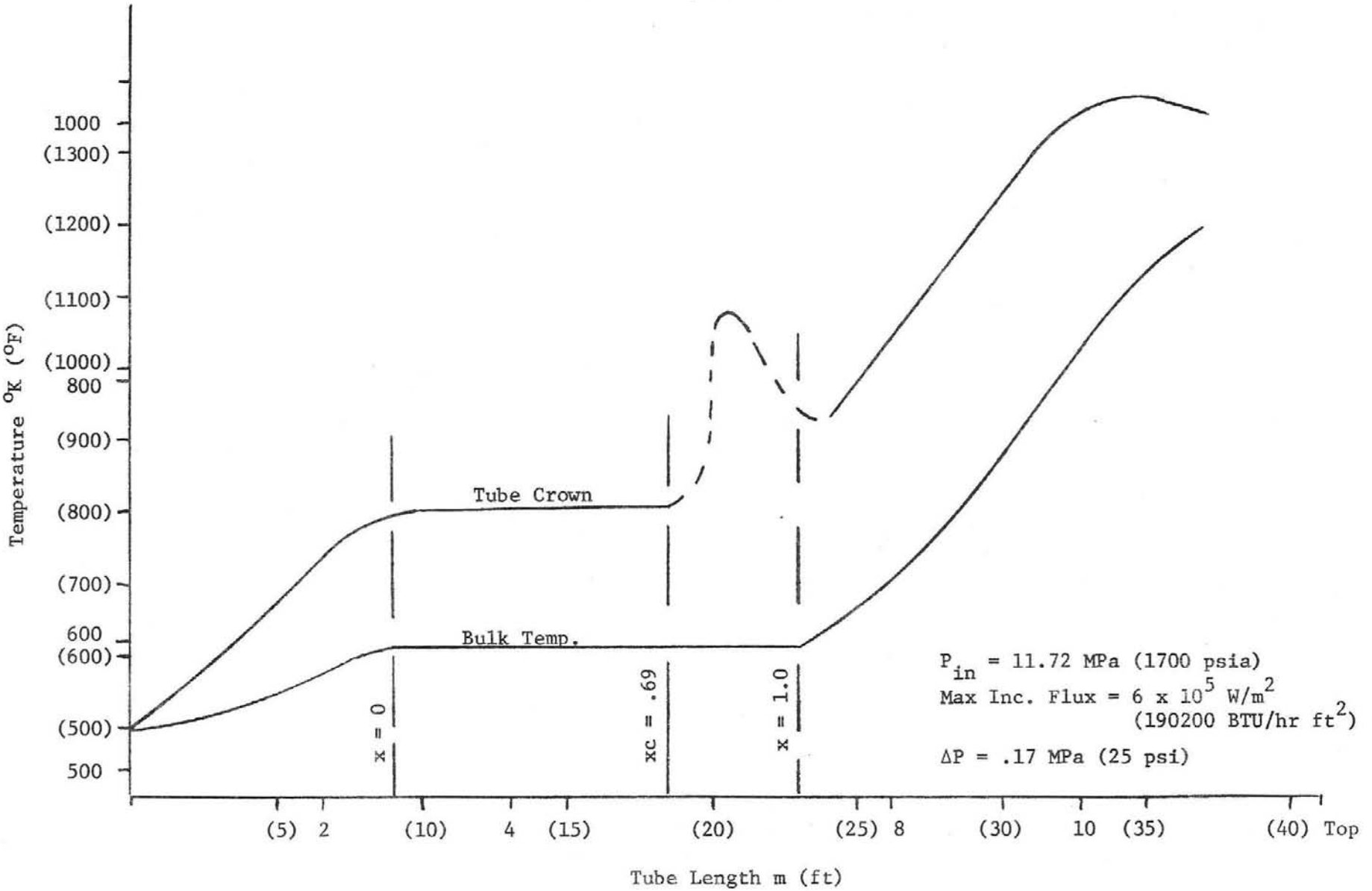

FIGURE 2.19

5-Tube Panel Test Predicted Performance

Max. Flux; High Flow

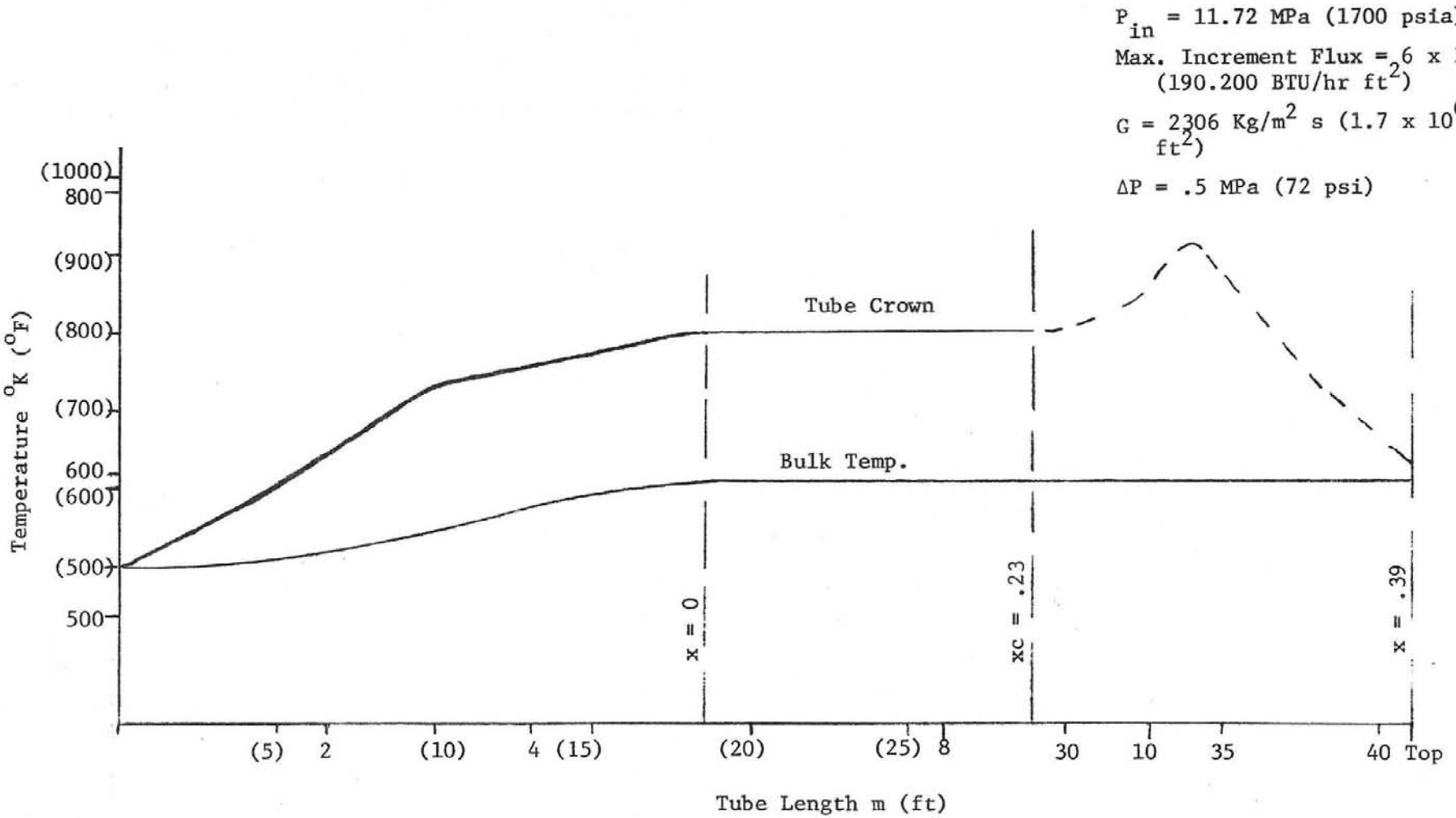

FIGURE 2.20

An area between 4.57 and 7 m (15 and 23 feet) was seen as including most of the CHF data of interest (high flux data). The area from 7 to 10 m (23 to 33 feet) is of a lesser interest. Thermocouples were concentrated in the area 4.57 to 7 m (15 to 23 feet), with spacing every 50.8 mm (2 inches). In the lesser region, spacing was selected as 76.2 mm (3 inches). Outside these two regions, 304.8 mm (12 inches) spacing is satisfactory. Figure 2.22 shows that the area can be narrowed by reducing panel subcooling. Figure 2.23 indicates the pressure effect on CHF location. These curves are for an inlet temperature of 260°F (500°F). Results of this thermal analysis indicate a general region exists where thermocouples can be concentrated to respond to the CHF phenomena over a wide range of input parameters.

Due to the fact that a number of the test points are "off-design", the pressure drop curves indicate static instability in certain regions (Figure 2.24). In order to assure stability during these tests, it is recommended that orifices be installed in the 5-tube panel. Figure 2.25 shows the minimum correction necessary. This requires orifices with a diameter ratio of 0.45. Tests may be run without orificing to check for instability. In static instability, the pump characteristic curve plays an important role. The effect of static instability should be manifested by gross flow excursions, which can occur between parallel tubes. Without sufficient orificing, test points should be approached cautiously to avoid the possibility of an actual burn-out. Dynamic instabilities may also be present, which are manifested by pressure and flow oscillations.

5-Tube Test Panel
Predicted Location of DNB, L_{xcrit}
Effect of Heat Flux

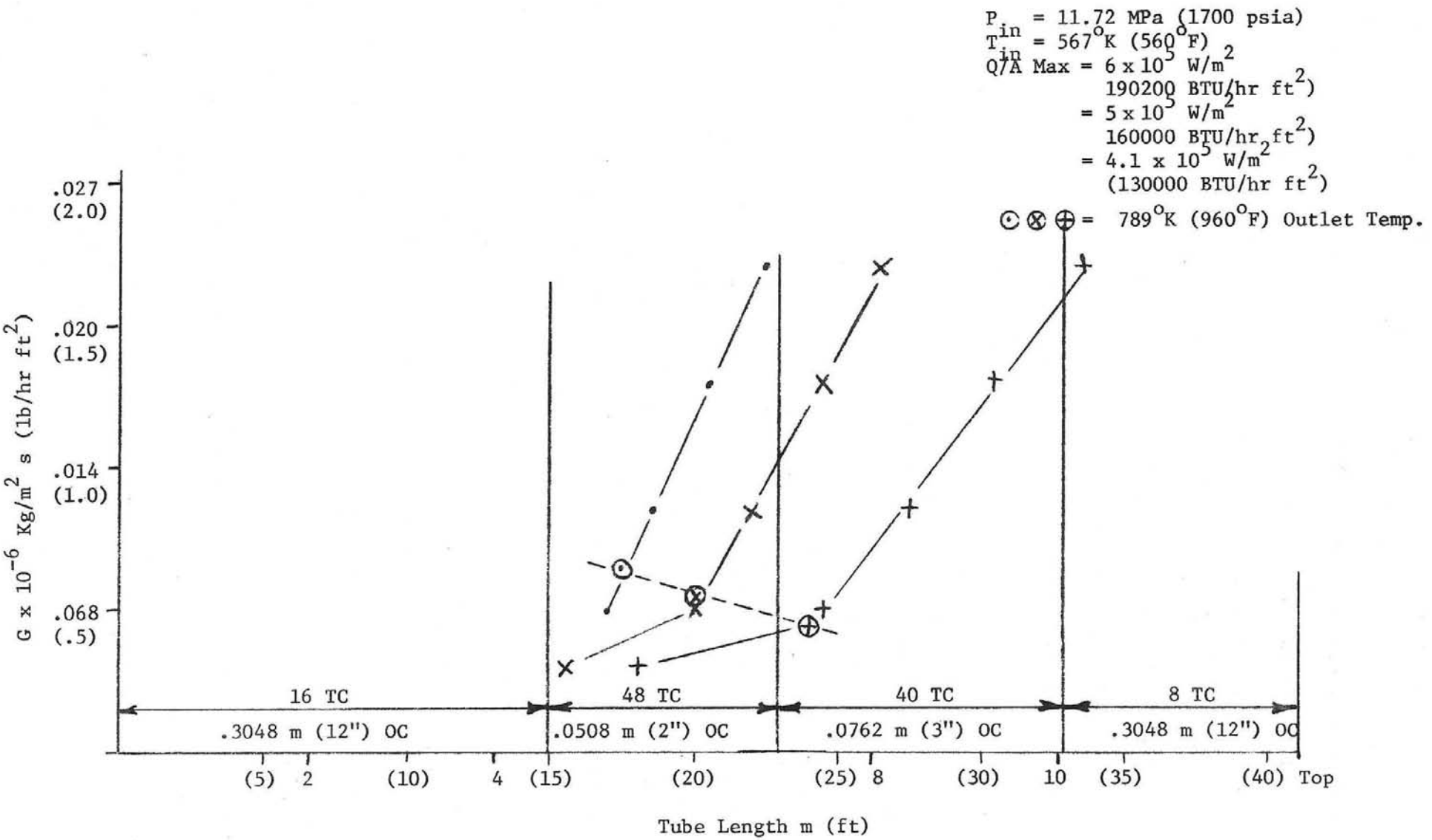

FIGURE 2.21

5-Tube Test Panel
Predicted Location of DNB, L_{crit}
Effect of Subcooling

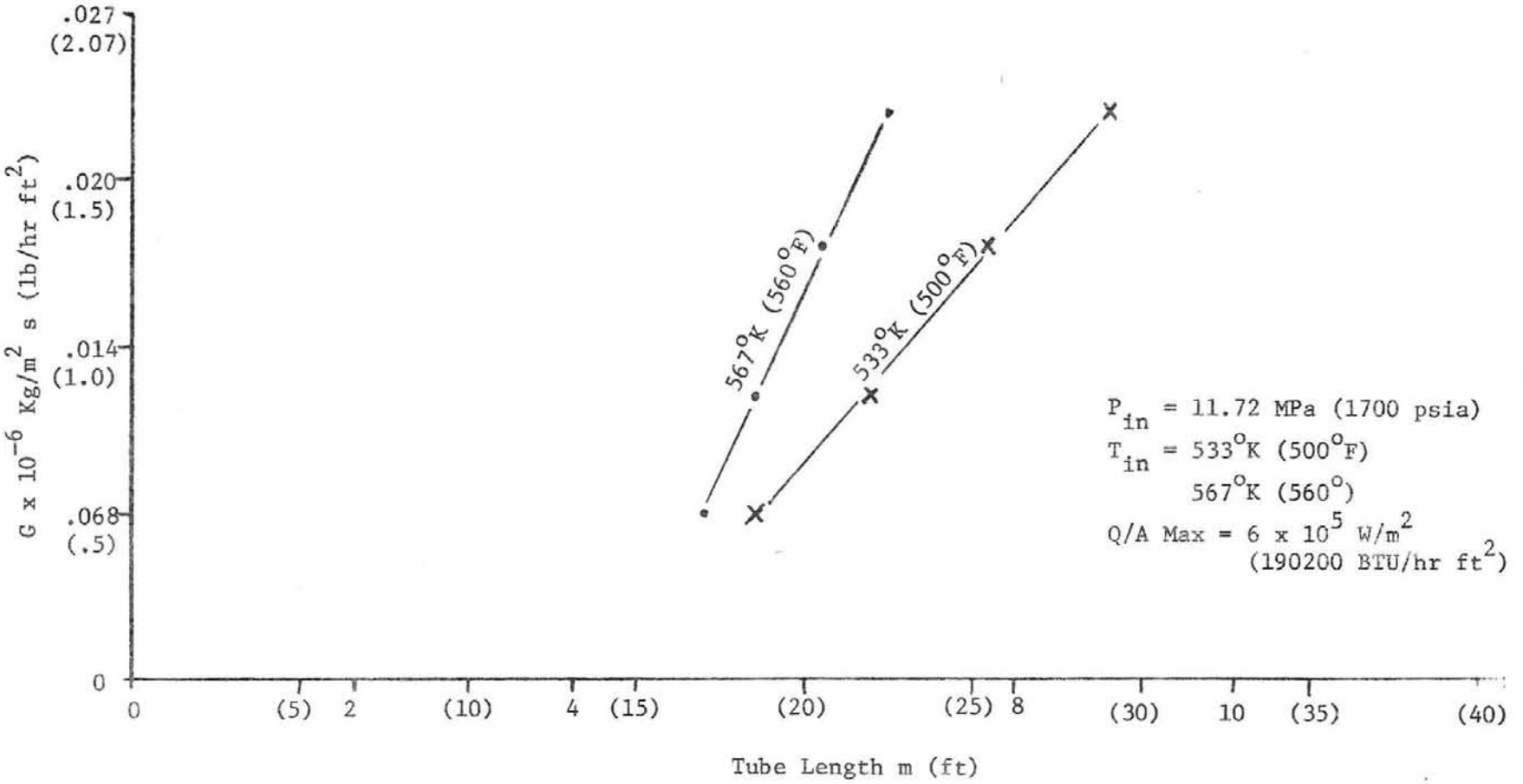

FIGURE 2.22

5-Tube Test Panel
Predicted Location of DNB, L_{crit}
Effect of Pressure

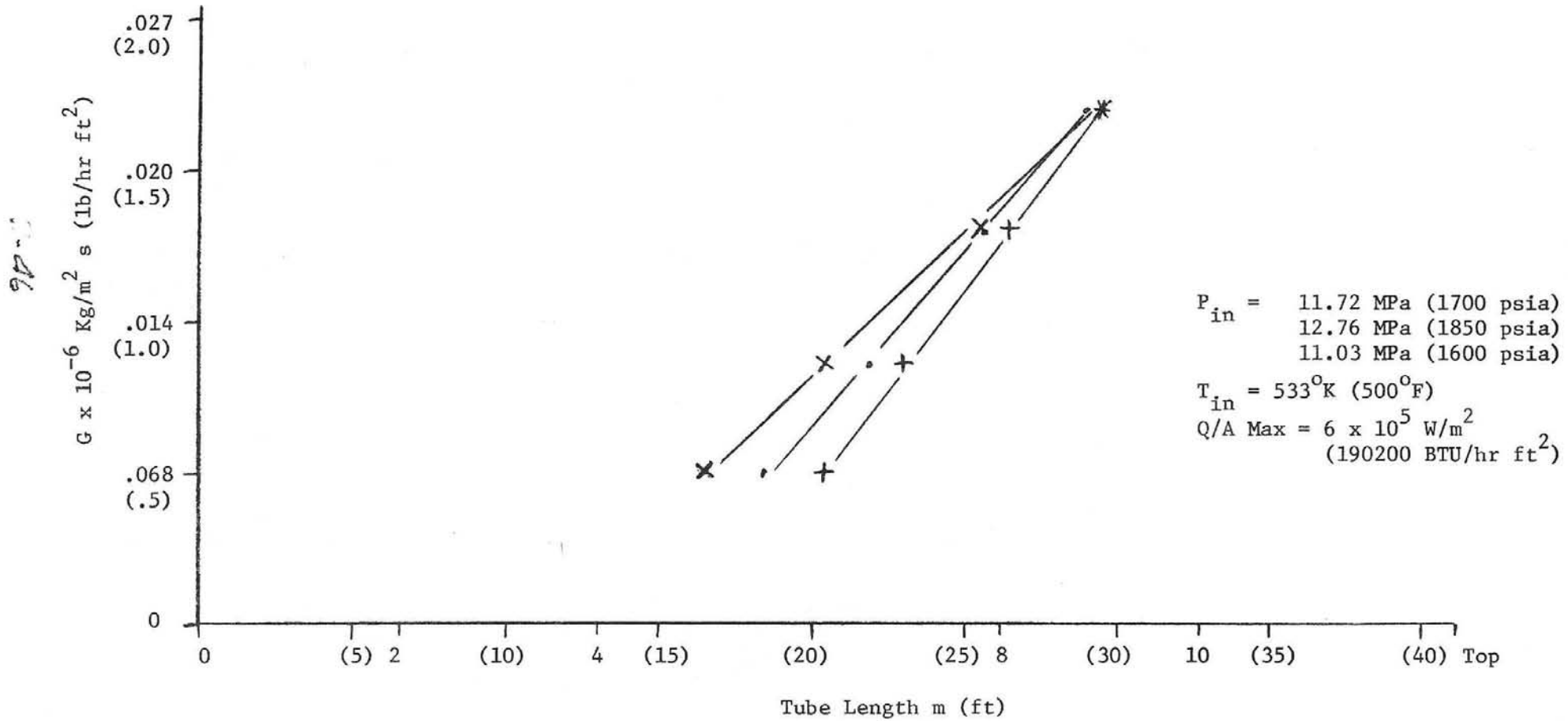

FIGURE 2.23

5-Tube Test Panel
Pressure Drop w/o Orifices

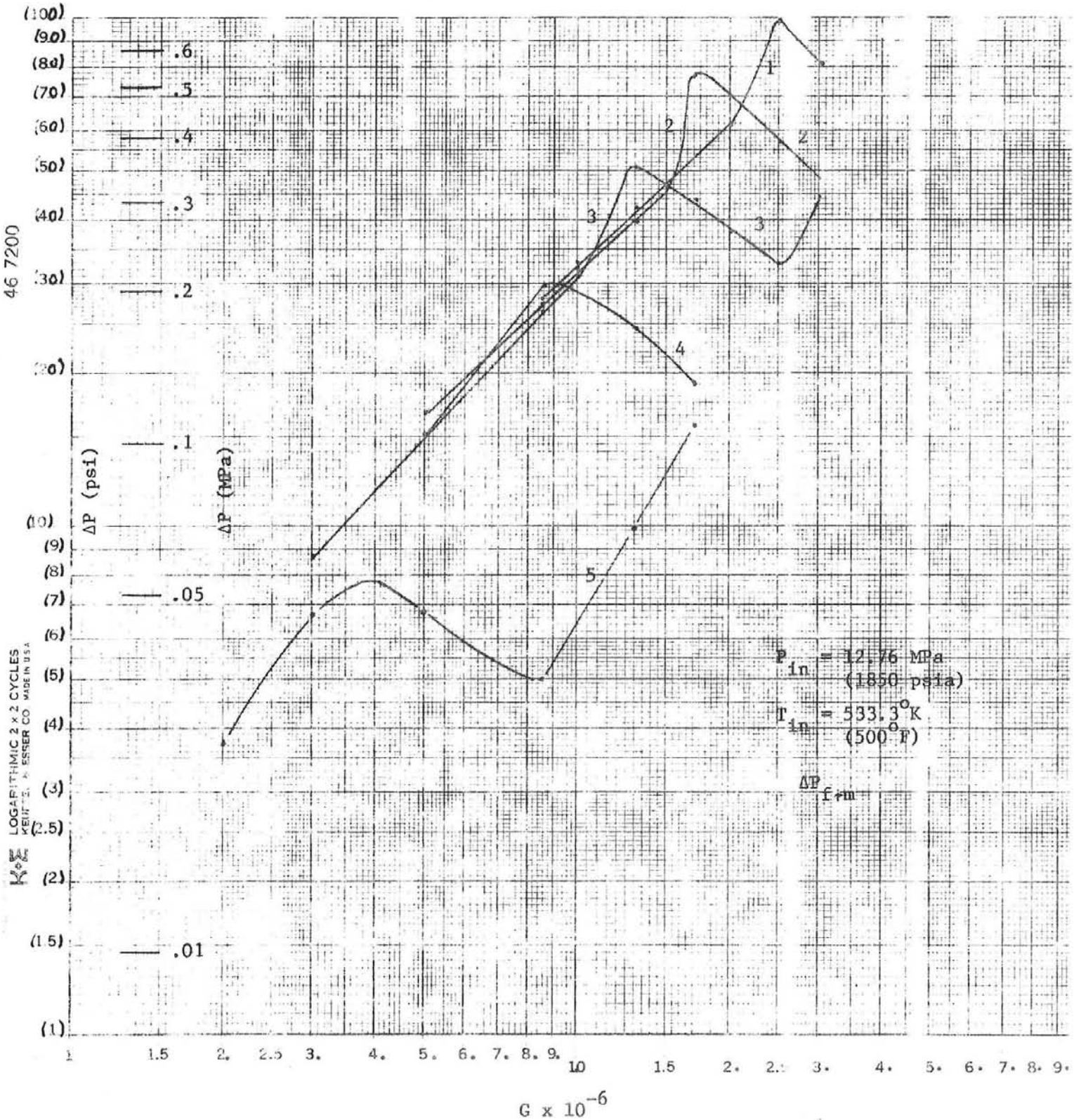

FIGURE 2.24

5-Tube Test Panel
Pressure Drop with Orifices

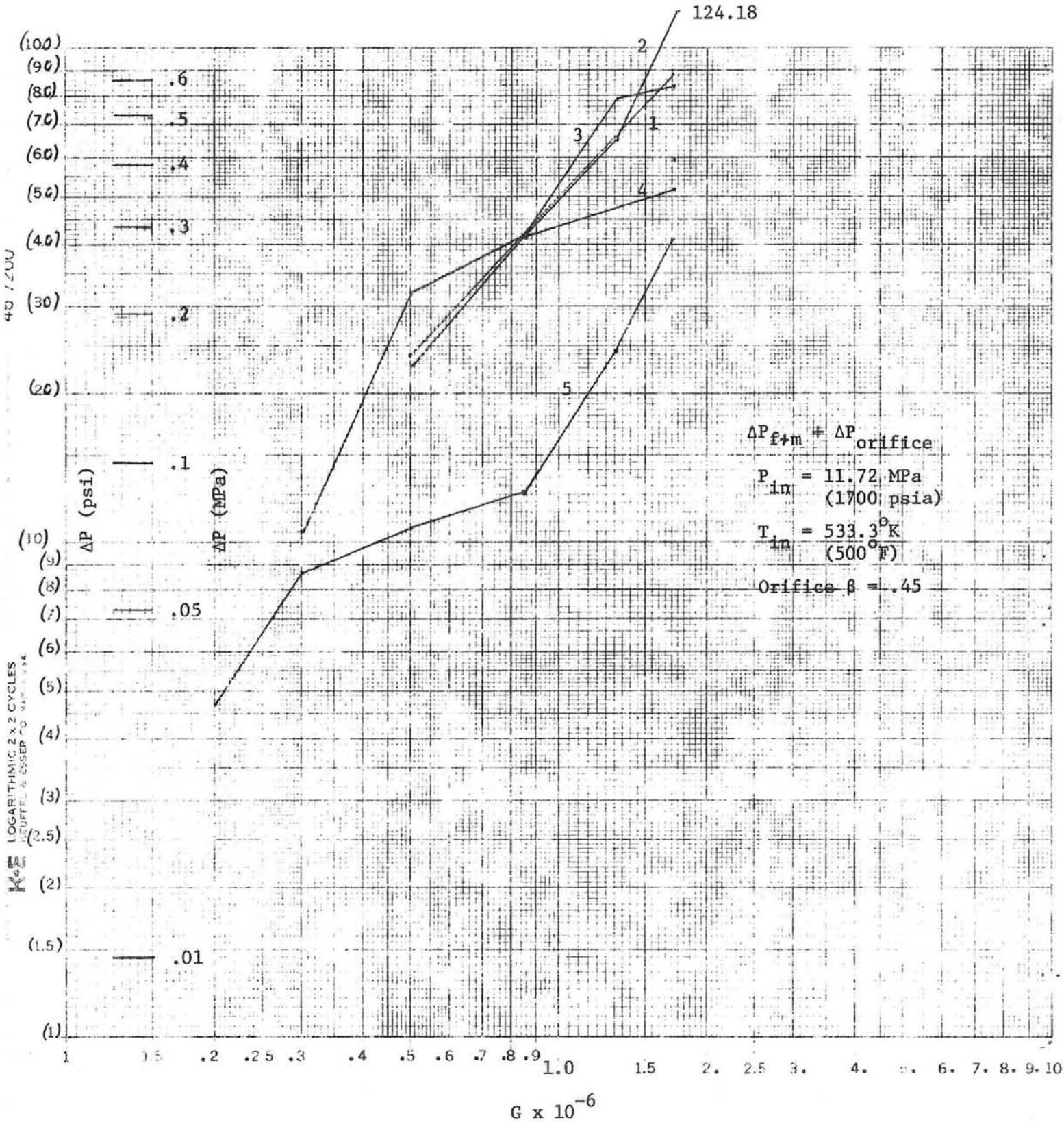

FIGURE 2.25

3.4 Water Chemistry

Since the STPS has a once-through steam generator, the water chemistry concepts which apply to C-E Combined Circulation (supercritical) Boilers are applicable to these units. Most of these concepts which include volatile water chemistry, condensate polishing, and a philosophy of zero solids entering the boiler have been incorporated in the design of both the pilot and commercial STPS.

However, the proposed feedwater pH of 9.5 is too high. A pH this high will cause excessive corrosion in the condenser (90/10; copper/nickel). The pH at the preheat panel inlet of HP heater outlet should be maintained between 9.0 and 9.2. If the condensate demineralizers are operated on a hydrogen cycle, high feedwater pH's will result in a greatly increased regeneration frequency due to ammonia exhaustion of the cation resin. The condensate demineralizers must be operated on the hydrogen cycle if there is any condenser leakage.

By its very nature, the STPS will have large load fluctuations. This type of operation results in increased amounts of preboiler oxide formation which eventually forms deposits on the heat transfer surfaces of the steam generator. Since the STPS will probably have to be chemically cleaned at a much higher frequency than normal high pressure boilers, necessary connections should be provided.

In addition to the nighttime standby procedures which maintain blanketing steam on the high pressure heaters and deaerator, there should be layup procedures for the preheat and evaporator panels. For short term shutdowns this whould consist of applying a nitrogen overpressure (20.7-345.5 KPa (3-5 psig)) and maintaining normal operational chemical limits.

During long term shutdowns the unit should be filled with condensate quality water treated with 200 ppm of hydrazine and 10 ppm of ammonia (pH 10.0) and a nitrogen overpressure (20.7-34.5 KPa (3-5 psig)) maintained. A typical layup procedure for a combined circulation unit is shown in Appendix D.

SECTION 3

STRESS ANALYSIS

3.1 Introduction

A heat transfer and an elastic stress analysis were performed for both the DOE/MDAC 100 MW commercial plant and a 10 MW pilot plant solar receiver designs.

The maximum stress of the commercial plant is 472.3 MPa (68,500 lb/in^2) and occurs at the film boiling point at the tube crown. This stress results in an estimated fatigue life of less than 200 cycles.

The maximum stress of the pilot plant is 185 MPa (26,850 lb/in^2). The estimated fatigue life of the pilot plant is 10^5 cycles.

The results of the stress analysis indicate the flux loading on the commercial plant is too severe. The high flux loading causes a large temperature gradient through the tubes, thereby causing large axial stresses. Table 3.7 summarizes the thermal cases analyzed. The fatigue life of the commercial plant is very low (200 cycles). Table 3.8 summarizes the fatigue lives of each case analyzed.

Two methods of reducing the temperature gradient across the tube were investigated, a thinner wall thickness and use of a ferritic steel. In each case, the gradient and, consequently, stress were reduced. A thinner tube reduced the gradient 35.6°C (96°F) and the ferritic reduced the gradient 31.7°C (89°F). The fatigue life of each was increased from 1100 cycles to 4500 cycles for the thin tube and from 1100 cycles to 3500 cycles for the ferritic. A combination of both produced a temperature gradient reduction of 61.7°C (143°F) and a fatigue life of 10,000 cycles.

A thermal transient analysis was performed on the pilot plant panel headers. Based on fluid temperature rise of 482°C/hr (900°F/hr) for 20 minutes, a fatigue life of 10^5 cycles was calculated.

The stresses on the pilot plant are low and the fatigue life of the pilot plant reflects this (10^5 cycles). The pilot plant could operate with the indicated flux .244 MW/m^2 (77,230 BTU/hr ft^2).

This stress analysis consisted of an elastic analysis only. The high flux loading and stresses should be analyzed inelastically. The fatigue life assessments would not be as conservative as the ones based on an elastic analysis. The scope of this review did not allow this type of analysis. However, a follow-on stress analysis should be conducted to determine the degree of conservation of the elastic analysis.

3.2 Analytical Procedures

A heat transfer and an elastic stress analysis were performed for the DOE/MDAC solar receiver design review. Loading conditions for the pilot plant and 100 MW commercial plant were analyzed. Design recommendations and fatigue life of the receiver were made based on these results.

A finite element model was generated based on panel geometry and constraint conditions from Rockwell International Corp. Drawing AP77-084. An 8-noded isoparametric element was used. Material properties for Incoloy 800H were obtained from Code Case 1592. Figures 3.1, 3.2, and 3.3 show the geometry and Tables 3.1, 3.2, 3.5 and Figure 3.4 show material properties. Four heat flux loading conditions were analyzed, three for the commercial plant (film boiling points, maximum crown temperature) and one for the pilot plant (maximum crown temperature).

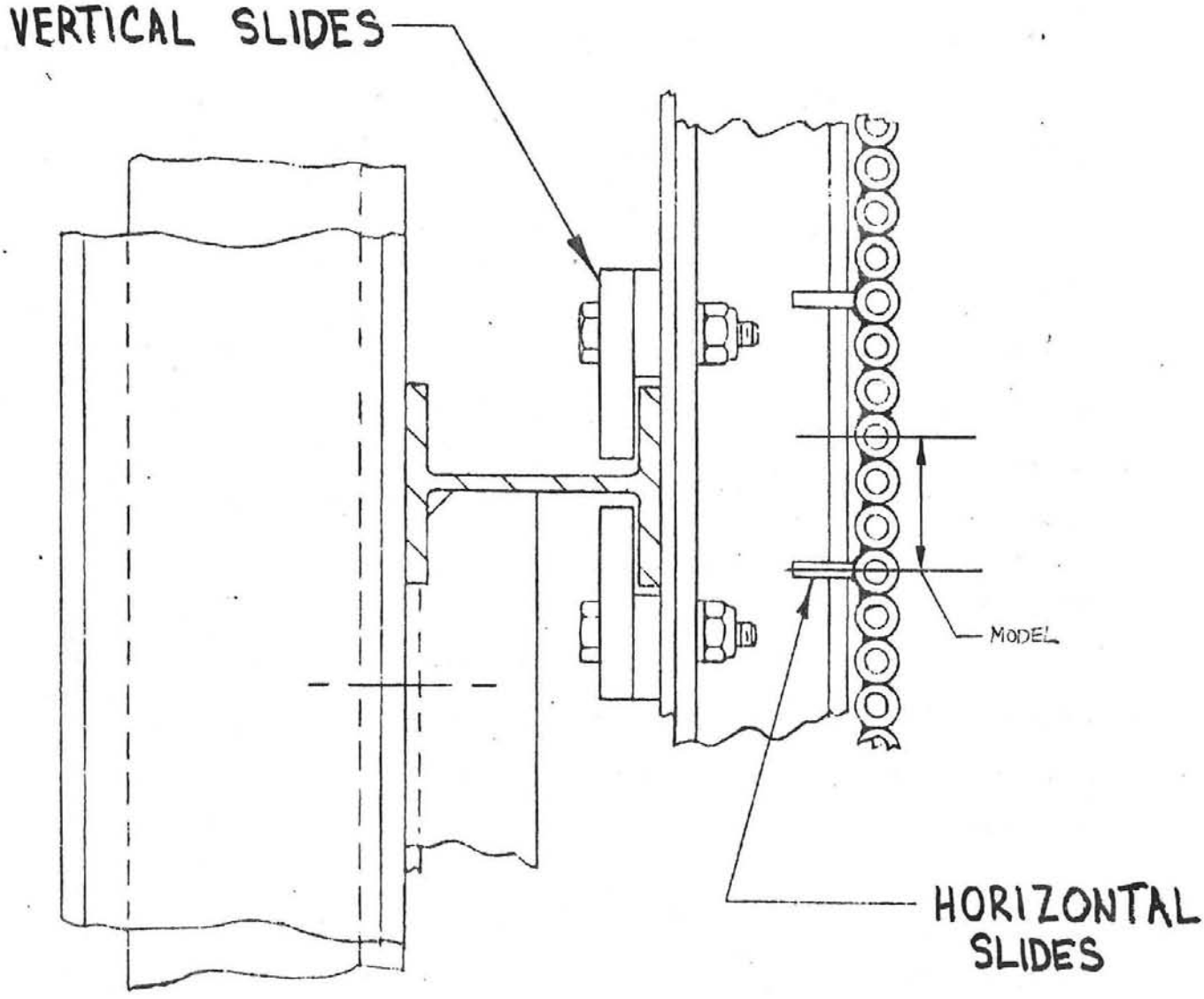

FIGURE 3.1

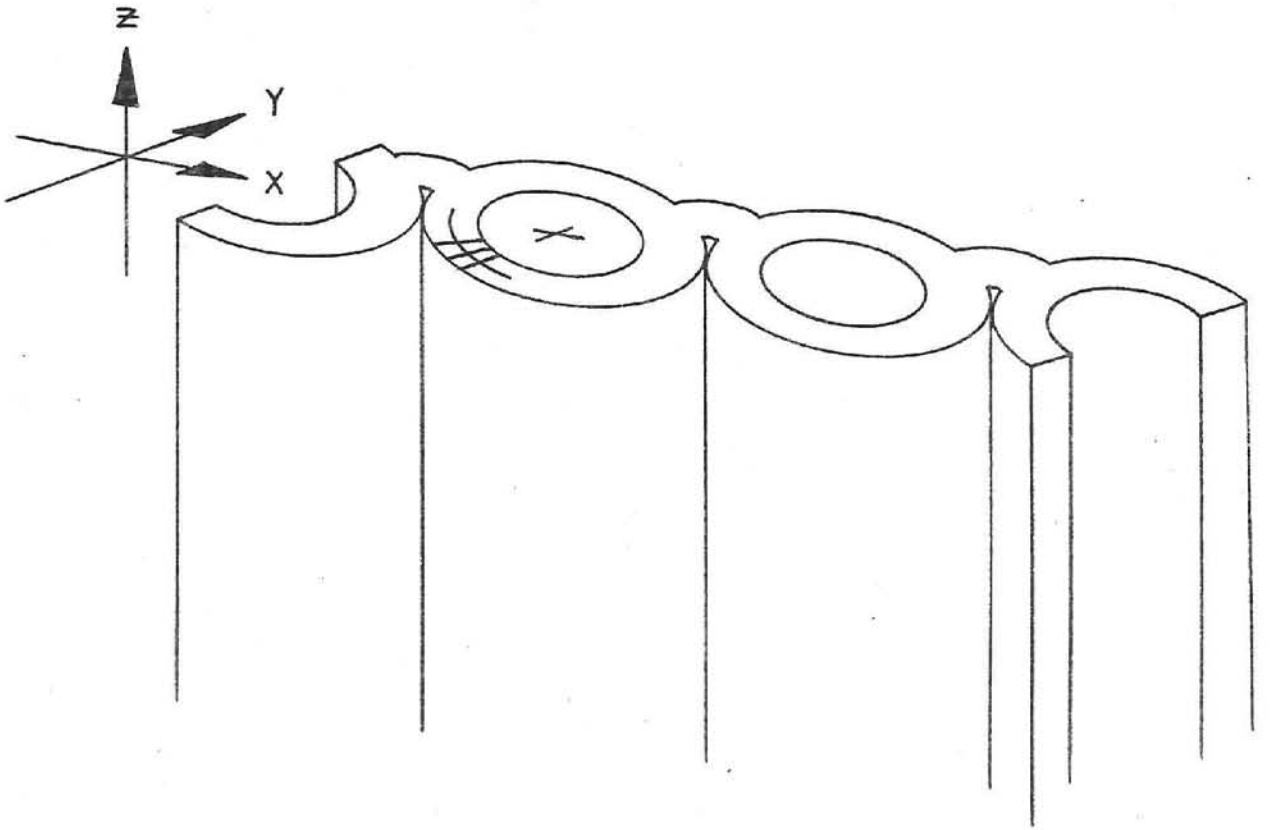

COORDINATE SYSTEM

FIGURE 3.2

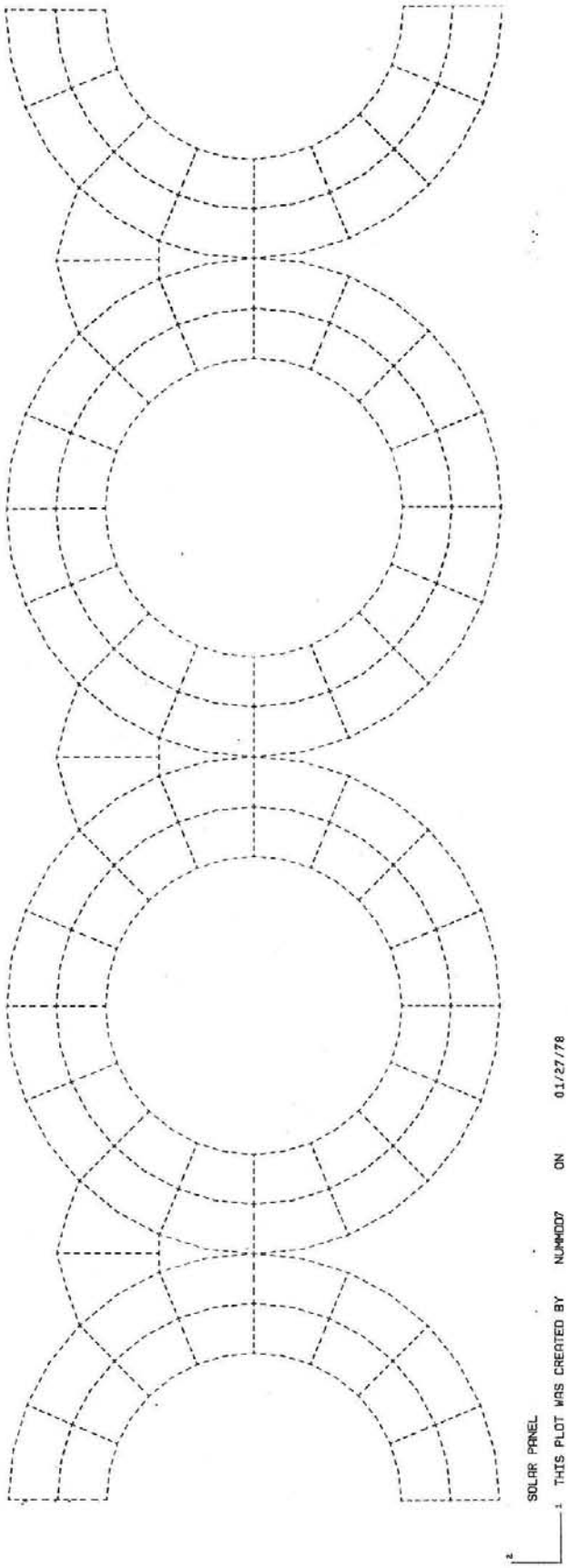

FIGURE 3.3

Thermal Conductivity of Inconel vs Temperature

9/9/65

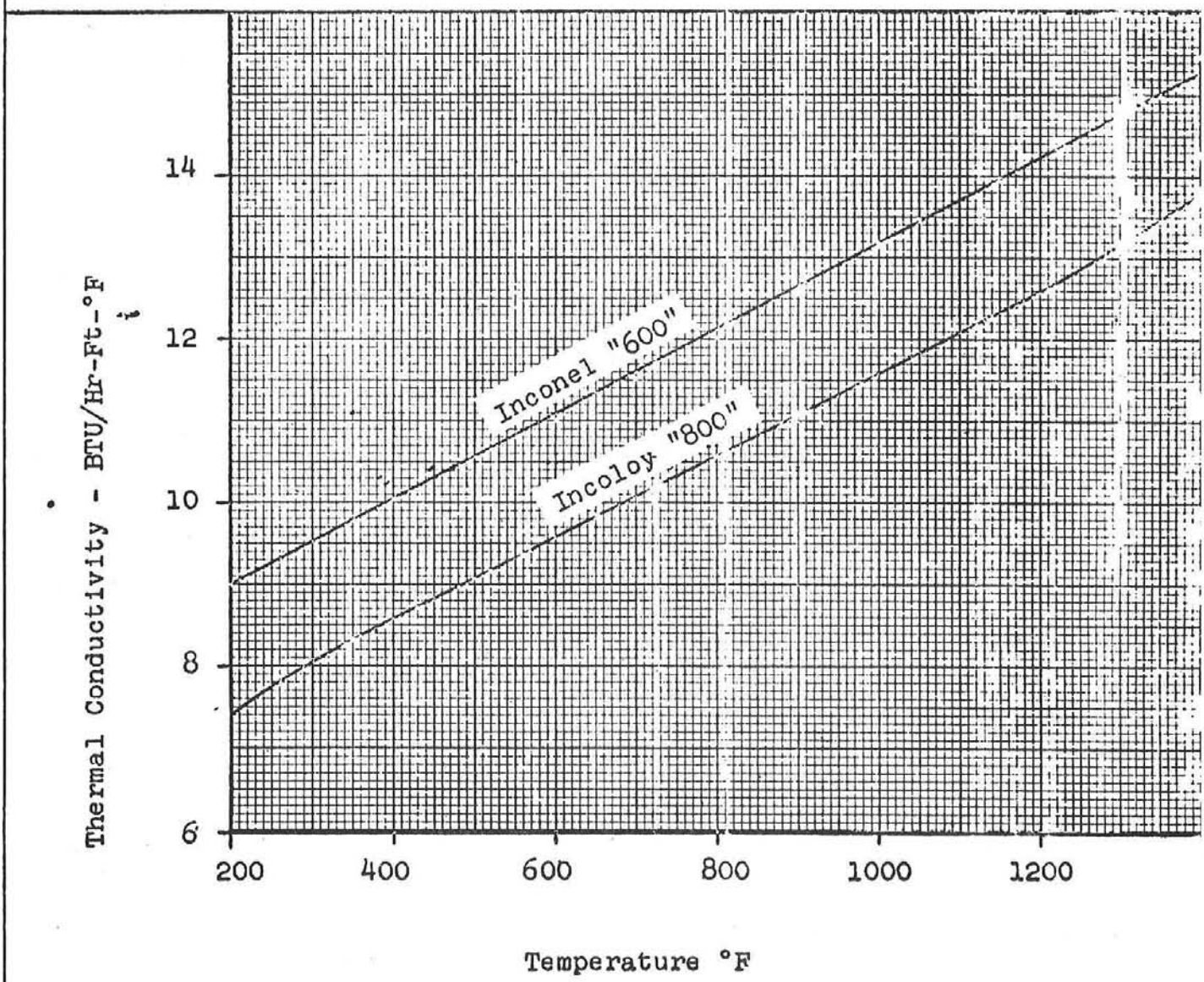

FIGURE 3.4

TABLE 3.1

Instantaneous Coefficient of Thermal Expansion vs. Temperature

Temp., °F	Instantaneous Coefficient of Thermal Expansion, in./in.-°F X 10^6			
	304 SS and 316 SS	Ni-Fe-Cr Alloy 800H	2¼ Cr - 1 Mo	Ni-Cr-Fe-Cb Alloy 718
70	9.11			
100	9.21		6.6	6.91
200	9.50	8.8	6.9	7.43
300	9.73	8.9	7.35	7.77
400	9.96	9.0	7.65	7.97
500	10.20	9.1	7.9	8.09
600	10.43	9.2	8.1	8.17
700	10.66	9.3	8.25	8.26
750	10.81			
800	10.90	9.5	8.4	8.42
850	11.00	9.65		
900	11.11	9.8	8.5	8.69
950	11.23	10.0		
1000	11.35	10.2	8.6	9.13
1050	11.46	10.4		9.46
1100	11.58	10.6	8.65	
1150	11.70	10.8		
1200	11.81	11.0	8.7	
1250	11.93	11.2		
1300	12.01	11.4		
1350	12.16	11.55		
1400	12.28	11.7		
1450	12.39	11.8		
1500	12.50	11.9		
1550		12.0		
1600		12.1		

TABLE 3.2

Modulus of Elasticity vs. Temperature

Temp., °F	(Static) Modulus of Elasticity, psi X 10^6			
	304 SS and 316 SS	Ni-Fe-Cr Alloy 800H	2¼ Cr - 1 Mo	Ni-Cr-Fe-Cb Alloy 718
70	28.3	28.5	29.9	–
100				29.0
200	27.7	27.8	29.5	28.38
300	27.1	27.3	29.0	27.93
400	26.6	26.8	28.6	27.51
500	26.1	26.3	28.0	27.10
600	25.4	25.7	27.4	26.69
700	24.8	25.2	26.6	26.26
750				–
800	24.1	24.6	25.7	25.82
850	23.7	24.4		–
900	23.3	24.1	24.5	25.35
950	22.9	23.8		–
1000	22.5	23.5	23.0	24.84
1050	22.1	23.3		24.56
1100	21.7	22.9	20.4	
1150	21.3	22.7		
1200	20.9	22.1	15.6	
1250	20.5	22.1		
1300	20.1	21.7		
1350	19.7	21.4		
1400	19.2	21.1		
1450	18.7	20.7		
1500	18.3	20.3		
1550		19.8		
1600		19.2		

The overall procedure consisted of inputting the heat flux loading into MARC Heat Program and generating steady-state temperature distributions across the model for each flux loading. These temperature distributions were then input into MARC Stress via a post tape. An elastic stress analysis was done for each case using the appropriate boundary conditions, pressure loading, and material properties. Using the results of these stress runs, fatigue life of both plants was calculated.

The 4 flux loading conditions analyzed are shown in Table 3.3. The first 3 are flux loadings on the commercial plant and the last is the flux loading on the pilot plant. The flux distribution was input on the tubes using a tube shading program. The model temperatures were put on tape to be input into the stress program. Results of the heat transfer analysis were also plotted for each case. Figures 3.5 through 3.8 show the temperature profiles for each loading condition.

The generated temperature distributions, pressure loads, and boundary conditions were input into MARC Stress. The panel geometry and the large front to back temperature loading necessitated the use of a generalized plane strain finite element. This element allowed the element to grow axially (strained T_{MEAN}) without constraint while still calculating the thermal strains due to differences in temperature from front to back.

The boundary conditions placed on the model are illustrated in Figure 3.9. Symmetry between horizontal slide locations cause the middle to be placed on rollers in the y direction. The horizontal slide weld point allows only x direction movement and symmetry forces the center line of tube to move the same amount. The tube rotation is fixed to zero in the z direction due to axial constraints.

TABLE 3.3

List of Loading Conditions

No.	Heat Flux MW/m^2 ($BTU/hr\ ft^2$)	Fluid Temp. C (F)	Film Coeff. $MW/m^2\ C$ ($BTU/hr\ ft^2\ ^oF$)	Pressure MPa (psia)
1	.779 (247,213)	328 (622)	.021 (3759)	12.5 (1815)
2	.779 (247,213)	328 (622)	5.3×10^{-3} (940)	12.5 (1815)
3	.757 (239,862)	426 (798)	.011 (1907)	11.67 (1693)
4	.244 (77,230)	432 (809)	2.6×10^{-3} (460)	10.97 (1592)

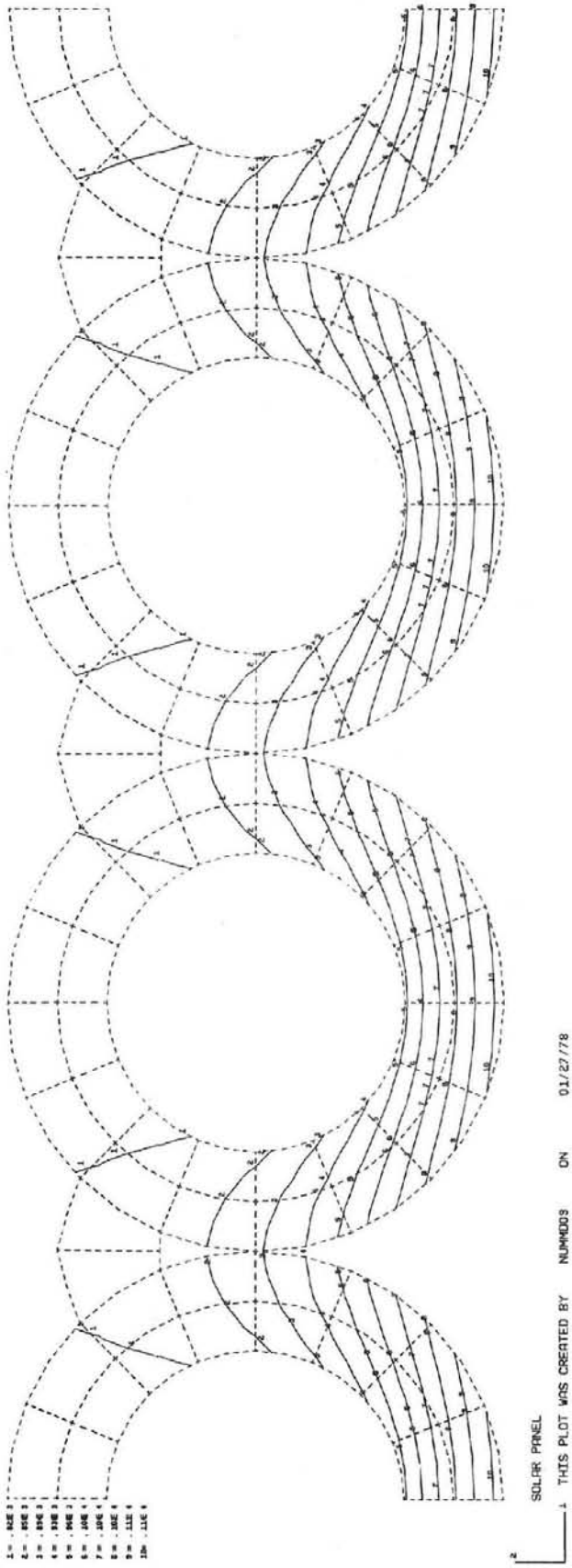

FIGURE 3.5

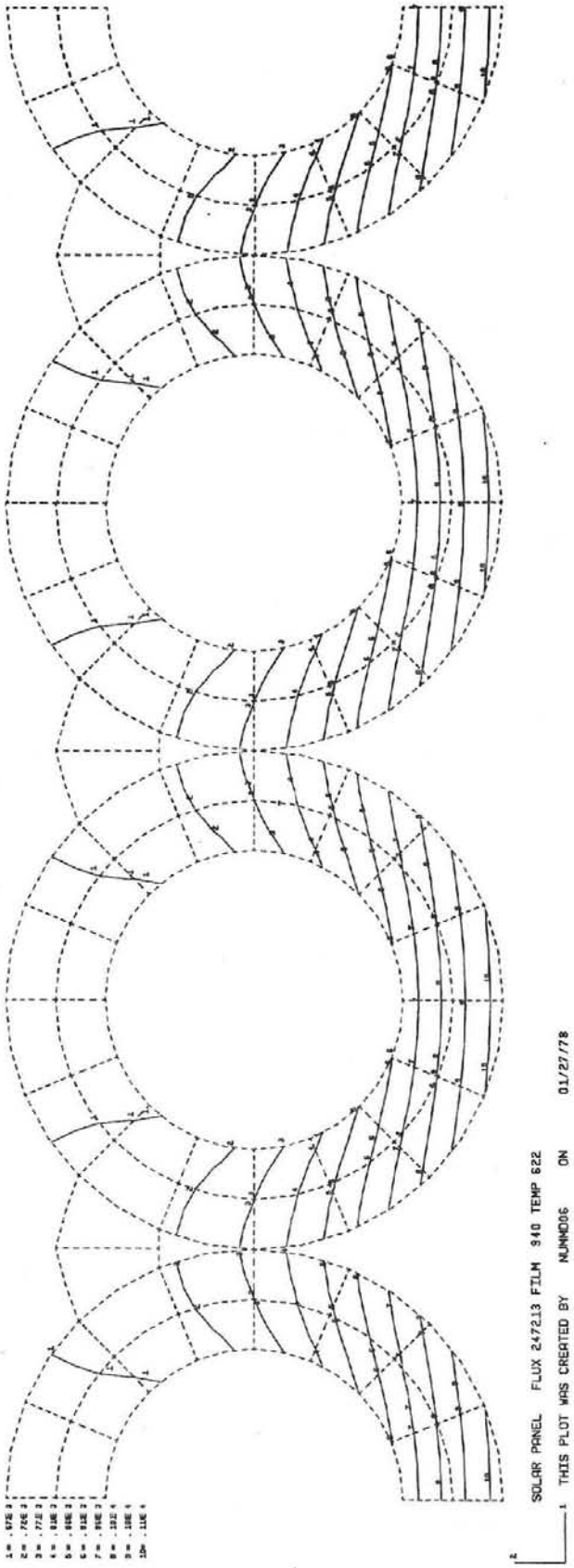
SOLAR PANEL FLUX 247213 FILM 940 TEMP 822
THIS PLOT WAS CREATED BY NUMMOD6 ON 01/27/78

FIGURE 3.6

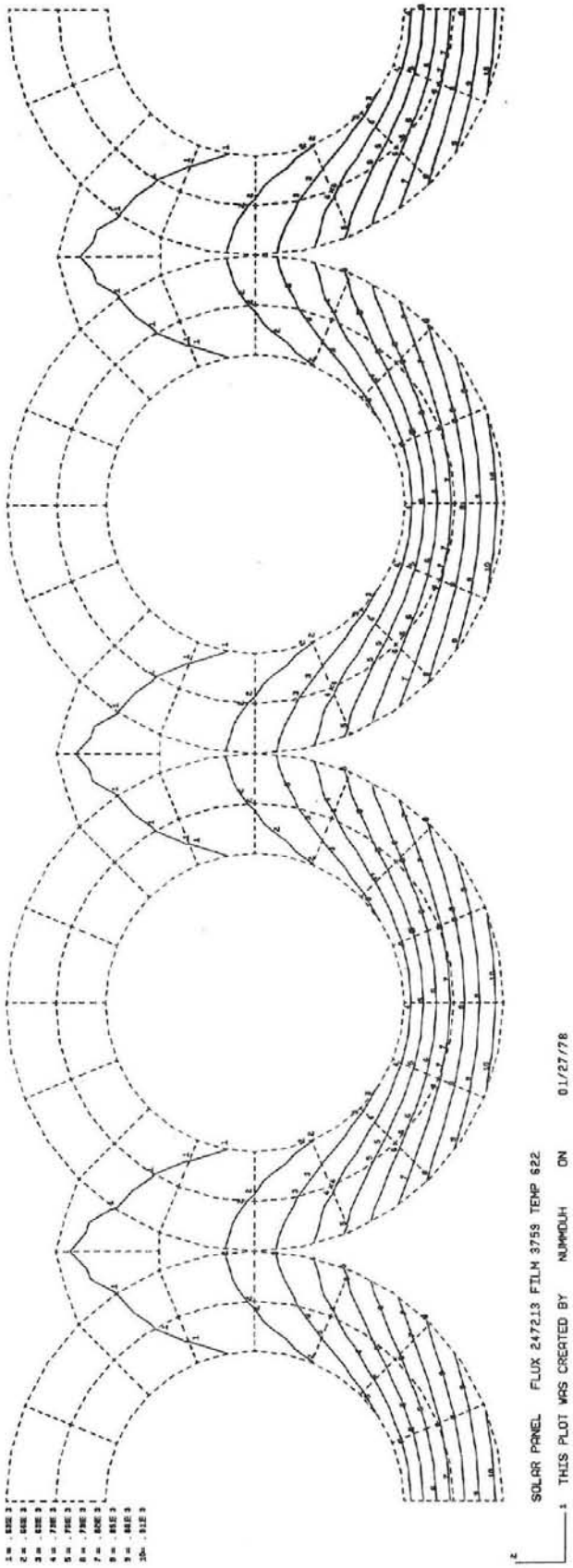
SOLAR PANEL FLUX 247213 FILM 3759 TEMP 622
THIS PLOT WAS CREATED BY NUMMOUH ON 01/27/78

FIGURE 3.7

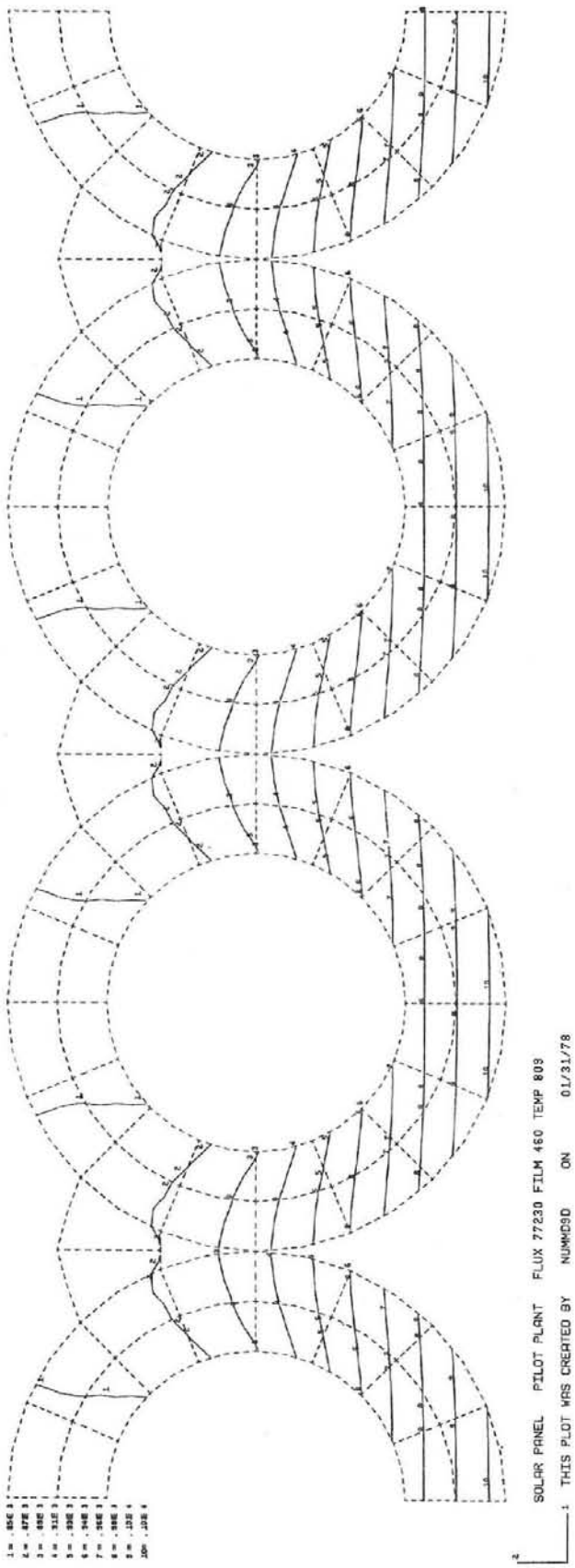
SOLAR PANEL PILOT PLANT FLUX 77230 FILM 460 TEMP 809
THIS PLOT WAS CREATED BY NUMMD9D ON 01/31/78

FIGURE 3.8

FIGURE 3.9

Table 3.4 shows the results of the elastic stress analysis for the highest stressed element for each loading condition (tube crown where the temperature loading is the highest). Stress contour plots for the commercial plant film boiling point are shown in Figures 3.10 to 3.13. These figures illustrate the stress pattern which arises for each case. Figure 3.14 shows the displacement of the model.

3.3 Fatigue Life Assessment

An assessment of the fatigue life of the commercial and pilot plant was made. Since an elastic analysis was performed, cyclic life had to be determined by using the calculated elastic strains. Fatigue life based on high elastic strains is very conservative. To fully evaluate the fatigue life, an inelastic analysis is required to determine the inelastic strain range.

Due to the high elastic strains calculated, it was necessary to modify the elastic strains. J. L. Houtman in the Westinghouse report, "Structural Evaluation of the In-Vessel FFTF Plant Unit Instrument Tree", presented a method to approximate inelastic strain using elastic analysis (Reference 25).

The procedure is as follows:

Step 1 Calculate the elastic stress.

Step 2 Calculate the elastic VonMises effective strain range.

Step 3 Determine the inelastic strain from the elastic strain by multiplying by the appropriate strain correction factor K from Figure 3.15.

Step 4 Using this strain follow up the stress strain curve to a maximum stress value (Figures 3.16, 3.17). Drop down from

TABLE 3.4

Stress Components

Loading Condition No.		σ_x	σ_y	σ_z	τ_{xy}	Von Mises
1	MPa	-30.97	8.07	-328	1.47	318.4
	(psi)	(4,492)	(1171)	(-47,580)	(214)	(46,180)
2	"	44.93	7.88	-44.8	-2.19	472.3
		(6,516)	(1143)	(-64,510)	(-318)	(68,500
3	"	-3.02	7.75	-363	.11	365.6
		(-438)	(1124)	(-52,670)	(16)	(53,030)
4	"	28.17	2.1	-168.6	-1.27	185.1
		(4086)	(305)	(-24,450)	(-184)	(26,850)

TABLE 3.5

Expected Minimum Yield Strength vs. Temperature

Temp., °F	304 SS	316 SS	Ni-Fe-Cr Alloy 800H	2¼ Cr-1 Mo	Ni-Cr-Fe-Cb Alloy 718
			(Stresses in ksi Units)		
RT	30.0	30.0	25.0	30.0	150.0
100	28.8	29.2	24.3	29.4	148.4
200	25.0	25.8	22.5	27.8	143.9
300	22.5	23.3	21.1	26.8	140.7
400	20.7	21.4	20.0	26.6	138.3
500	19.1	19.9	19.0	26.5	136.7
600	18.2	18.8	18.3	26.5	135.4
700	17.7	18.1	17.5	26.5	134.3
750	17.3	17.8	17.2	26.5	133.7
800	16.8	17.6	16.8	26.5	133.1
850	16.5	17.4	16.5	26.3	132.1
900	16.2	17.3	16.3	25.6	131.5
950	15.9	17.1	16.1	24.7	130.5
1000	15.6	17.0	15.8	23.6	129.4
1050	15.2	16.7	15.6	22.1	128.0
1100	14.7	16.5	15.3	20.4	
1150	14.4	16.1	15.0	18.4	
1200	14.1	16.2	14.8	16.1	
1250	13.7	15.8	14.5		
1300	13.2	15.3	14.3		
1350	12.5	14.9	14.0		
1400	11.6	14.1	13.7		
1450	10.6	13.3	13.4		
1500	9.5	13.1	13.0		
1550			12.3		
1600			11.0		

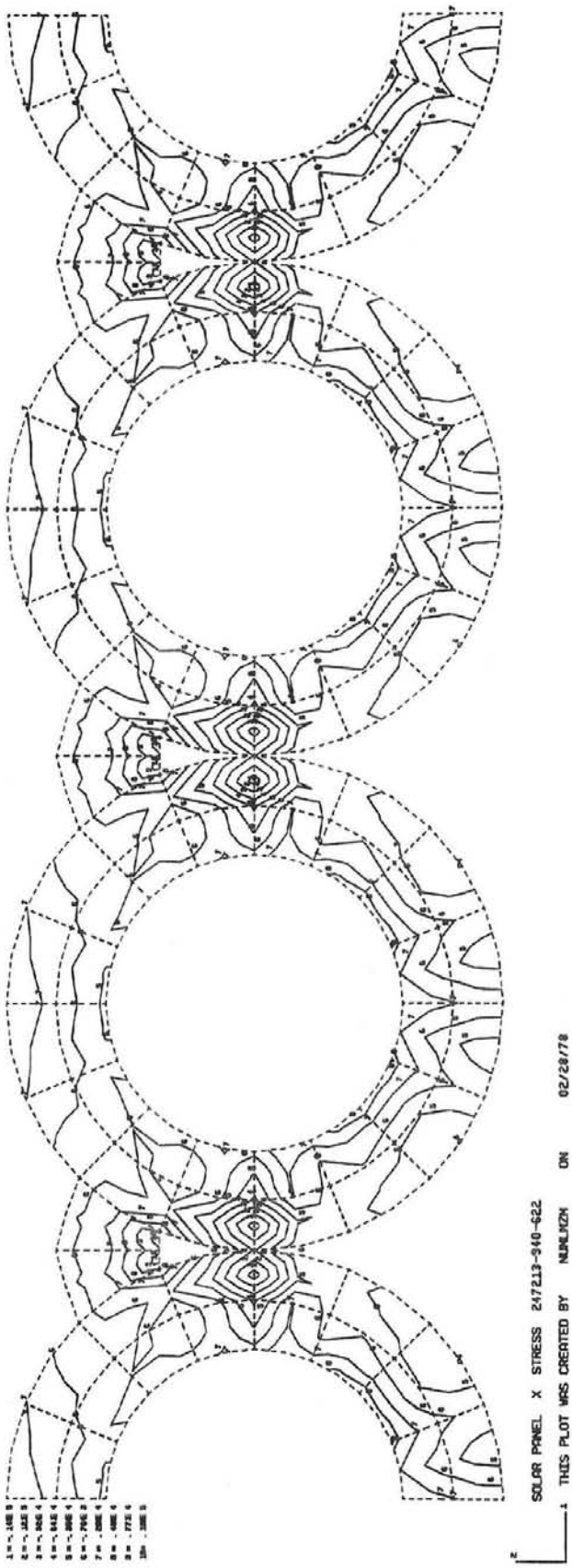
SOLAR PANEL X STRESS 247213-910-622
THIS PLOT WAS CREATED BY NUNLMGN ON 02/28/78

FIGURE 3.10

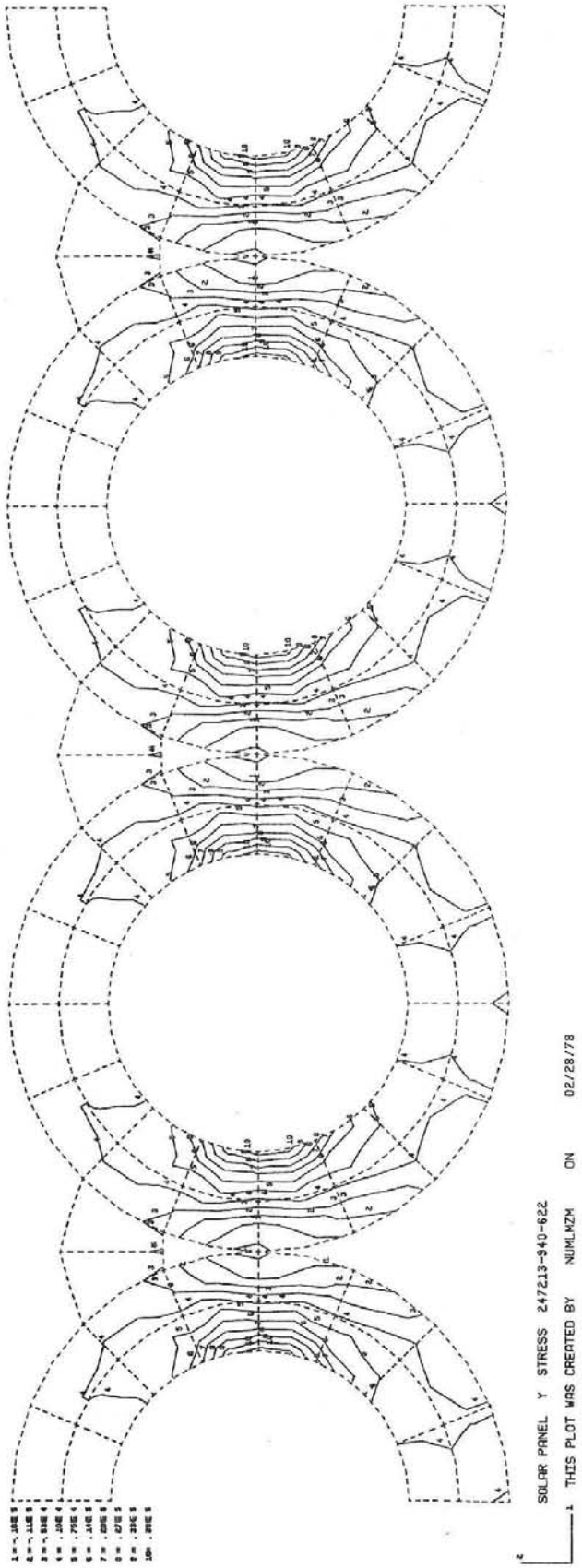
SOLAR PANEL Y STRESS 247213-940-622
THIS PLOT WAS CREATED BY NUMLMZM ON 02/28/78

FIGURE 3.11

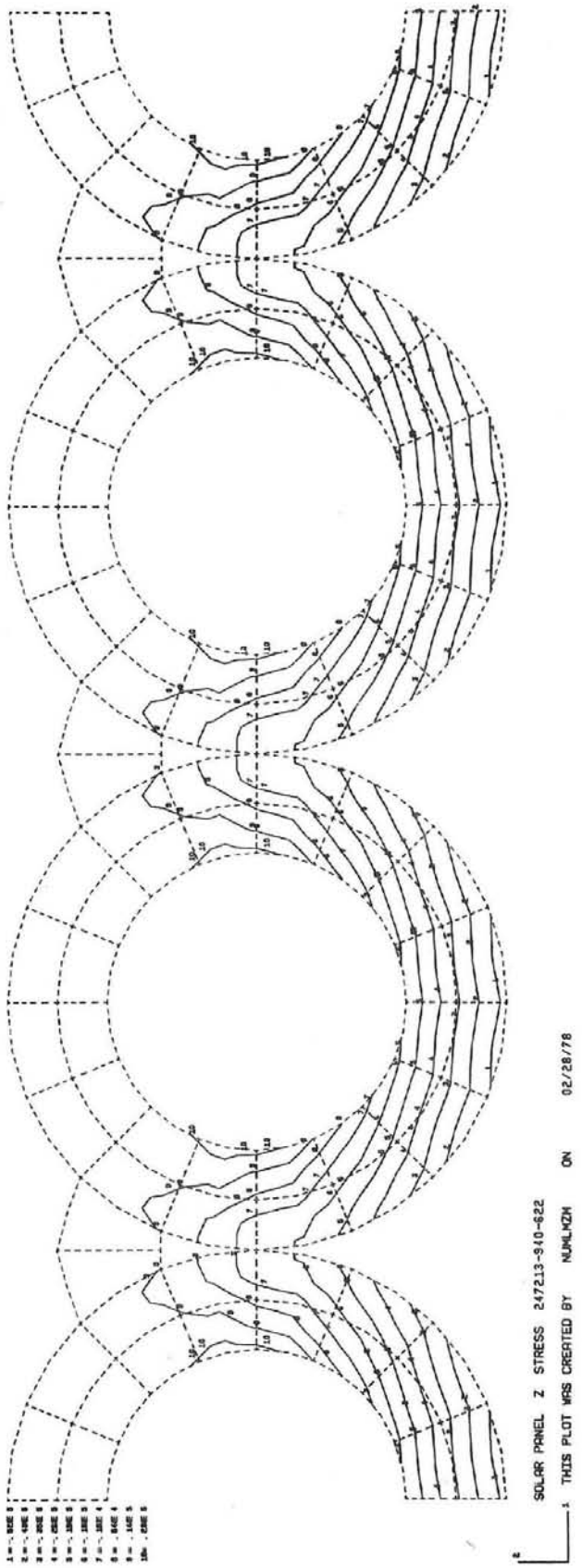
SOLAR PANEL Z STRESS 247213-910-622
THIS PLOT WAS CREATED BY NUMLIKZM ON 02/28/78

FIGURE 3.12

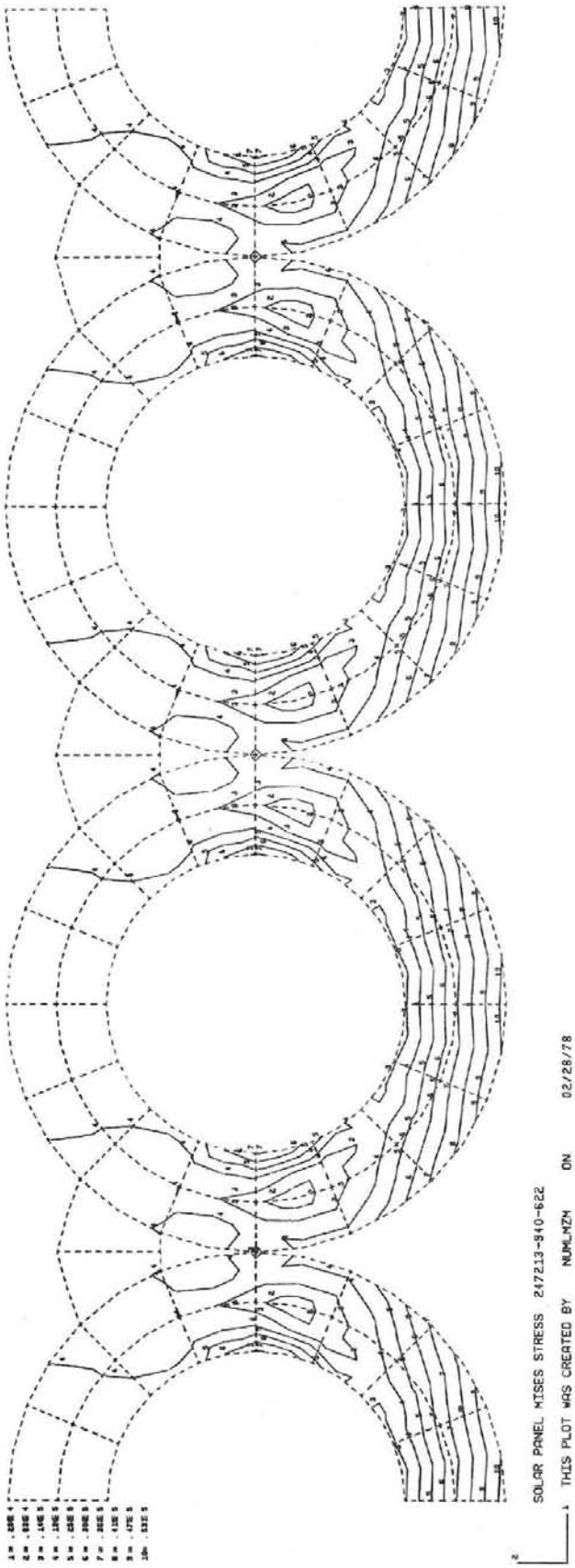
SOLAR PANEL MISES STRESS 247213-940-622
THIS PLOT WAS CREATED BY NUMLMZN ON 02/28/78

FIGURE 3.13

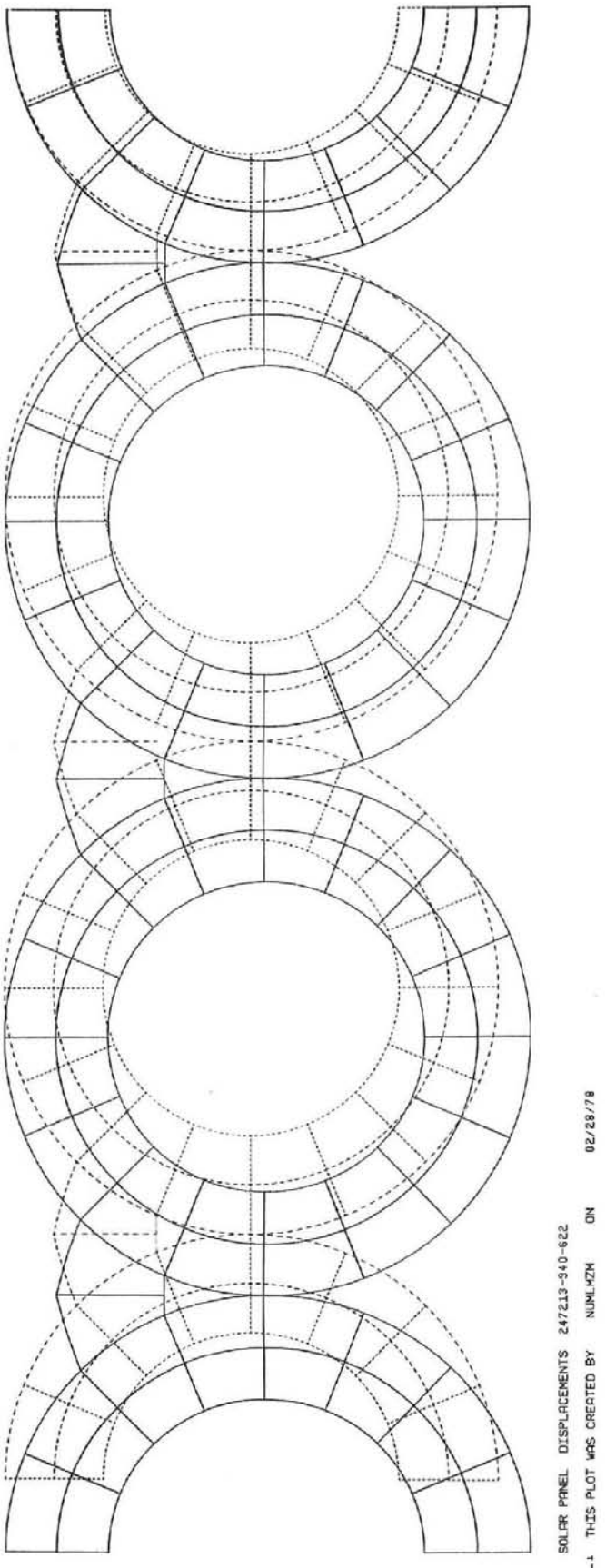
SOLAR PANEL DISPLACEMENTS 247213-940-622
THIS PLOT WAS CREATED BY NUNLMZM ON 02/28/78

FIGURE 3.14

STRAIN CORRECTION FACTOR

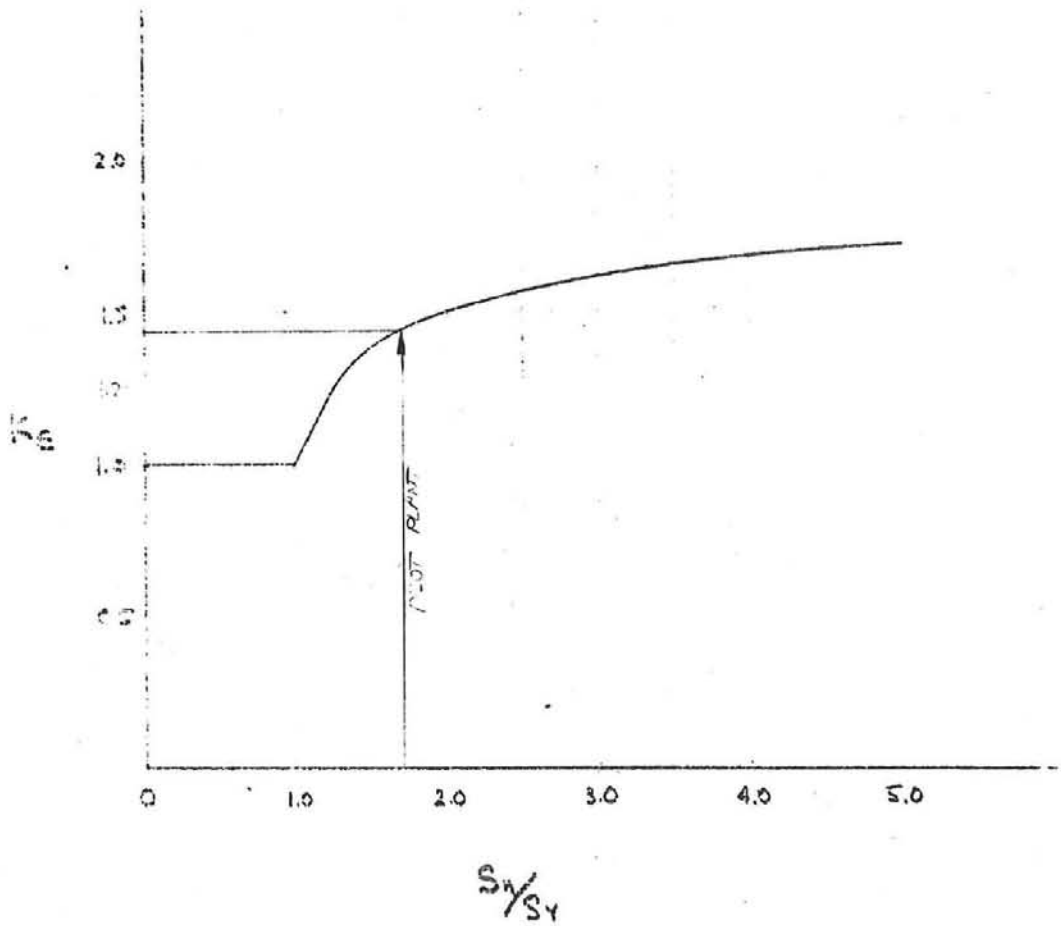

S_n - ELASTIC STRESS

S_y - YEILD STRESS (SEE TABLE 5)

FIGURE 3.15

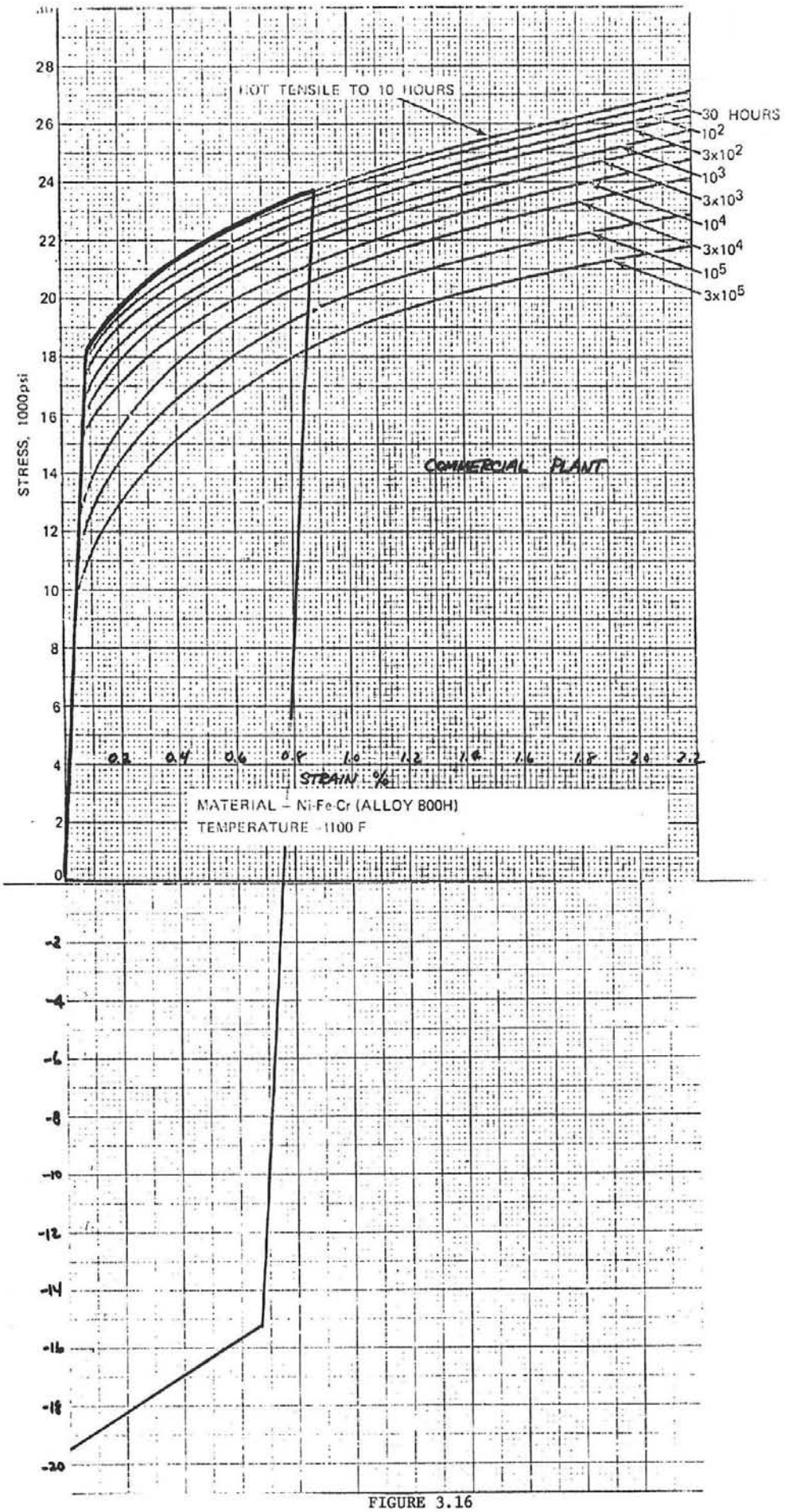
HOT TENSILE TO 10 HOURS
30 HOURS
10^2
$3x10^2$
10^3
$3x10^3$
10^4
$3x10^4$
10^5
$3x10^5$
STRESS, 1000psi
COMMERCIAL PLANT
STRAIN %
MATERIAL – Ni-Fe-Cr (ALLOY 800H)
TEMPERATURE – 1100 F

FIGURE 3.16

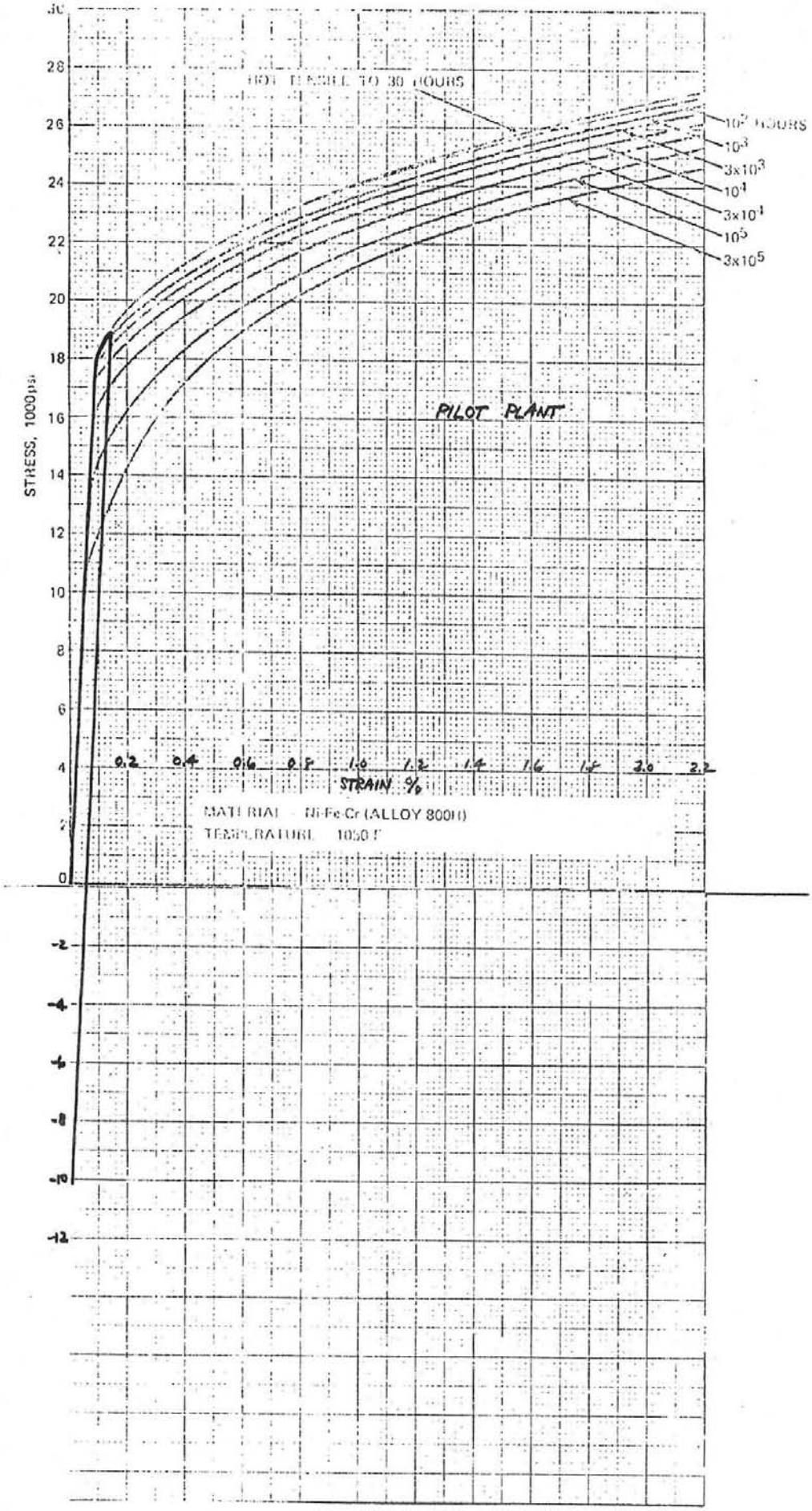
HOT TENSILE TO 30 HOURS
10^{-2} HOURS
10^{-3}
3×10^{-3}
10^{-1}
3×10^{-1}
10^{5}
3×10^{5}
PILOT PLANT
STRESS, 1000psi
STRAIN %
MATERIAL Ni-Fe-Cr (ALLOY 800H)
TEMPERATURE 1050 F

FIGURE 3.17

this point elastically until a comprehensive yield value is reached. Proceed along the plastic slope back to the stress axis at zero strain.

Step 5 Using the determined inelastic effective strain and the appropriate fatigue design curve (Figure 3.18) fatigue damage is evaluated.

Using this method, the fatigue life of the two plants are:

	Strain Range	Cycles
Commercial Plant	8.8×10^{-3}	150
Pilot Plant	1.4×10^{-3}	10^5

This technique calculates the first cycle strain range. Relaxation of this stress with time has not been taken into account. This method produces a conservative fatigue life.

3.4 Thermal Transient Analysis

A thermal analysis was done on the panel headers to determine how the start-up rates would effect fatigue life of the headers. The analysis was done on CREPLACYL, an elastic-plastic-creep analysis program for long, thick-walled cylinders.

Input into the program includes header geometry, film coefficients, material properties and fluid heat-up rates. Stress concentration factors due to header tees were included in the analysis. Exact dimensions of the panel headers could not be obtained from the design reports. Based on dimensioned figures, approximate dimensions were used (inside radius 76.2 mm (3 inches), thickness 25.4 mm (1 inch). The entire start-up loading profile for the unit was not contained

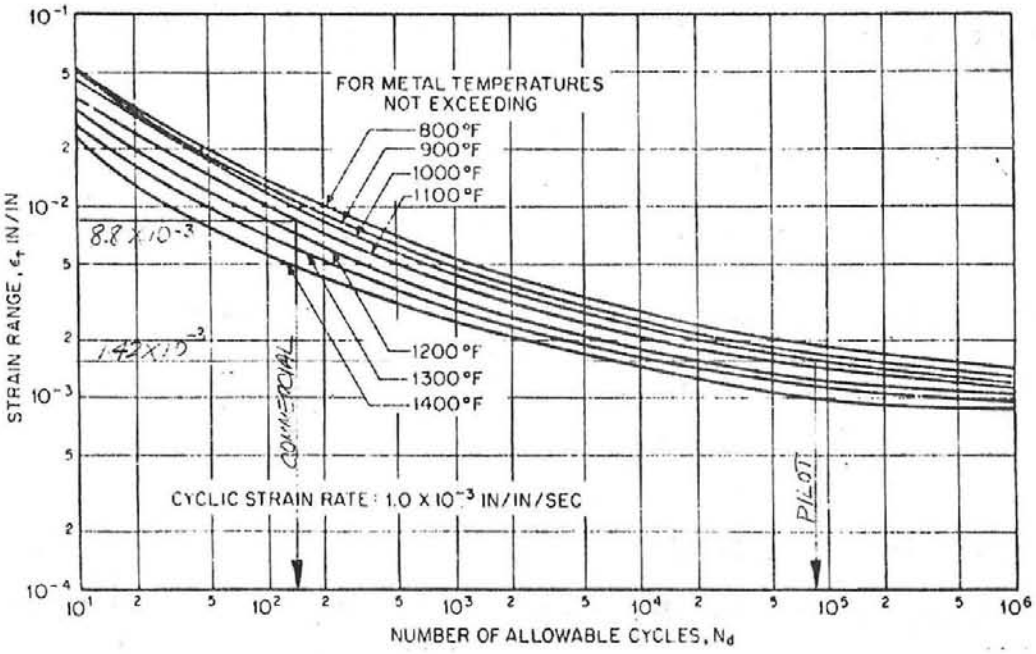

FIGURE 3.18

Design Fatigue Strain Range
ϵ_t for Incalloy 800

in the report, although the report stated that within the start-up cycle, the maximum fluid temperature rise was 482°C (900°F/hr) for 20 minutes.

Results of the cycling indicated header fatigue life due to this loading was greater than 10^5 cycles. However, this is only a small portion of the start-up cycle. A full start-up, shut-down loading history is needed in order to provide a better indication of header life.

3.5 Thin Tube Analysis

The tube thickness from the design report is significantly greater than the minimum wall thickness from the ASME Boiler and Pressure Vessel Code. Because of less metal resistance, a thin tube provides better heat flow to the fluid. An analysis was performed to determine what reduction in stress would occur if the minimum ASME wall thickness was used.

From Section I - Power Boilers, Pg 27, the minimum allowable tubing thickness is defined as:

$$t = \frac{PD}{2S+P} + 0.005D + e$$

where: P = maximum allowable working pressure

D = outside diameter of cylinder

S = maximum allowable stress value at the operating temperature of the metal

e = thickness factor for expanded tube ends

For the operating conditions:

P = 11.72 MPa (1700 psi)

D = 12.7 mm (0.5 in.)

S = 47.6 MPa (6900 psi) (800H at 1260°F)

e = 0

The calculated minimum wall thickness is

t = 1.448 mm (0.057 in.)

A thermal and stress analysis was performed using a heat flux of .757 MW/m^2 (239,862 BTU/hr ft^2), film coefficient .011 MW/m^2 (1907 BTU/hr ft^2 °F), and fluid temperature 425°C (798°F) and compared to the previous analysis with the same loading with the tube thickness of 2.54 mm (0.1 in.).

The tube crown temperature (and the front to back temperature gradient) was reduced by 41.7°C (107°F). The axial stress was reduced 30%. This reduced the effective stress from 365 MPa (53,000 psi) to 293 MPa (42,500 psi). Using the same method as outlined in Section 4.3, a fatigue life of 4500 cycles was calculated. This jump in life from 1100 to 4500 was due not only to the reduction in stress but also the reduction in tube crown temperature.

3.6 Ferritic Material Tube Analysis

Ferritic steels have a much better heat conductivity than stainless steels and consequently better thermal performance. However, at high temperatures ferritic steels have poor creep resistance. An analysis was done using the material properties for an advanced ferritic and compared to the Incoloy 800H analysis. Table 3.6 compares the material properties for the ferritic and Incoloy 800H.

Using ferritic material properties, a thermal and stress analysis was performed using a heat flux .757 MW/m^2 (239,862 BTU/hr ft^2), film

TABLE 3.6

Comparison of Ferritic and Incoloy

	SC/510 (950)	800H/510 (950)
Thermal Expansion		
C^{-1}	1.404×10^{-5}	1.8×10^{-5}
(F^{-1})	(7.8×10^{-6})	(10×10^{-6})
Thermal Conductivity		
W/m·K	29.41	19.55
(BTU/hr ft F)	(17)	(11.3)
Specific Heat		
J/kg·K	669.9	669.9
(BTU/lbm ^{o}F)	(.16)	(.16)
Modules of Elasticity		
MPa	$.16 \times 10^{6}$	$.16 \times 10^{6}$
(psi)	(23.3×10^{6})	(23.8×10^{6})
Yield Strength		
MPa	176.5	111
(psi)	(25,600)	(16,100)

TABLE 3.7

Tube Crown Temperatures

Loading No.	Thickness mm	Thickness in.	Material	Crown Temp. °C	Crown Temp. (°F)	ΔT (Tube) °C	ΔT (Tube) (°F)
4 - Pilot Plt	2.54	(.1)	800H	557	(1035)	103	(186)
2 - Comm Plt	2.54	(.1)	800H	607	(1125)	258	(464)
1 - Comm Plt	2.54	(.1)	800H	497	(926)	166	(299)
3 - Comm Plt	2.54	(.1)	800H	628	(1162)	196	(353)
3 - Comm Plt	1.488	(.057)	800H	568	(1055)	143	(257)
3 - Comm Plt	2.54	(.1)	9Cr	580	(1077)	147	(264)

TABLE 3.8

Fatigue Life Comparison - 100 MW

Loading	Thickness mm	Thickness (in.)	Material	Effective Stress MPa	Effective Stress (psi)	Fatigue Life Cycles
2	2.54	(.1)	800H	472	(68,500)	200
1	2.54	(.1)	800H	318	(46,200)	5,000
3	2.54	(.1)	800H	365	(53,000)	1,100
3	1.448	(.057)	800H	293	(42,500)	4,500
3	2.54	(.1)	9Cr	273	(39,600)	3,500
3	1.448	(.057)	9Cr	248	(36,000)	10,000

coefficient .011 MW/m^2 ^oC (1907 BTU/hr ft^2 ^oF) and fluid temperature 426^oC (798^oF) and compared to the same loading using 800H material properties. The tube crown temperature was reduced by 29^oC (85^oF) The axial stress was reduced from -363 MPa (-52,700 psi) to -257 MPa (-37,300 psi). This reduced the effective stress 25%. A fatigue life of 3500 cycles was calculated. This fatigue calculation does not include effects of creep. Because of low creep resistance of ferritics at 581^oC (1077^oF) (tube crown temperature), the calculated fatigue life would be reduced.

SECTION 4

PROPOSED REDESIGN WITH RIFLED TUBING

4.1 Introduction

The design review of the DOE/MDAC once-through central receiver for the 100 MWe commercial plant indicated that the anticipated service life for the receiver is severely restricted, due to the thermal stresses created mainly by the high heat fluxes incident on the north side receiver panels, coupled with a low film boiling coefficient. Because of the cyclic operating conditions expected, these high stresses have a large impact on the fatigue life. These thermal stresses are most severe at two locations on the panels, in the CHF-film boiling zone, and in the superheater zone of the once-through panels. Possible solutions to these problems areas are to: 1) lower the heat flux and thereby increase the receiver surface, and 2) rearrange the heat surface to take advantage of turbulators to enhance the evaporative heat absorption process. In the first solution thermal efficiency would be sacrificed, and the cost and weight would increase. In the second case, a preliminary analysis indicates that a rearrangement of circuits is possible, which will maintain the same heat flux and receiver size without significant loss of overall efficiency. This redesign of absorption circuitry assumes the efficient performance of rifled tubing in the evaporator region.

4.2 Description of Proposed Redesign

The basic arrangement of the external central receiver remains intact, as seen in Figure 4.1, with 24 separate panels. Assuming symmetry about the N-S axis, the 12 panels are divided as follows: 1-6 are evaporator panels, each producing a slight superheat temperature. Each is individually controlled with subcooled water entering at the bottom. This section of the receiver is identical with the DOE/MDAC design except that the panel tubes are replaced with rifled tubes of approximately 12.7 mm

KEY PLAN

EXTERNAL CENTRAL RECEIVER

Symmetrical about N-S Axis

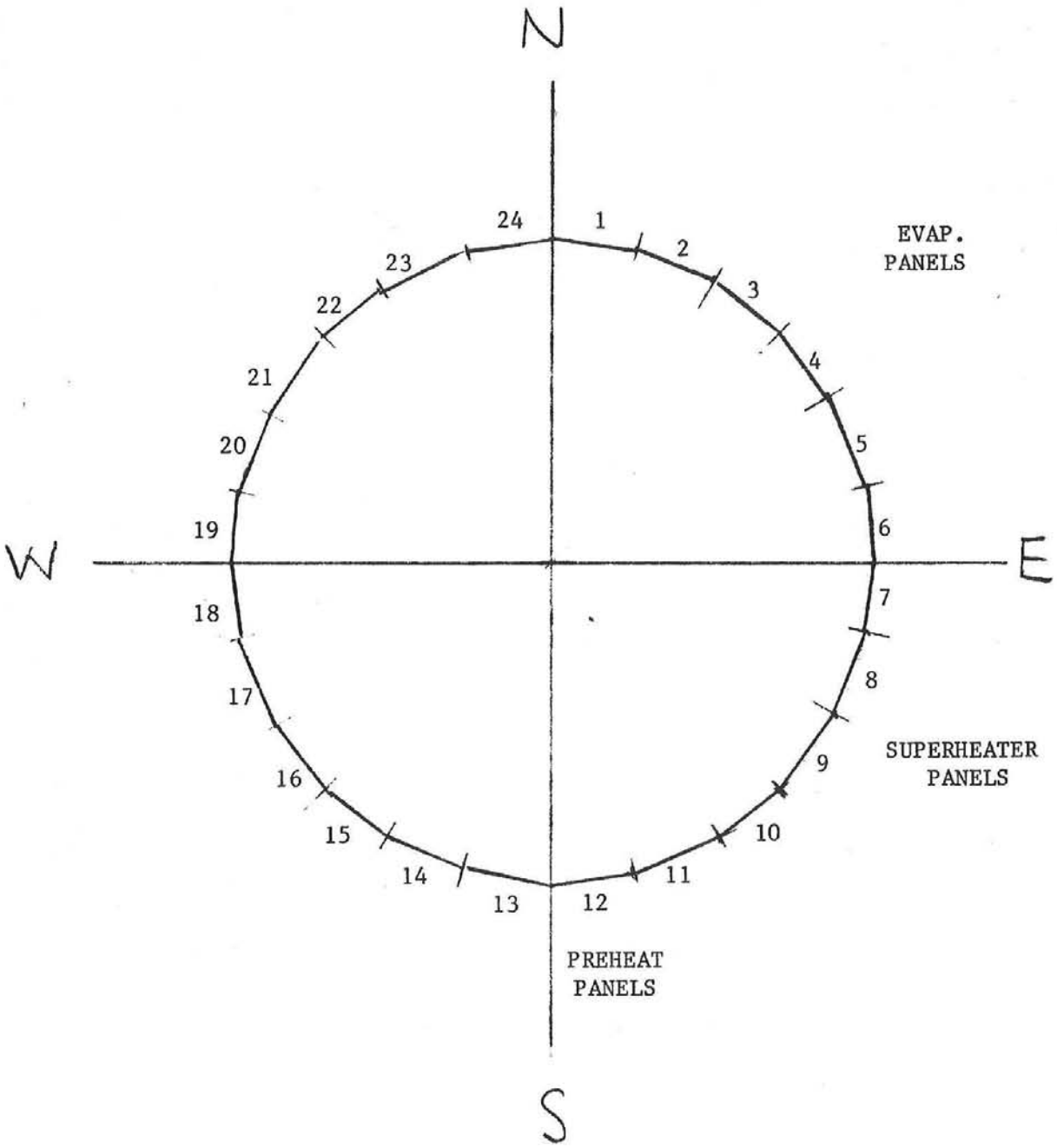

FIGURE 4.1

(1/2") O.D. Performance of the rifled tubing is assumed to eliminate DNB and film boiling. If the rifled tubing performance is proven to be as efficient as is indicated, nucleate boiling may exist all the way to 100% quality. This would allow the high heat flux to be retained without the associated problems with high thermal stress.

Panels 1-6 discharge 343°C (650°F) steam into a collecting header, where it is routed to the superheater portion of the receiver, represented by panel Nos. 7-10. These panels have a lower average heat flux than Nos. 1-6, and are therefore more adapted for superheating. Two possible arrangements were analyzed. One was a series arrangement with 38 mm (1.5") O.D. tubes and the other was a series/parallel arrangement using 25.4 mm (1") O.D. tubes. Both produce approximately 510°C (950°F) rated steam. See Figure 4.2 and Figure 4.3. Preliminary calculations indicate that the metal temperatures are not as high as in the present design, and the temperature differences are lower, resulting in apparent lower stress values. Again, the crux of this design is the potential of the rifled tubing for elimination of the CHF/film boiling phenomena.

The thermal analysis program was utilized in the prediction of the performance of each panel involved in the redesign. Table 4.1 shows the physical dimensions of the various panels, tubes, and selected values of conductivity. In anticipation of lowered metal temperatures, values of conductivity selected correspond to T-11 and C-steel boiler tubing. This assumption of carbon steel may be too optimistic. Conductivity decreases as temperatures rise, reflecting the conductivity of Incoloy 800H for the high temperature superheater.

Parallel Evaporator - Series Superheater

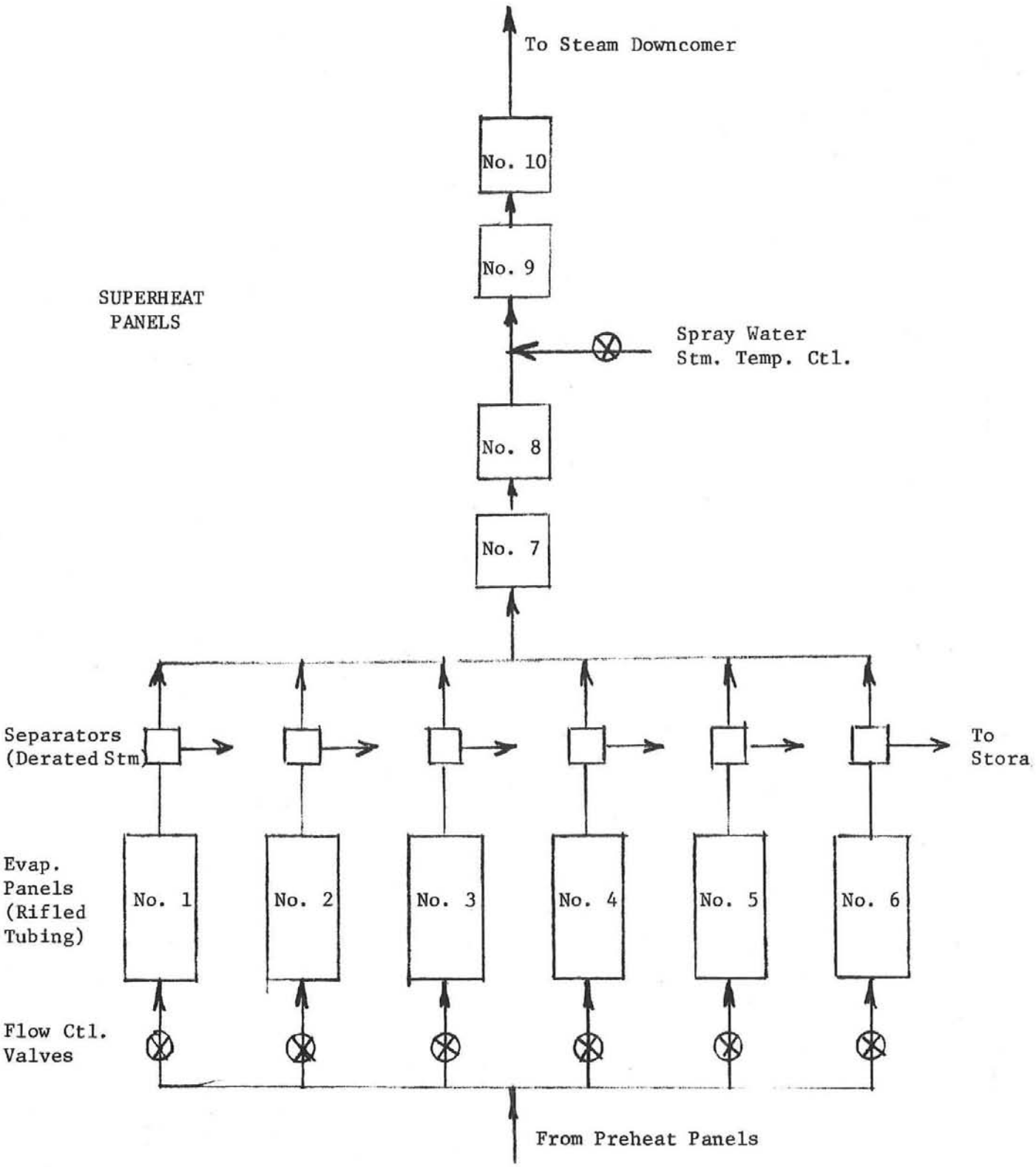

FIGURE 4.2

Parallel Evaporator - Series/Parallel Superheater

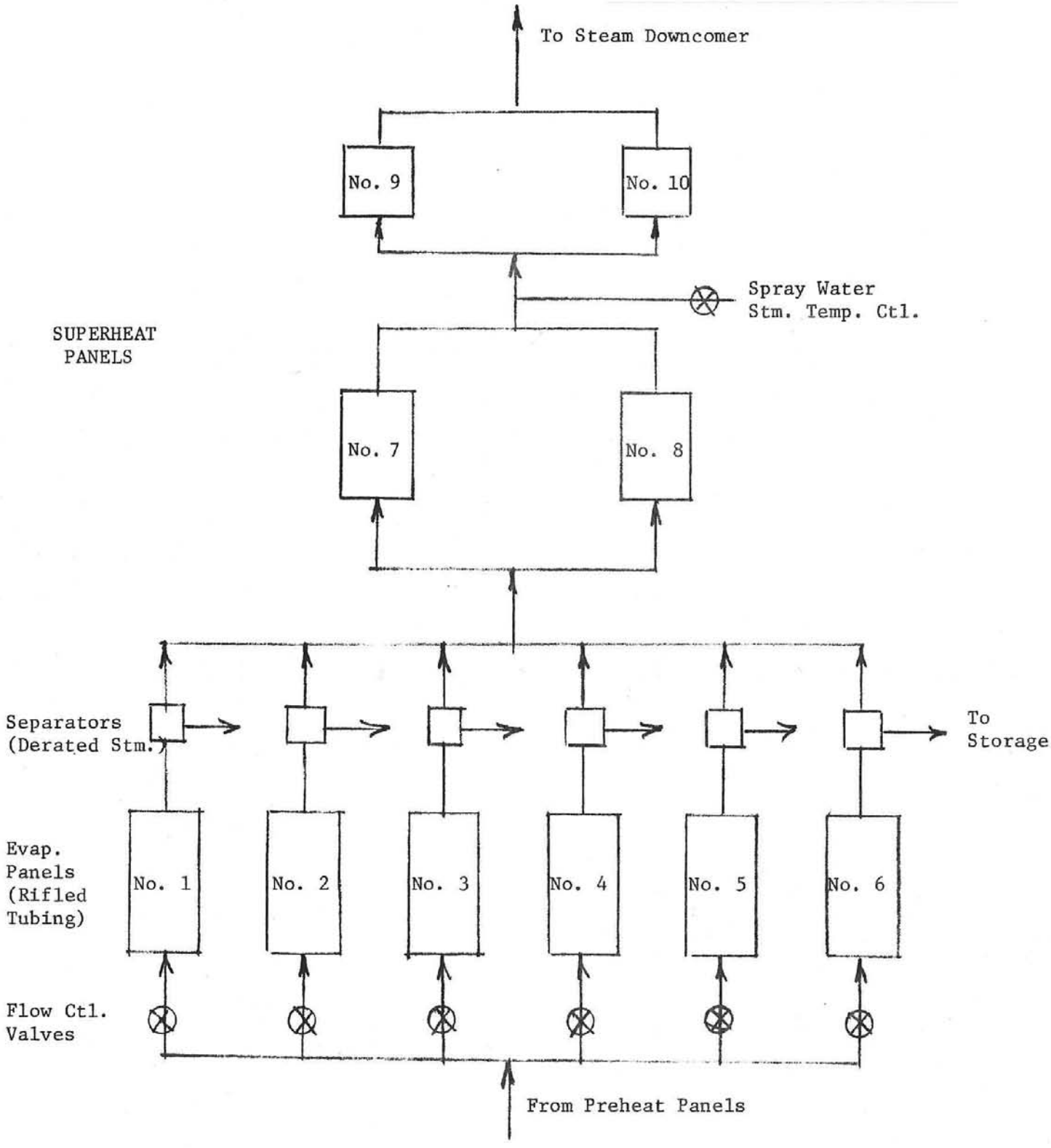

FIGURE 4.3

TABLE 4.1

Alt. Design Using Rifled Tubing Evaporator
Ext. Central Receiver - Physical Dimensions

Series S.H.

Panel No.	Heated Length m	(ft)	Width Ft. m	(ft)	No. Tubes	Tube OD mm	(in)	Tube ID mm	(in)	Tube Condition w/m·k	(BTU/hr ft^2 $^\circ$F)
1-6	25.6	(84)	2.158	(7.083)	170	12.7	(0.5)	10.67*	(0.42)	519.2	(300)
7	25.6	(84)	2.17	(7.125)	57	38.1	(1.50)	32.36	(1.27)	346	(200)
8	25.6	(84)	2.17	(7.125)	57	38.1	(1.50)	32.26	(1.27)	346	(200)
9	25.6	(84)	2.17	(7.125)	57	38.1	(1.50)	32.26	(1.27)	259.6	(150)
10	25.6	(84)	2.17	(7.125)	57	38.1	(1.50)	32.26	(1.27)	259.6	(150)

Series/Parallel S.H.

7	25.6	(84)	2.16	(7.083)	85	2.54	(1.0)	21.6	(0.85)	346	(200)
8	25.6	(84)	21.6	(7.083)	85	2.54	(1.0)	21.6	(0.85)	346	(200)
9	25.6	(84)	2.16	(7.083)	85	2.54	(1.0)	21.6	(0.85)	259.6	(150)
10	25.6	(84)	2.16	(7.083)	85	2.54	(1.0)	21.6	(0.85)	259.6	(150)

*Nominal ID - variable with rifled tube geometry.

Results of the performance analysis appear in Table 4.2. The incident heat flux profiles, projected heated surface area, and loss model were not changed from the MDAC/Rocketdyne commercial receiver. The panel efficiencies remain high, with some reduction in the superheater panels. Overall receiver efficiency, however, was 93.3%. This compares favorably with the original receiver. The series superheater pressure drop is probably too high. The serials/parallel superheater has a better ΔP, and the overall efficiency is not changed. In the series/parallel arrangement streams of different temperatures must be mixed. This should not be a problem, since the temperature difference is not great. This is the preferred arrangement.

Table 4.3 lists maximum metal temperatures, and temperature differences from the tube crown to the rear. These are representative of relative thermal stress levels, and they indicate a 70% reduction of stress over the original design. Maximum tube temperatures are somewhat lower in the superheater, and very much lower in the evaporator section. This is because of the assumption that rifled tubing will be effective in eliminating CHF, thus allowing nucleate boiling to exist to 100% quality.

Figure 4.4 shows typical dimensions of a rifled tube.

4.3 Conclusion

Based on this preliminary analysis, it is concluded that the use of rifled tubing in the evaporator has a potential for significantly increasing the fatigue life of the commercial plant receiver, by eliminating CHF and film boiling, thus reducing the panel thermal stress.

TABLE 4.2

Alternate Design Using Rifled Tubing Evaporator
Predicted Performance Using MDAC Solar Flux
Taken at Sum. Solsitice Noon
(Series Superheater)

Panel No.	P_{in} MPa (psia)	P_{out} MPa (psia)	T_{in} C (^{o}F)	T_{out} C (^{o}F)	Max. Solar Flux MW/m^2 (BTU/hr ft^2)	Mass Flow Kg/s (lb/hr)	G x 10^{-6} Kg/m^2 s_2 (lb/hr ft^2)	Heat Abs. MW (BTU/hr x 10^{-6})	Panel Eff. %
1	12.7 (1850)	11 (1599)	284 (543)	342 (648)	.85 (269,500)	20.6 (163,600)	1333 (0.983)	32.9 (112.23)	95.2*
2	12.7 (1850)	11.2 (1626)	284 (543)	343 (649)	.83 (254,550)	19.5 (154,700)	1261 (0.93)	31 (105.81)	95
3	12.7 (1850)	11.4 (1651)	284 (543)	344 (651)	.76 (239,600)	18.4 (145,900)	1189 (0.877)	29.2 (99.65)	95
4	12.7 (1850)	11.5 (1668)	284 (543)	344 (651)	.72 (228,530)	17.6 (139,700)	1138 (0.839)	27.8 (94.99)	95
5	12.7 (1850)	11.6 (1681)	284 (543)	342 (648)	.69 (217,460)	16.9 (134,100)	1093 (0.806)	26.5 (90.52)	95.2
6	12.7 (1850)	11.8 (1710)	284 (543)	344 (651)	.60 (191,150)	14.9 (118,000)	962 (0.709)	23.3 (79.53)	95.2
7	11 (1600)	10.6 (1536)	343 (650)	383 (722)	.52 (164,840)	108 (856,000)	2315 (1.707)	19.3 (65.91)	91.4
8	10.6 (1536)	10 (1458)	383 (722)	428 (802)	.45 (141,220)	108 (856,000)	2315 (1.707)	16.3 (55.64)	90.1
9	10 (1458)	9.4 (1365)	428 (802)	470 (877)	.37 (117,600)	108 (856,000)	2315 (1.707)	13 (44.51)	86.6
10	9.4 (1365)	8.7 (1257)	469 (877)	502 (936)	.30 (93,980)	108 (856,000)	2315 (1.707)	10 (34.24)	83.3

*Panel efficiency includes radiation and still air conv. losses only.

Total Abs. in Evap. - 582.73 x 10^6 BTU/hr.

Total Abs. in SH = 200.3 x 10^6 BTU/hr. Overal unit efficiency = 93.3%.

TABLE 4.2 (Cont'd.)

Alt. Design Using Rifled Tubing With
Series/Parallel Superheater

Performance of Evap. Panels No. 1-6 Same

Panel No.	P_{in} MPa (psia)	P_{out} MPa (psia)	T_{in} C (^{o}F)	T_{out} C (^{o}F)	Max. Solar Flux MW/m^2 ($BTU/hr\ ft^2$)	Mass Flow Kg/s (lb/hr)	G x 10^{-6} $Kg/m^2\ s$ ($lb/hr\ ft^2$)	Heat Abs. MW ($BTU/hr \times 10^{-6}$)	Panel Eff. %
7	11 (1600)	10.6 (1532)	342 (648)	440 (824)*	.52 (164,840)	53.9 (428,000)	1741 (12.84)	19.2 (65.48)	90.8
8	11 (1600)	10.6 (1534)	342 (648)	422 (792)*	.45 (141,200)	53.9 (428,000)	1741 (1.284)	16.3 (55.64)	90.1
9	10.6 (1533)	9.9 (1443)	431 (808)	518 (964)	.37 (117,600)	53.9 (428,000)	1741 (1.284)	12.8 (43.66)	84.9
10	10.6 (1533)	9.96 (1445)	431 (808)	498 (928)	.296 (93,980)	53.9 (428,000)	1741 (1.284)	10 (34.24)	83.3

*Note: Outlet streams are mixed to produce an average temperature entering the next panel-pair.

Overall unit efficiency = 93.2%.

TABLE 4.3

Alt. Design Using Rifled Tubing Evaporators
Predicted Maximum Tube Temperatures

Panel No.	Max. Tube Temp. C	Max. Tube Temp. (°F)	ΔT* C	ΔT* (°F)	Heat Flux MW/m²	Heat Flux (BTU/hr ft²)	
1	391	(736)	69.4	(125)	.62	(197,518)	
2	390	(734)	67.2	(121)	.59	(186,595)	
3	389	(732)	65	(117)	.55	(175,890)	
4	387	(728)	62.2	(112)	.526	(167,023)	
5	382	(720)	57.8	(104)	.48	(152,571)	
6	380	(717)	54.8	(98)	.42	(133,736)	
7	484	(904)	108	(194)	.47	(149,761)	Series SH
8	517	(963)	96	(173)	.40	(126,176)	Series SH
9	554	(1030)	90.5	(163)	.32	(102,091)	Series SH
10	569	(1056)	71	(128)	.25	(79,125)	Series SH
7	528	(982)	104	(187)	.47	(148,167)	Ser/Par SH
8	497	(927)	88	(158)	.40	(126,962)	Ser/Par SH
9	587	(1088)	81	(145)	.32	(100,767)	Ser/Par SH
10	553	(1027)	64	(115)	.25	(79,799)	Ser/Par SH

* T - Tube Crown - Bulk Liquid)

Note: Based on the assumption that rifled tubing allows nucleate boiling to exist to 100% quality.

Max. metal temps. occur in SH region.

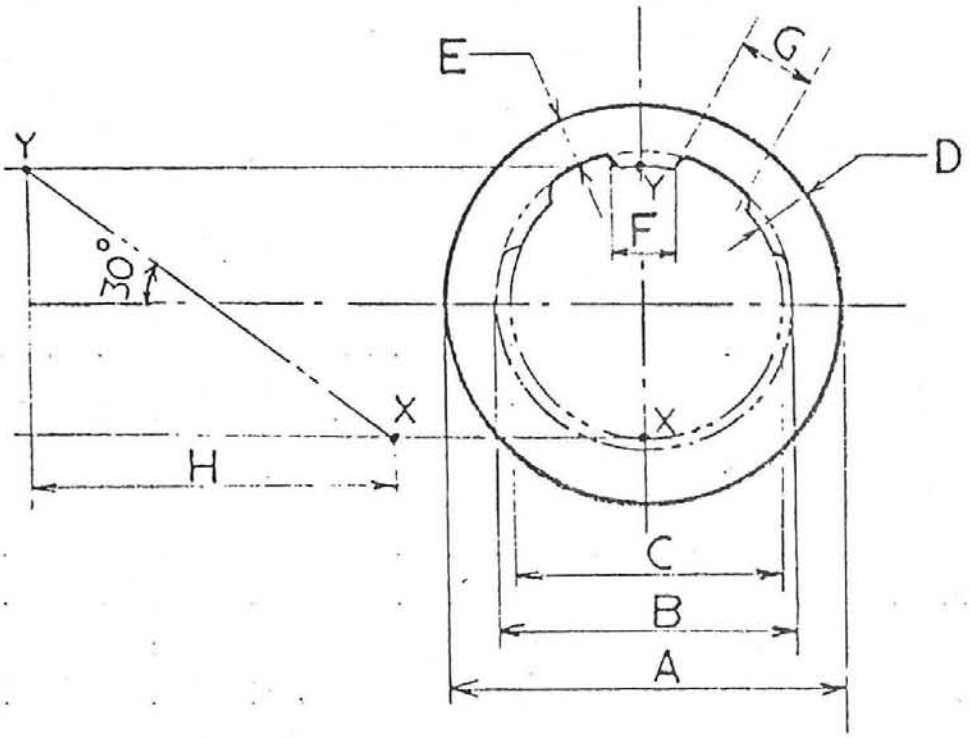

CROSS SECTION OF 6 RIB RIFLED TUBE

NOTATIONS

A	OUTSIDE DIAMETER
B	MAJOR DIAMETER
C	MINOR DIAMETER
D	RIB WALL THICNESS
E	ROOT WALL THICNESS
F	RIB WIDTH
G	ROOT WIDTH
H	RIFLE PITCH (180° TWIST)

FIGURE 4.4

SECTION 5

APPENDICES

APPENDIX A

Thompson-MacBeth Correlation

I. The low velocity correlation for $G \leq 0.3 \times 10^6$ lbm/hr ft^2:

$$\frac{q_{crit}}{10^6} = .00633\, H_{fg}\, D^{-.1} \left(\frac{G}{10^6}\right)^{.51} (1-x)$$

where: q_{crit} = critical heat flux (BTU/hr ft^2) (inside surface)

H_{fg} = heat of evaporation (BTU/lbm)

D = tube I.D. (in.)

G = mass flux (lbm/hr ft^2)

x = critical quality

II. The high velocity correlation for $G > 0.3 \times 10^6$ lbm/hr ft^2:

$$\frac{q_{crit}}{10^6} = \frac{A^1 - \frac{1}{4}D\,(G \times 10^{-6}) \times H_{fg}}{C^1}$$

where: A^1 and C^1 contain Y constants based on pressure ranges.

Constants (Y) were determined from Ref. 15 at 1550 psia.

$$\therefore\ A^1 = 36D^{.509}(G \times 10^{-6})^{-.109}\left[1-.19D+0.24(G \times 10^{-6})+.463D(G \times 10^{-6})\right]$$

$$\text{and } C^1 = 41.7D^{.053}(G \times 10^{-6})^{.0109}\left[1+.231D+.0767(G \times 10^{-6})+.117D(G \times 10^{-6})\right]$$

NOTE: In the thermal analysis program, a linear interpolation is made between 1550 psia and 2000 psia for the above (Y) constants.

APPENDIX B

Groeneveld Film Boiling Correlation

The film boiling coefficient, (h), is given as a function of quality, (x).

$$h = a \frac{Kg}{D} \left[Reg \left(x + \frac{\rho g}{\rho l} (1 - x)\right)\right]^{b} Pr_w^{c} Y^{d} \phi^{e}$$

where:

- h = film coefficient, BTU/hr ft^2 ^oF
- a = 1.85×10^{-4}, const.
- Kg = sat. steam conductivity, BTU/hr ft^2 ^oF
- D = tube diameter, feet.
- Reg = Reynolds Number at sat. steam condition.
- x = local quality
- ρg = density sat. steam
- ρl = density sat. liquid
- b = 1.0, const.
- Pr_w = Prandtl Number evaluated at wall temperature
- c = 1.57, const.
- Y = see below
- d = -1.12, const.
- ϕ = heat flux, BTU/hr ft^2, inside surface
- e = .131, const.

$$Y = 1 - .1 \left(\frac{\rho l}{\rho g - 1}\right)^{.4} (1 - x)^{.4}$$

and $X_{h_{min}}$ is given by

$$(X_{h_{min}} - X_{DNB}) = .045 + \frac{.048}{2.3 - .01\ p}$$

where: p, pressure, is in bar.

APPENDIX C

Description of Thermal Analysis Program

An energy and mass balance is made for each increment of tube length. The heat conduction equations are written for the axisymmetric flow at the tube crown. The incident heat flux is assumed normal to the tube at this point. A correction factor is incorporated into the one-dimensional, axisymmetrical case to correct the crown temperature for the effect of 2-D heat flux and heat flow. The pressure drop is calculated assuming the homogeneous model.

The absorbed crown heat flux is given by:

$$\dot{q}_{abs} = \dot{q}_{inc} \cdot \alpha_s - \sigma\epsilon(T_{s1}^4 - T_o^4) - h_{ext}(T_{s1} - T_o)$$

where:
- $\dot{q}_{abs}$ = absorbed heat flux, BTU/hr ft^2
- $\dot{q}_{inc}$ = incident solar flux, BTU/hr ft^2
- α_s = solar absorptance
- σ = Stefan-Baltzmann Constant
- ϵ = infrared emittance
- h_{ext} = external convection coefficient
- T_{s1} = absolute surface temperature ^{o}R
- T_{so} = absolute ambient temperature ^{o}R

Also, by: $$\dot{q}_{abs} = (T_{s1} - T_f) / \left[D_o \Psi / h_i D_i + (D_o/2K) \ln\left(\frac{D_o}{D_i}\Psi\right)\right]$$

where:
- $\dot{q}_{abs}$ = crown absorbed heat flux, BTU/hr ft^2
- T_{s1} = absolute surface temperature ^{o}R
- T_{sf} = absolute fluid bulk temperature ^{o}R
- D_o = tube outside diameter, inches
- D_i = tube inside diameter, inches
- h_i = inside film convection coefficient, BTU/hr ft^2 ^{o}F
- K = tube conductivity BTU in/hr ft^2 ^{o}F
- Ψ = correction factor for 2-D heat flow.

These 2 equations can be combined into a quartic equation in T_{s1}. This is then solved by formula from a standard math reference:

$$T_{s1}^4 + \left\{ h_{ext}/\sigma\epsilon + 1/\sigma\epsilon\left[D_o\Psi/h_i D_i + (D_o/2K)\,Ln(D_o\Psi/D_i)\right]\right\} T_{s1}$$

$$- \left\{ \dot{q}_{inc}\,\alpha_s/\sigma\epsilon + h_{ext}\,T_o/\sigma\epsilon + T_o^4 + T_f/\sigma\epsilon\left[D_o\Psi/h_i D_i + (D_o/2K)\,Ln(D_o\Psi/D_i)\right]\right\} = 0$$

The 2-D correlation, Ψ, is calculated by an equation of the form:

$$\Psi = B1 + B2\ (BIOT)^{B3}$$

where: B1, B2, B3 are constants that depend on the diameter ratio.

$$BIOT = \frac{HT}{K}$$

where: H = inside film conductance

T = tube thickness

K = tube conductivity

The incremental increase in fluid enthalpy is then calculated from the absorbed heat flux based on the following energy balance:

$$\dot{q}_{net\ in} = \frac{M * \Delta h_f}{\Delta A}$$

where: M = mass flow rate

Δh_f = change in enthalpy

ΔA = incremental area of the element

The program then calculates the fluid quality. If this quality lies between 0 and 1, the critical heat flux is determined and compared to the absorbed heat flux as an indicator of the point at which CHF occurs.

Finally, the pressure drop (ΔP) through the increment of tube length is determined as a function of frictional, momentum, and gravitational components. The detailes of this calculation are as follows:

$$f = 0.46/Re^{.2}$$

where: f = friction factor

Re = Reynold's Number

$$\Delta P_{friction} = 4 \times 10^{-10} \; f \frac{\Delta l}{Di} \; v \; G^2$$

where: Δl = incremental tube length

Di = inside tube diameter

v = average specific volume in increment.

G = mass flow rate per unit area per tube.

$$\Delta P_{momentum} = 1.667 \times 10^{-11} \; (v_2 - v_1) \; G^2$$

where: v_2 = element outlet sp. vol.

v_1 = element inlet sp. vol.

$$\Delta P_{gravity} = \frac{\Delta l}{144 \; v}$$

$$\Delta P_{total} = \Delta P_{friction} + \Delta P_{momentum} + \Delta P_{gravity}$$

Pressure at the increment's exit is then simply:

$$P = P_{in} - \Delta P_{total}$$

The inside film coefficient for use in the above equations is determined by the following correlations, depending on the fluid state existing in a particular element.

1. Single phase, liquid and vapor: (Dittus-Boelter)

$$\frac{hD}{K} = .023 \; Re^{.8} \; Pr^{.4}$$

2. Two-phase, nucleate boiling region:

$$h = 5000 \text{ BTU/hr ft}^2 \; ^{o}F$$

3. Film boiling region: (Groeneveld correlation, Appendix B)

4. Transitional boiling region (X_c to $X_{h_{min}}$):

   A linear interpolation is made between $h_i = 5000$ and $h_i = h_{min}$, from the Groeneveld Correlation.

The program recalculates the above variables for each increment of the tube length. If desired, the program will test the final increment output for proper steam temperature. The program will then automatically adjust the flow rate and recalculate the above parameters until the desired steam temperature is achieved.

BOILER PANEL NO. 1
(USING GROENEVELD CORRELATION)

COMMERCIAL PLANT

PRESS PSIA	TEMP F	ENTHALPY BTU/LB	L1 FT	L2 FT*	NO.TUBES	TUBE OD IN	*TUBE ID IN	TUBE LGTH FT	INCREMENT FT
1850.	550.	560.	27.7	67.2	170	0.50	0.27	84.	0.50

CONDUCTIVITY B-IN/H-SF-F	EXT.COEFF B/H-SF-F	EMISSIVITY *	ABSORPTANCE	*AMB.TEMP F	MAX.SOLAR FLUX BTU/HR-SQFT
150.	3.	0.89	0.95	100.	269500.

TUBE LGTH FT	PRESS PSIA	BULK TEMP F	ENTHALPY BTU/LB	INSIDE FILM COEF B/H-SF-F	OUTSIDE HEAT FLUX B/H-SF	TUBE *CROWN TEMP F	BULK QUAL	CRIT QUAL
0.50	1849.6	557.	560.	4992.	2470.	559.	-.19	0.0
1.00	1849.3	557.	560.	4992.	7051.	564.	-.19	0.0
1.50	1848.9	557.	561.	4993.	11474.	569.	-.19	0.0
2.00	1848.5	558.	561.	4994.	16056.	575.	-.19	0.0
2.50	1848.2	558.	562.	4995.	21142.	581.	-.19	0.0
3.00	1847.8	559.	562.	4996.	25624.	586.	-.19	0.0
3.50	1847.4	559.	563.	4998.	29924.	591.	-.18	0.0
4.00	1847.1	560.	564.	5001.	34388.	597.	-.18	0.0
4.50	1846.7	561.	566.	5003.	39268.	603.	-.18	0.0
5.00	1846.3	562.	567.	5006.	43584.	609.	-.18	0.0
5.50	1846.0	563.	568.	5009.	48375.	615.	-.17	0.0
6.00	1845.6	564.	570.	5013.	53010.	621.	-.17	0.0
6.50	1845.2	566.	572.	5017.	57558.	627.	-.17	0.0
7.00	1844.9	567.	573.	5022.	61891.	633.	-.16	0.0
7.50	1844.5	569.	575.	5027.	66641.	640.	-.16	0.0
8.00	1844.1	570.	578.	5032.	71116.	646.	-.15	0.0
8.50	1843.8	572.	580.	5037.	75349.	653.	-.15	0.0
9.00	1843.4	574.	582.	5044.	79846.	659.	-.14	0.0
9.50	1843.0	576.	585.	5051.	84642.	666.	-.14	0.0
10.00	1842.6	578.	587.	5058.	89289.	673.	-.13	0.0
10.50	1842.3	580.	590.	5066.	93573.	680.	-.13	0.0
11.00	1841.9	583.	593.	5075.	98343.	687.	-.12	0.0
11.50	1841.5	585.	596.	5085.	102625.	694.	-.12	0.0
12.00	1841.2	587.	599.	5096.	107407.	702.	-.11	0.0
12.50	1840.8	590.	603.	5107.	111988.	709.	-.10	0.0
13.00	1840.4	593.	606.	5120.	116178.	716.	-.10	0.0
13.50	1840.1	596.	610.	5134.	120753.	724.	-.09	0.0
14.00	1839.7	598.	613.	5150.	125579.	732.	-.08	0.0
14.50	1839.3	601.	617.	5168.	129713.	739.	-.07	0.0
15.00	1838.9	604.	621.	5185.	134486.	747.	-.06	0.0
15.50	1838.6	606.	625.	5203.	138801.	754.	-.06	0.0
16.00	1838.2	609.	630.	5222.	143368.	762.	-.05	0.0
16.50	1837.8	612.	634.	5244.	147908.	769.	-.04	0.0
17.00	1837.4	615.	639.	5269.	152365.	777.	-.03	0.0
17.50	1837.1	618.	643.	5296.	156945.	784.	-.02	0.0
18.00	1836.7	621.	648.	5328.	161647.	792.	-.01	0.0
18.50	1836.3	624.	653.	5363.	165847.	800.	0.00	0.0
19.00	1835.8	624.	658.	5000.	170497.	810.	0.01	0.0
19.50	1835.2	624.	663.	5000.	174968.	815.	0.02	0.0
20.00	1834.5	624.	669.	5000.	179418.	820.	0.03	0.0
20.50	1833.7	624.	674.	5000.	183872.	824.	0.04	0.0
21.00	1832.8	624.	680.	5000.	188620.	829.	0.05	0.0
21.50	1831.7	623.	685.	5000.	193026.	834.	0.07	0.0
22.00	1830.5	623.	691.	5000.	197731.	839.	0.08	0.0
22.50	1829.2	623.	697.	5000.	202063.	844.	0.09	0.0
23.00	1827.8	623.	703.	5000.	206786.	849.	0.10	0.0

23.50	1826.2	623.	710.	5000.	211259.	854.	0.12	0.0
24.00	1824.5	623.	716.	5000.	215904.	859.	0.13	0.0
24.50	1822.7	623.	723.	5000.	220178.	863.	0.14	0.0
25.00	1820.7	623.	729.	5000.	224781.	868.	0.16	0.0
25.50	1818.5	623.	736.	5000.	229301.	873.	0.17	0.17
26.00	1817.8	622.	743.	4983.	234024.	878.	0.18	0.18
26.50	1817.0	622.	750.	4352.	238367.	890.	0.20	0.20
27.00	1816.2	622.	757.	3710.	242581.	906.	0.21	0.21
27.50	1815.4	622.	765.	3057.	246862.	926.	0.23	0.23
28.00	1814.6	622.	772.	2392.	248189.	952.	0.24	0.24
28.50	1813.7	622.	780.	1724.	247327.	992.	0.26	0.26
29.00	1812.8	622.	787.	1059.	245224.	1076.	0.27	0.27
29.50	1811.9	622.	794.	944.	244578.	1100.	0.29	0.29
30.00	1811.0	622.	801.	975.	244800.	1093.	0.30	0.30
30.50	1810.0	622.	809.	1006.	244969.	1086.	0.32	0.32
31.00	1809.0	622.	816.	1037.	245107.	1080.	0.33	0.33
31.50	1808.0	622.	823.	1067.	245252.	1074.	0.35	0.35
32.00	1807.0	622.	831.	1098.	245358.	1068.	0.36	0.36
32.50	1805.9	622.	838.	1128.	245575.	1063.	0.38	0.38
33.00	1804.8	621.	845.	1158.	245632.	1058.	0.39	0.39
33.50	1803.7	621.	852.	1187.	245813.	1053.	0.40	0.40
34.00	1802.6	621.	860.	1217.	245902.	1048.	0.42	0.42
34.50	1801.4	621.	867.	1246.	246017.	1044.	0.43	0.43
35.00	1800.2	621.	874.	1274.	246125.	1040.	0.45	0.45
35.50	1799.0	621.	882.	1303.	246214.	1036.	0.46	0.46
36.00	1797.8	621.	889.	1331.	246364.	1032.	0.48	0.48
36.50	1796.5	621.	896.	1359.	246399.	1028.	0.49	0.49
37.00	1795.2	621.	904.	1386.	246481.	1025.	0.51	0.51
37.50	1793.9	621.	911.	1413.	246659.	1021.	0.52	0.52
38.00	1792.6	621.	918.	1440.	246627.	1018.	0.54	0.54
38.50	1791.2	620.	926.	1466.	246709.	1015.	0.55	0.55
39.00	1789.8	620.	933.	1492.	246775.	1012.	0.57	0.57
39.50	1788.3	620.	940.	1518.	246950.	1009.	0.58	0.58
40.00	1786.9	620.	948.	1544.	246914.	1007.	0.59	0.59
40.50	1785.4	620.	955.	1569.	246919.	1004.	0.61	0.61
41.00	1783.9	620.	962.	1593.	247108.	1002.	0.62	0.62
41.50	1782.3	620.	970.	1617.	247130.	999.	0.64	0.64
42.00	1780.8	620.	977.	1641.	247268.	997.	0.65	0.65
42.50	1779.2	619.	984.	1665.	247220.	995.	0.67	0.67
43.00	1777.6	619.	992.	1688.	247277.	993.	0.68	0.68
43.50	1775.9	619.	999.	1710.	247314.	991.	0.70	0.70
44.00	1774.2	619.	1007.	1732.	247454.	989.	0.71	0.71
44.50	1772.5	619.	1014.	1754.	247460.	987.	0.72	0.72
45.00	1770.8	619.	1021.	1775.	247382.	985.	0.74	0.74
45.50	1769.0	619.	1029.	1795.	247517.	983.	0.75	0.75
46.00	1767.2	619.	1036.	1815.	247497.	982.	0.77	0.77
46.50	1765.4	618.	1043.	1835.	247572.	980.	0.78	0.78
47.00	1763.6	618.	1051.	1853.	247522.	978.	0.80	0.80
47.50	1761.7	618.	1058.	1871.	247728.	977.	0.81	0.81
48.00	1759.8	618.	1065.	1889.	247678.	976.	0.83	0.83
48.50	1757.8	618.	1073.	1906.	247720.	975.	0.84	0.84
49.00	1755.9	618.	1080.	1921.	247736.	973.	0.85	0.85
49.50	1753.9	618.	1088.	1936.	247757.	972.	0.87	0.87
50.00	1751.9	617.	1095.	1950.	247842.	971.	0.88	0.88
50.50	1749.8	617.	1102.	1963.	247905.	970.	0.90	0.90
51.00	1747.7	617.	1110.	1975.	247834.	969.	0.91	0.91
51.50	1745.6	617.	1117.	1984.	247926.	969.	0.92	0.92
52.00	1743.5	617.	1124.	1993.	247927.	968.	0.94	0.94
52.50	1741.3	617.	1132.	1998.	247839.	967.	0.95	0.95
53.00	1739.1	616.	1139.	2001.	247819.	967.	0.97	0.97
53.50	1736.9	616.	1147.	1999.	247910.	967.	0.98	0.98
54.00	1734.6	616.	1154.	1990.	247810.	967.	1.00	1.00

54.50	1732.8	618.	1161.	1959.	247747.	969.	1.01	1.00
55.00	1730.8	622.	1169.	3541.	249100.	912.	1.02	1.00
55.50	1728.9	626.	1176.	3400.	248888.	919.	1.04	1.00
56.00	1726.8	631.	1183.	3276.	248714.	926.	1.05	1.00
56.50	1724.8	635.	1191.	3167.	248745.	933.	1.07	1.00
57.00	1722.7	640.	1198.	3069.	248602.	940.	1.08	1.00
57.50	1720.6	645.	1206.	2977.	248333.	948.	1.09	1.00
58.00	1718.4	650.	1213.	2889.	248275.	955.	1.11	1.00
58.50	1716.2	656.	1220.	2789.	248164.	964.	1.12	1.00
59.00	1714.0	662.	1228.	2695.	247737.	972.	1.14	1.00
59.50	1711.7	668.	1235.	2607.	247662.	981.	1.15	1.00
60.00	1709.3	674.	1243.	2522.	247458.	990.	1.16	1.00
60.50	1706.9	681.	1250.	2443.	247214.	1000.	1.18	1.00
61.00	1704.4	687.	1257.	2369.	246942.	1009.	1.19	1.00
61.50	1701.9	694.	1265.	2298.	246686.	1019.	1.20	1.00
62.00	1699.3	702.	1272.	2246.	246523.	1028.	1.22	1.00
62.50	1696.7	709.	1279.	2203.	246334.	1038.	1.23	1.00
63.00	1694.1	717.	1287.	2163.	246059.	1047.	1.24	1.00
63.50	1691.4	725.	1294.	2127.	245859.	1057.	1.26	1.00
64.00	1688.6	733.	1301.	2094.	245607.	1066.	1.27	1.00
64.50	1685.9	742.	1308.	2064.	245454.	1076.	1.28	1.00
65.00	1683.0	750.	1316.	2036.	245180.	1086.	1.30	1.00
65.50	1680.1	759.	1323.	2011.	244837.	1096.	1.31	1.00
66.00	1677.2	768.	1330.	1988.	244535.	1105.	1.32	1.00
66.50	1674.2	778.	1338.	1967.	244340.	1116.	1.34	1.00
67.00	1671.2	787.	1345.	1948.	244076.	1126.	1.35	1.00
67.50	1668.1	796.	1352.	1930.	239621.	1130.	1.36	1.00
68.00	1665.0	806.	1359.	1915.	232271.	1130.	1.38	1.00
68.50	1661.8	815.	1366.	1901.	224996.	1130.	1.39	1.00
69.00	1658.6	824.	1372.	1889.	217763.	1129.	1.40	1.00
69.50	1655.4	833.	1378.	1879.	210507.	1128.	1.41	1.00
70.00	1652.2	841.	1384.	1869.	203250.	1127.	1.42	1.00
70.50	1648.9	850.	1390.	1861.	196058.	1126.	1.43	1.00
71.00	1645.5	858.	1396.	1854.	188892.	1124.	1.44	1.00
71.50	1642.1	866.	1401.	1848.	181561.	1122.	1.45	1.00
72.00	1638.7	873.	1406.	1842.	174424.	1120.	1.46	1.00
72.50	1635.3	881.	1411.	1837.	167140.	1117.	1.47	1.00
73.00	1631.9	888.	1416.	1833.	160046.	1114.	1.48	1.00
73.50	1628.4	895.	1421.	1830.	152754.	1111.	1.48	1.00
74.00	1624.9	901.	1425.	1826.	145631.	1108.	1.49	1.00
74.50	1621.3	908.	1429.	1824.	138426.	1104.	1.50	1.00
75.00	1617.7	914.	1433.	1821.	131249.	1100.	1.50	1.00
75.50	1614.2	919.	1437.	1819.	124139.	1095.	1.51	1.00
76.00	1610.5	925.	1440.	1817.	116945.	1091.	1.51	1.00
76.50	1606.9	930.	1443.	1816.	109861.	1086.	1.52	1.00
77.00	1603.3	934.	1446.	1814.	102794.	1080.	1.52	1.00
77.50	1599.6	939.	1449.	1813.	95562.	1074.	1.53	1.00
78.00	1595.9	943.	1452.	1812.	88386.	1068.	1.53	1.00
78.50	1592.2	946.	1454.	1811.	81306.	1062.	1.54	1.00
79.00	1588.5	950.	1457.	1810.	74273.	1055.	1.54	1.00
79.50	1584.7	953.	1459.	1809.	67146.	1048.	1.54	1.00
80.00	1581.0	955.	1460.	1809.	59987.	1041.	1.54	1.00
80.50	1577.2	958.	1462.	1808.	52833.	1033.	1.54	1.00
81.00	1573.4	960.	1463.	1807.	45791.	1025.	1.55	1.00
81.50	1569.7	962.	1464.	1806.	38751.	1017.	1.55	1.00
82.00	1565.9	963.	1465.	1806.	31671.	1008.	1.55	1.00
82.50	1562.1	964.	1466.	1805.	24655.	999.	1.55	1.00
83.00	1558.3	964.	1467.	1804.	17497.	989.	1.55	1.00
83.50	1554.5	965.	1467.	1804.	10428.	980.	1.55	1.00
84.00	1550.7	965.	1467.	1803.	3341.	969.	1.55	1.00

MASS FLOW =0.1191E 06LB/HR G =0.1762E 07LB/HR-SQ FT HMIN = 914.388.

COMMERCIAL PLANT PANEL No. 1

$$\eta = \frac{(19{,}100)(1467-560)}{(269{,}500)(437.4)} = .916$$

$$R = .909$$

CUMULATIVE PRESSURE DROP		
FRICTION PSI	MOMENTUM PSI	GRAVITY PSI
0.2083	0.0001	0.1577
0.4166	0.0004	0.3154
0.6250	0.0008	0.4730
0.8335	0.0014	0.6306
1.0420	0.0023	0.7881
1.2507	0.0033	0.9454
1.4595	0.0044	1.1026
1.6685	0.0058	1.2596
1.8776	0.0073	1.4164
2.0870	0.0090	1.5730
2.2967	0.0109	1.7294
2.5066	0.0130	1.8854
2.7167	0.0152	2.0412
2.9272	0.0176	2.1967
3.1381	0.0202	2.3518
3.3493	0.0230	2.5066
3.5609	0.0260	2.6609
3.7728	0.0291	2.8149
3.9852	0.0324	2.9685
4.1981	0.0359	3.1216
4.4114	0.0395	3.2742
4.6252	0.0434	3.4264
4.8395	0.0474	3.5781
5.0543	0.0516	3.7292
5.2696	0.0560	3.8798
5.4856	0.0605	4.0298
5.7020	0.0652	4.1792
5.9191	0.0701	4.3281
6.1369	0.0764	4.4762
6.3557	0.0843	4.6235
6.5756	0.0924	4.7699
6.7967	0.1007	4.9152
7.0191	0.1093	5.0596
7.2426	0.1182	5.2029
7.4674	0.1274	5.3453
7.6935	0.1372	5.4865
7.9213	0.1505	5.6265
8.1579	0.2637	5.7613
8.4037	0.4798	5.8910
8.6589	0.8016	6.0160
8.9237	1.2321	6.1364
9.1985	1.7743	6.2524
9.4834	2.4313	6.3644
9.7789	3.2061	6.4723
10.0850	4.1017	6.5765
10.4022	5.1213	6.6771
10.7307	6.2681	6.7742
11.0708	7.5453	6.8680

11.4228	8.9560	6.9586
11.7870	10.5036	7.0462
12.1636	12.1912	7.1309
12.7035	12.3286	7.1900
13.2684	12.4685	7.2465
13.8588	12.6110	7.3006
14.4752	12.7560	7.3523
15.1179	12.9019	7.4020
15.7870	13.0474	7.4497
16.4824	13.1916	7.4956
17.2040	13.3355	7.5398
17.9517	13.4797	7.5825
18.7256	13.6240	7.6237
19.5259	13.7684	7.6636
20.3525	13.9130	7.7022
21.2056	14.0577	7.7397
22.0851	14.2027	7.7760
22.9911	14.3477	7.8112
23.9237	14.4929	7.8454
24.8830	14.6382	7.8787
25.8690	14.7837	7.9111
26.8818	14.9294	7.9426
27.9215	15.0751	7.9733
28.9881	15.2211	8.0033
30.0818	15.3671	8.0325
31.2027	15.5134	8.0610
32.3508	15.6598	8.0888
33.5262	15.8063	8.1160
34.7290	15.9530	8.1425
35.9592	16.0999	8.1685
37.2169	16.2469	8.1939
38.5023	16.3940	8.2187
39.8154	16.5413	8.2431
41.1562	16.6888	8.2669
42.5248	16.8364	8.2902
43.9214	16.9843	8.3131
45.3461	17.1322	8.3356
46.7988	17.2803	8.3576
48.2797	17.4285	8.3791
49.7889	17.5770	8.4003
51.3265	17.7256	8.4211
52.8925	17.8743	8.4415
54.4870	18.0232	8.4616
56.1102	18.1723	8.4813
57.7621	18.3215	8.5006
59.4429	18.4709	8.5196
61.1525	18.6205	8.5383
62.8912	18.7702	8.5567
64.6590	18.9201	8.5748
66.4559	19.0702	8.5926
68.2822	19.2205	8.6101
70.1379	19.3709	8.6274
72.0231	19.5216	8.6444
73.9380	19.6723	8.6611
75.8826	19.8233	8.6775
77.8569	19.9745	8.6937
79.8613	20.1258	8.7097
81.8956	20.2772	8.7254
83.9601	20.4289	8.7409
86.0549	20.5807	8.7562
87.6736	20.7972	8.7712
89.3259	21.0612	8.7860

91.0151	21.3284	8.8004
92.7420	21.5935	8.8145
94.5071	21.8538	8.8282
96.3099	22.1201	8.8417
98.1531	22.3812	8.8550
100.0417	22.6476	8.8679
101.9773	22.9119	8.8806
103.9604	23.1785	8.8931
105.9923	23.4480	8.9053
108.0742	23.7161	8.9172
110.2069	23.9859	8.9290
112.3918	24.2567	8.9405
114.6224	24.5284	8.9518
116.8967	24.8015	8.9629
119.2154	25.0762	8.9738
121.5792	25.3511	8.9845
123.9885	25.6275	8.9950
126.4440	25.9039	9.0054
128.9460	26.1817	9.0155
131.4951	26.4589	9.0255
134.0916	26.7377	9.0353
136.7361	27.0168	9.0449
139.4290	27.2966	9.0544
142.1706	27.5771	9.0637
144.9611	27.8530	9.0729
147.7998	28.1210	9.0819
150.6857	28.3809	9.0908
153.6179	28.6329	9.0996
156.5955	28.8766	9.1082
159.6174	29.1125	9.1168
162.6827	29.3394	9.1252
165.7901	29.5591	9.1335
168.9388	29.7702	9.1417
172.1275	29.9734	9.1498
175.3552	30.1685	9.1578
178.6207	30.3549	9.1658
181.9229	30.5336	9.1737
185.2606	30.7041	9.1814
188.6326	30.8656	9.1892
192.0377	31.0194	9.1968
195.4747	31.1652	9.2044
198.9423	31.3030	9.2119
202.4393	31.4328	9.2194
205.9646	31.5547	9.2268
209.5168	31.6684	9.2341
213.0948	31.7739	9.2414
216.6982	31.8710	9.2487
220.3258	31.9596	9.2559
223.9763	32.0389	9.2631
227.6482	32.1094	9.2702
231.3403	32.1715	9.2773
235.0512	32.2252	9.2843
238.7796	32.2704	9.2914
242.5241	32.3071	9.2984
246.2833	32.3353	9.3053
250.0559	32.3548	9.3123
253.8404	32.3658	9.3192
257.6353	32.3681	9.3261

$\Delta T = 334\ ^\circ F$

279.34

/HR-SF-F

$\Delta P_{fm} = 290.0034$

BOILER PANEL NO. 1
(USING GROENEVELD CORRELATION) PILOT PLANT

PRESS PSIA	TEMP F	ENTHALPY BTU/LB	L1 FT	L2 FT*	NO.TUBES	TUBE OD IN	*TUBE ID IN	TUBE LGTH FT	INCREMENT FT
1600.	505.	493.	9.8	32.8	70	0.50	0.27	41.	0.50

CONDUCTIVITY B-IN/H-SF-F	EXT.COEFF B/H-SF-F	EMISSIVITY *	ABSORPTANCE	*AMB.TEMP F	MAX.SOLAR FLUX BTU/HR-SQFT
150.	3.	0.89	0.95	100.	98000.

TUBE LGTH FT	PRESS PSIA	BULK TEMP F	ENTHALPY BTU/LB	INSIDE FILM COEF B/H-SF-F	OUTSIDE HEAT FLUX B/H-SF	TUBE *CROWN TEMP F	BULK QUAL	CRIT QUAL
0.50	1599.8	505.	493.	1181.	2759.	509.	-.24	0.0
1.00	1599.6	506.	495.	1182.	7408.	518.	-.24	0.0
1.50	1599.5	507.	497.	1182.	12144.	527.	-.24	0.0
2.00	1599.3	509.	500.	1184.	16725.	537.	-.23	0.0
2.50	1599.1	512.	503.	1185.	21321.	547.	-.22	0.0
3.00	1598.9	516.	508.	1187.	25997.	558.	-.21	0.0
3.50	1598.8	520.	513.	1190.	30586.	569.	-.21	0.0
4.00	1598.6	525.	519.	1193.	35167.	581.	-.19	0.0
4.50	1598.4	530.	526.	1197.	39752.	594.	-.18	0.0
5.00	1598.2	536.	534.	1201.	44523.	608.	-.17	0.0
5.50	1598.1	542.	542.	1205.	48995.	621.	-.15	0.0
6.00	1597.9	550.	552.	1210.	53623.	636.	-.13	0.0
6.50	1597.7	557.	562.	1215.	58063.	650.	-.11	0.0
7.00	1597.6	566.	573.	1222.	62662.	666.	-.09	0.0
7.50	1597.4	575.	584.	1229.	67147.	682.	-.07	0.0
8.00	1597.2	584.	597.	1237.	71678.	698.	-.05	0.0
8.50	1597.1	595.	610.	1247.	76310.	715.	-.03	0.0
9.00	1596.9	605.	624.	1261.	80840.	733.	0.00	0.0
9.50	1596.8	605.	639.	5000.	86532.	699.	0.03	0.0
10.00	1596.6	605.	654.	5000.	89685.	702.	0.06	0.0
10.50	1596.5	605.	670.	5000.	89697.	702.	0.09	0.0
11.00	1596.3	605.	686.	5000.	89709.	702.	0.11	0.0
11.50	1596.2	605.	701.	5000.	89720.	702.	0.14	0.0
12.00	1596.0	605.	717.	5000.	89732.	702.	0.17	0.0
12.50	1595.9	605.	732.	5000.	89745.	702.	0.20	0.0
13.00	1595.7	605.	748.	5000.	89757.	702.	0.23	0.0
13.50	1595.5	604.	763.	5000.	89770.	702.	0.26	0.0
14.00	1595.3	604.	779.	5000.	89347.	702.	0.29	0.0
14.50	1595.1	604.	794.	5000.	89361.	702.	0.32	0.0
15.00	1594.9	604.	810.	5000.	89376.	702.	0.34	0.0
15.50	1594.7	604.	825.	5000.	89391.	702.	0.37	0.0
16.00	1594.5	604.	841.	5000.	89407.	702.	0.40	0.0
16.50	1594.3	604.	856.	5000.	89424.	702.	0.43	0.0
17.00	1594.0	604.	872.	5000.	89442.	702.	0.46	0.0
17.50	1593.8	604.	887.	5000.	89460.	702.	0.49	0.0
18.00	1593.6	604.	903.	5000.	89479.	702.	0.52	0.0
18.50	1593.3	604.	918.	5000.	89498.	702.	0.54	0.0
19.00	1593.0	604.	934.	5000.	89519.	702.	0.57	0.0
19.50	1592.7	604.	949.	5000.	89540.	702.	0.60	0.0
20.00	1592.4	604.	965.	5000.	89562.	702.	0.63	0.0
20.50	1592.1	604.	980.	5000.	89585.	702.	0.66	0.0
21.00	1591.8	604.	996.	5000.	89609.	702.	0.69	0.0
21.50	1591.4	604.	1011.	5000.	89633.	702.	0.72	0.0
22.00	1591.1	604.	1027.	5000.	89659.	702.	0.74	0.0
22.50	1590.7	604.	1042.	5000.	89685.	702.	0.77	0.0

23.00	1590.4	604.	1058.	5000.	89712.	702.	0.80	0.0
23.50	1590.2	604.	1073.	5000.	89740.	702.	0.83	0.0
24.00	1589.6	604.	1089.	5000.	89768.	702.	0.86	0.0
24.50	1589.2	604.	1104.	5000.	89358.	702.	0.89	0.0
25.00	1588.8	604.	1120.	5000.	89388.	702.	0.92	0.0
25.50	1588.4	604.	1135.	5000.	89420.	702.	0.95	0.95
26.00	1588.3	604.	1151.	5003.	89663.	702.	0.97	0.97
26.50	1588.2	605.	1166.	2534.	89120.	720.	1.00	0.97
27.00	1588.1	614.	1182.	808.	87856.	790.	1.03	0.97
27.50	1588.0	624.	1197.	750.	87512.	805.	1.06	0.97
28.00	1587.9	635.	1212.	704.	87297.	821.	1.09	0.97
28.50	1587.7	648.	1227.	665.	87002.	838.	1.11	0.97
29.00	1587.6	661.	1242.	629.	86723.	855.	1.14	0.97
29.50	1587.5	675.	1257.	590.	86373.	874.	1.17	0.97
30.00	1587.4	691.	1272.	556.	86052.	894.	1.20	0.97
30.50	1587.2	707.	1287.	527.	85646.	914.	1.22	0.97
31.00	1587.1	724.	1301.	509.	85261.	933.	1.25	0.97
31.50	1587.0	742.	1316.	495.	84857.	953.	1.28	0.97
32.00	1586.8	761.	1331.	483.	84459.	972.	1.30	0.97
32.50	1586.7	781.	1345.	473.	84081.	992.	1.33	0.97
33.00	1586.5	800.	1359.	465.	81648.	1007.	1.36	0.97
33.50	1586.4	819.	1373.	459.	76326.	1013.	1.38	0.97
34.00	1586.2	837.	1385.	454.	71023.	1019.	1.40	0.97
34.50	1586.1	854.	1396.	450.	65792.	1023.	1.43	0.97
35.00	1585.9	871.	1407.	448.	60543.	1025.	1.44	0.97
35.50	1585.7	885.	1416.	446.	55314.	1027.	1.46	0.97
36.00	1585.6	899.	1425.	444.	50147.	1027.	1.48	0.97
36.50	1585.4	911.	1433.	443.	45007.	1027.	1.49	0.97
37.00	1585.3	922.	1440.	443.	39900.	1025.	1.51	0.97
37.50	1585.1	932.	1446.	442.	34741.	1021.	1.52	0.97
38.00	1584.9	940.	1451.	442.	29707.	1017.	1.53	0.97
38.50	1584.8	947.	1455.	442.	24657.	1010.	1.53	0.97
39.00	1584.6	953.	1459.	442.	19688.	1003.	1.54	0.97
39.50	1584.4	957.	1461.	442.	14698.	995.	1.54	0.97
40.00	1584.3	960.	1463.	442.	9720.	985.	1.55	0.97
40.50	1584.1	961.	1464.	442.	4785.	973.	1.55	0.97
41.00	1583.9	961.	1464.	442.	-102.	961.	1.55	0.97

MASS FLOW =0.8419E 04LB/HR G =0.3025E 06LB/HR-SQ FT HMIN = 265.068

$$S = \frac{\log \frac{12.017}{11.11}}{\log \frac{.3176}{.3025}}$$

PILOT PLANT PANEL NO. 1

$\eta = .890$

CUMULATIVE PRESSURE DROP		
FRICTION PSI	MOMENTUM PSI	GRAVITY PSI
0.0082	0.0000	0.1704
0.0165	0.0001	0.3407
0.0248	0.0002	0.5105
0.0330	0.0003	0.6798
0.0413	0.0004	0.8485
0.0497	0.0006	1.0162
0.0581	0.0008	1.1829
0.0665	0.0010	1.3485
0.0750	0.0013	1.5127
0.0835	0.0016	1.6754
0.0921	0.0020	1.8366
0.1007	0.0023	1.9960
0.1094	0.0027	2.1536
0.1183	0.0032	2.3093
0.1272	0.0036	2.4630
0.1361	0.0041	2.6146
0.1452	0.0046	2.7639
0.1544	0.0054	2.9108
0.1648	0.0159	3.0400
0.1766	0.0366	3.1549
0.1896	0.0675	3.2584
0.2040	0.1087	3.3525
0.2196	0.1600	3.4388
0.2365	0.2215	3.5185
0.2548	0.2932	3.5925
0.2743	0.3751	3.6616
0.2952	0.4672	3.7263
0.3173	0.5695	3.7873
0.3407	0.6820	3.8449
0.3655	0.8046	3.8994
0.3915	0.9374	3.9513
0.4188	1.0805	4.0007
0.4474	1.2337	4.0478
0.4774	1.3971	4.0929
0.5086	1.5707	4.1361
0.5411	1.7545	4.1776
0.5749	1.9486	4.2175
0.6101	2.1529	4.2559
0.6465	2.3674	4.2929
0.6843	2.5922	4.3287
0.7233	2.8272	4.3633
0.7637	3.0725	4.3967
0.8054	3.3280	4.4291
0.8484	3.5939	4.4605

0.8927	3.8700	4.4910
0.9585	4.1564	4.5205
0.9852	4.4532	4.5493
1.0334	4.7602	4.5773
1.0830	5.0776	4.6045
1.1338	5.4052	4.6311
1.1860	5.7432	4.6569
1.2826	5.7534	4.6709
1.3576	5.7641	4.6845
1.4353	5.7810	4.6976
1.5164	5.7982	4.7102
1.6008	5.8155	4.7223
1.6889	5.8329	4.7340
1.7811	5.8503	4.7452
1.8778	5.8677	4.7560
1.9790	5.8852	4.7664
2.0839	5.9027	4.7765
2.1927	5.9203	4.7862
2.3052	5.9378	4.7957
2.4217	5.9553	4.8049
2.5421	5.9728	4.8137
2.6663	5.9898	4.8224
2.7943	6.0058	4.8308
2.9258	6.0206	4.8390
3.0605	6.0343	4.8470
3.1983	6.0469	4.8549
3.3388	6.0584	4.8626
3.4820	6.0688	4.8702
3.6274	6.0781	4.8777
3.7749	6.0864	4.8851
3.9242	6.0935	4.8925
4.0751	6.0996	4.8997
4.2273	6.1047	4.9069
4.3806	6.1087	4.9141
4.5347	6.1117	4.9212
4.6894	6.1137	4.9283
4.8445	6.1146	4.9354
4.9997	6.1146	4.9425

16.0568

'HR-SF-F

$\Delta P_{f+m} = 11.11$ psi

$= \frac{.63408}{.02116} = 1.61$

RECOMMENDED LAY–UP PROCEDURES
C-E DRUM TYPE UTILITY UNITS

TYPE OF SHUTDOWN	PROCEDURE
Pre-Operational Period Post Hydro (See Note 1)	With the economizer, waterwalls, superheater, and reheater filled to overflowing pressurize the unit with nitrogen to 5 psig pressure (See Notes 4 & 5).
Pre-Operational Period Post Chemical Cleaning	1. Introduce demineralized or condensate quality water containing 10 ppm of ammonia and 200 ppm of hydrazine into the superheater, reheater, feedwater heaters, (tube side) and associated piping, economizer and waterwalls (Refer to Notes 3 & 4). 2. Nitrogen cap the superheater, feedwater heaters (shell side) and drum. Maintain 5 psig nitrogen pressure (See Note 5).
Short Outage - 4 Days or Less	1. Maintain the same hydrazine and ammonia concentrations as those present during normal operation. 2. Establish and maintain a 5 psig nitrogen cap on the superheater and the steam drum (See Note 5). 3. Nitrogen cap the shell side of the feedwater heaters.
Short Outage - 4 Days or Less Unit Partially Drained for Repairs	1. Drain and open only those sections requiring repairs. 2. Isolate remainder of unit under 5 psig nitrogen pressure where possible (See Note 5). 3. Maintain the same hydrazine and ammonia concentrations for water remaining in the cycle as those present during normal operation. 4. Nitrogen cap the shell side of the feedwater heaters.
Long Outage - Longer than 4 Days	1. Fill the superheater and reheater with demineralized or condensate quality water containing 10 ppm of ammonia and 200 ppm of hydrazine. The pH of the solution should be approximately 10.0. Add the fill water to the outlet of the non-drainable sections (See Note 4). 2. Increase the hydrazine and ammonia concentration in the waterwalls, economizer and feedwater heaters (tube side) and associated piping to 200 ppm and 10 ppm respectively (See Notes 2, 3, and 4). 3. Establish and maintain a 5 psig nitrogen cap on the superheater and steam drum (See Note 5). 4. Nitrogen cap the shell side of the feedwater heaters.
Long Outage - Longer than 4 Days Unit Partially Drained for Repairs	1. Drain and open only those sections requiring repairs. 2. Fill the superheater and reheater (if not requiring draining for repairs) with demineralized or condensate quality water containing 10 ppm of ammonia and 200 ppm of hydrazine. The pH of the solution should be approximately 10.0. Add the fill water to the outlet of the non-drainable sections (See Note 4). 3. Increase the hydrazine and ammonia concentrations in the tube side of the feedwater heaters and the undrained circuits of the economizer and waterwalls to 200 ppm and 10 ppm respectively (See Notes 2, 3 & 4). 4. Establish and maintain a 5 psig nitrogen cap on the undrained sections of the unit, where possible (See Note 5). 5. Nitrogen cap the shell side of the feedwater heaters. 6. After completion of the repair, fill the drained sections with demineralized or condensate quality water containing 10 ppm of ammonia and 200 ppm of hydrazine. Cap with nitrogen (See Notes 2, 3, & 4).

NOTES

1. All non-drainable sections to be hydrostatically tested should be filled with demineralized or condensate quality water containing 10 ppm of ammonia and 200 ppm of hydrazine. This should produce a solution pH of approximately 10.0. The superheater should be filled first, to overflow into the boiler drum. Then the economizer and waterwalls can be filled through normal fill connections (See Note 2) with demineralized or condensate quality water, or if not available, any source of clean, filtered water may be used. This water should also contain 10 ppm of ammonia and 200 ppm of hydrazine.
2. Hydrazine and ammonia should be added in a manner that results in a uniform concentration throughout. They may be added to the system in several ways, as for example:
   a. By pumping concentrated solutions through the chemical feed equipment and blend filling to achieve the desired concentrations.
   b. If condenser leakage is not a cause for shutdown, concentrated solutions can be introduced directly into the hotwell where they can be mixed to achieve the desired concentrations. If condensate demineralizers are employed, they must be bypassed during this operation.

   It is important to have the fluid temperature in the cycle below 400°F before addition of hydrazine. If this temperature is exceeded, the hydrazine will decompose.
3. The tube side of copper alloy feedwater heaters should be filled with demineralized water containing 0.5 ppm of ammonia and 50 ppm of hydrazine.
4. If freezing is a problem, the water in drainable circuits can be displaced with nitrogen and the unit layed up under 5 psig nitrogen pressure. Auxiliary heat may be applied to keep the non-drainable sections from freezing.
5. Nitrogen cap should be applied through the drum vent, superheater outlet header drain/vent, and reheater outlet header drain/vent, as the unit is cooled, when pressure drops to 5 psig. Admission of air through atmospheric vents should be avoided.

SECTION 6

References

1. MDAC - Preliminary Design Report, Vol. IV, Receiver Subsystem.
2. MDAC - Preliminary Design Report, Vol. II.
3. Rockwell - S.R.E. Test Report.
4. Sandia Thermal/Structural Analysis of DNB in the MDAC Receiver.
5. MDAC/Rocketdyne - Thermal/Structural Analysis of DNB in their Receiver.
6. MDAC - Predictions for Incident and Absorbed Heat Flux on Panels 1 and 9.
7. Letter from Sandia stating lateral flux variations on Panels 7 and 8.
8. Test plan for Retest of MDAC SRE boiler panel.
9. Plots of solar insolation vs. time of day for August 1, 1975 to July 31, 1976.
10. GE Reports:
    a. "An Evaluation of Strain Cycling Effects in the DNB Zone of the CR BR Evaporators".
    b. "Thermal/Hydraulic Test Results Including Critical Heat Flux Conditions for a Sodium-Heated Steam Generator Test Model".
11. Tentative Test Plan for Materials Testing at ANL.
12. MDAC-PDR - Vol. VI.
13. Notes on Pilot Plant and Commercial Plant Panel Performance.
14. Drawings:
    Rocketdyne - 99R5010503
    Rocketdyne - 99R5010503, Sheet 2
    Rocketdyne - 99R5010504
    Rocketdyne - 99R5010501
15. Yin-Yun Hsu and R. W. Graham, "Transport Process in Boiling and Two-Phase Systems", McGraw Hill, New York, 1976.
16. John Collier, "Convective Boiling and Condensation", McGraw Hill, London, 1972.
17. H. Herkenenerath, P. Mork-Morkenstein, U. Jung, F.-J. Weckerman, "Warneubergang an Wasser bei Erzwungener Stromung im Druckenberich 140 bis 250 bar", Darstellung der Versuche.

18. D. C. Groeneveld, "An Investigation of Heat Transfer in the Liquid Deficient Regime", AECL-3281, Chalk River, Ontario, 1964.

19. Richard Dougall and Warren Rohsenow, "Film Boiling on the Inside of Vertical Tubes with Upward Flow of the Fluid at Low Qualities", MIT Report 9079-26, September, 1963.

20. V. E. Doroshchuck and F. P. Lantsman, "Selecting Magnitudes of Critical Heat Fluxes with Water Boiling in Vertical Uniformly Heated Tubes", Teploenergetika, 1970, 17(12), 17-19.

21. M. Buzina, "Development Problems with Once-Through Forced-Flow Steam Generators", Sulzer Technical Review 1/1976, Wintherthur, Switzerland. Reprinted in Combustion Magazine, September, 1977.

22. J. C. Chen, R. K. Sundaram, F. T. Ozkaynak, "A Phenomenological Correlation for Post CHF Heat Transfer", Lehigh University Report for the U. S. Nuclear Regulatory Commission, NUREG--237, Bethlehem, Pennsylvania, June, 1977.

23. B. Thompson and R. V. MacBeth, "Boiling Water Heat Transfers, Burnout in Uniformly Heated Round Tubes: A Compilation of World Data with Accurate Correlations", AEEW R-356, 1964.

24. H. M. Payne, "Preliminary Assessment of the DOE/MDAC Solar Receiver Design", Interim Report, Combustion Engineering, Inc., January, 1978.

25. J. L. Houtman, "Structural Evaluation of the In-Vessel FFTF Plant Unit Instrument Tree", Westinghouse Advanced Reactors Division, FRA 1143, December 14, 1973.

UNLIMITED RELEASE

INITIAL DISTRIBUTION:

Large Power Systems Branch (4)
Division of Central Power Systems
U.S. Department of Energy
Washington, D.C. 20545
Attn: G. W. Braun, Asst. Director
J. Zingeser, Project Officer
J. Weisiger, Program Manager
G. M. Kaplan, Chief

Aerospace Corporation (2)
P. O. Box 92957
Los Angeles, CA 90009
Attn: R. Leatherman
K. Zondervan

Babcock & Wilcos (2)
1562 Beeson
Alliance, OH 44601
Attn: T. B. Brown
M. Wiener

Black & Veatch Consulting Engineers
P.O. Box 8405
Kansas City, MO 64114
Attn: J. E. Harder

Combustion Engineering, Inc. (3)
1000 Prospect Hill Road
Windsor, CT 06095
Attn: C. R. Bozzuto
M. J. Davidson
H. M. Payne

ETEC/STMPO (3)
9550 Flair Park Drive
Suite 210
El Monte, CA 91731
Attn: K. L. Adler
G. C. French
R. W. Wiese

Division of Solar Technology
U.S. Department of Energy
San Francisco Operations Office
1333 Broadway
Oakland, CA 94612
Attn: S. D. Elliott

Foster Wheeler Energy Corp. (2)
110 South Orange Avenue
Livingston, NJ 07039
Attn: S. F. Wu
R. J. Zoschak

Los Angeles Department of Water & Power (2)
P. O. Box 111
Los Angeles, CA 90051
Attn: J. M. Hayashi
C. Singman

Martin Marietta Aerospace (2)
P. O. Box 178
Denver, CO 80201
Attn: D. Gorman
T. R. Tracey

McDonnell Douglas (3)
5301 Bolsa Avenue
Huntington Beach, CA 92647
Attn: I. Catton
G. Coleman
R. Gervais

Rocketdyne Division (3)
Rockwell International Corp.
6633 Canoga Avenue
Canoga Park, CA 91304
Attn: J. M. Friefeld
A. Liebman
D. Vanevenhoven

Riley-Stoker
P. O. Box 547
Worcester, MA 01613
Attn: A. H. Rawdon

Southern California Edison (2)
P. O. Box 800
Rosemead, CA 91770
Attn: L. Rasband
W. H. von KleinSmid

Stearns-Roger (2)
P. O. Box 5888
Denver, CO 80217
Attn: A. W. McKenzie
H. C. Welz

W. B. Jones, 5835
T. B. Cook, Jr., 8000; Attn: W. J. Spencer, 8100
A. N. Blackwell, 8200
B. F. Murphey, 8300
J. F. Jones, 8122
M. Abrams, 8124
L. Gutierrez, 8400; Attn: R. A. Baroody, 8410
J. W. Pearce, 8420
G. W. Anderson, 8440
C. M. Tapp, 8460
C. S. Selvage, 8470
R. C. Wayne, 8450
W. G. Wilson, 8451
A. C. Skinrood, 8452
E. T. Cull, 8452 (20)
L. A. Hiles, 8452
J. W. Liebenberg, 8452
M. B. Loll, 8452
C. W. Moore, 8452
L. N. Tallerico, 8452
Publications & Public Information Division, 8265, for TIC (27)
F. J. Cupps, 8265/Technical Library Processes Division, 3141
Technical Library Processes Division, 3141 (2)
Library & Security Classification Division, 8266-2 (3)